



**PRELIMINARY ELECTRICAL DESIGNS FOR CTEX AND  
AFIT SATELLITE GROUND STATION**

THESIS

Arthur L. Morse, Captain, USAF

AFIT/GA/ENY/10-M08

**DEPARTMENT OF THE AIR FORCE  
AIR UNIVERSITY**

**AIR FORCE INSTITUTE OF TECHNOLOGY**

**Wright-Patterson Air Force Base, Ohio**

APPROVED FOR PUBLIC RELEASE; DISTRIBUTION UNLIMITED.

The views expressed in this thesis are those of the author and do not reflect the official policy or position of the United States Air Force, Department of Defense, or the United States Government. This material is declared a work of the U.S. Government and is not subject to copyright protection in the United States.

AFIT/GA/ENY/10-M08

PRELIMINARY ELECTRICAL DESIGNS FOR CTEX AND  
AFIT SATELLITE GROUND STATION

THESIS

Presented to the Faculty  
Department of Aeronautics and Astronautics  
Graduate School of Engineering and Management  
Air Force Institute of Technology  
Air University  
Air Education and Training Command  
In Partial Fulfillment of the Requirements for the  
Degree of Master of Science in Astronautical Engineering

Arthur L. Morse, BS  
Captain, USAF

March 2010

APPROVED FOR PUBLIC RELEASE; DISTRIBUTION UNLIMITED.

PRELIMINARY ELECTRICAL DESIGNS FOR CTEX AND  
AFIT SATELLITE GROUND STATION

Arthur L. Morse, BS  
Captain, USAF

Approved:

<hr/>	<hr/>
//signed//	18 Mar 2010
Dr. Jonathan Black (Chairman)	Date
<hr/>	<hr/>
//signed//	18 Mar 2010
Eric D. Swenson, Lt Col, USAF (Member)	Date
<hr/>	<hr/>
//signed//	18 Mar 2010
Dr. Richard Cobb (Member)	Date

## *Abstract*

This thesis outlines the design of the electrical components for the space-based ChromoTomography Experiment (CTEx). CTEx is the next step in the development of high-speed chromotomography at the Air Force Institute of Technology. The electrical design of the system is challenging due to the large amount of data that is acquired by the imager and the limited resources that is inherent with space-based systems. Additional complication to the design is the need to know the angle of a spinning prism that is in the field of view very precisely for each image. Without this precise measurement any scene that is reconstructed from the data will be blurry and incomprehensible. This thesis also outlines how the control software for the CTEx space system should be created. The software flow is a balance of complex real time target pointing angles and simplicity to allow the system to function as quick as possible.

This thesis also discusses the preliminary design for an AFIT satellite ground station based upon the design of the United States Air Force Academy's ground station. The AFIT ground station will be capable of commanding and controlling satellites produced by USAFA and satellites produced by a burgeoning small satellite program at AFIT.

## *Acknowledgements*

I'd like to thank my wife for all of the support she has given me and allowing me to focus on my studies while she took care of our 2 year old daughter and, as of committee turn in, our 2 week old son.

Arthur L. Morse

# *Table of Contents*

	Page
Abstract . . . . .	iv
Acknowledgements . . . . .	v
List of Figures . . . . .	viii
List of Tables . . . . .	x
I. Introduction . . . . .	1
1.1 Motivation . . . . .	1
1.2 CTE <sub>x</sub> . . . . .	2
1.3 Purpose . . . . .	3
1.4 Scope . . . . .	3
1.5 Organization . . . . .	3
II. Background . . . . .	5
2.1 Spectral Imaging Basics . . . . .	5
2.1.1 Spectroscopy . . . . .	5
2.1.2 Hyperspectral Imaging . . . . .	7
2.2 Hyperspectral Imagers . . . . .	10
2.2.1 HICO . . . . .	10
2.2.2 ARTEMIS . . . . .	15
2.3 CTE <sub>x</sub> Software Foundation . . . . .	21
2.3.1 RIGEX . . . . .	21
2.4 AFIT Ground Station Foundation . . . . .	24
2.4.1 United States Air Force Academy . . . . .	24
2.4.2 United States Naval Academy . . . . .	28
2.5 CTE <sub>x</sub> Application . . . . .	30
2.5.1 Electrical . . . . .	30
2.5.2 Software . . . . .	31
2.5.3 Ground Station . . . . .	31
III. CTE <sub>x</sub> Overview . . . . .	32
3.0.4 Chromotomography . . . . .	35
3.0.5 AFIT Chromotomography . . . . .	37

	Page
IV. Designs . . . . .	42
4.1 CTE <sub>x</sub> Electrical Subsystem . . . . .	42
4.1.1 Data Collection and Command Unit . . . . .	44
4.1.2 Power Switching Unit . . . . .	47
4.1.3 CTE <sub>x</sub> Imaging System . . . . .	47
4.1.4 Attitude Determination System . . . . .	50
4.1.5 Telescope Assembly Control . . . . .	51
4.2 CTE <sub>x</sub> Software . . . . .	52
4.2.1 Main Software Function . . . . .	52
4.2.2 Flight Verification Test Software Function . . . . .	57
4.2.3 Slewing Control Software (Target Init) . . . . .	60
4.2.4 Camera Control Software (Camera Init) . . . . .	63
4.2.5 Prism Control Software (Encoder Init) . . . . .	66
4.2.6 Data Collection Example Sequence . . . . .	69
4.3 AFIT Ground Station . . . . .	71
V. Conclusions . . . . .	73
5.1 Overview of Designs . . . . .	73
5.2 Future Work . . . . .	75
5.3 Conclusions . . . . .	77
Appendix A. Satellite Ground Station Parts List . . . . .	79
Appendix B. Data Collection & Command Unit Component Datasheets . . . . .	82
Appendix C. CTE <sub>x</sub> Imaging System Component Datasheets . . . . .	99
Appendix D. Attitude Determination System Component Datasheets . . . . .	105
Appendix E. Telescope Assembly Component Datasheets . . . . .	110
Appendix F. Proposed AFIT Ground Station Parts List . . . . .	136
Bibliography . . . . .	138
Index . . . . .	140



## *List of Figures*

Figure		Page
2.1	Electromagnetic Spectrum [1] . . . . .	5
2.2	The Different Types of Spectra [2] . . . . .	6
2.3	Emission and Absorption Spectra of Hydrogen . . . . .	8
2.4	Comparison of Multi and Hyper spectral resolution [2] . . . . .	9
2.5	Hyperspectral Datacube. <i>Image courtesy of the NEMO project office</i> . . . .	10
2.6	HICO Image of Hong Kong. <i>Image courtesy of NASA</i> . . . . .	11
2.7	Subsystem overview of HREP [3] . . . . .	12
2.8	Instrument Interface Unit Diagram [3] . . . . .	13
2.9	Instrument Control Unit [3] . . . . .	14
2.10	Power Distribution Unit [3] . . . . .	15
2.11	TERMA Star Tracker [4] . . . . .	16
2.12	ARTEMIS Payload Processor Configuration [5] . . . . .	17
2.13	Functional Block Diagram of the G4-SBC 6U Single Board Computer [5]	18
2.14	Functional Block Diagram of the Reconfigurable Computer [6] . . . . .	19
2.15	ARTEMIS Mezzanine Cards [6] . . . . .	20
2.16	RIGEX Schedule of Events [7] . . . . .	22
2.17	USAFA Ground Station Schematic <i>Diagram Courtesy of USAFA</i> . . . . .	26
2.18	Simplified USAFA Ground Station Downlink Schematic . . . . .	27
2.19	Simplified USAFA Ground Station Uplink Schematic . . . . .	28
2.20	USNA MidSTAR Ground Station Schematic [8] . . . . .	29
3.1	AVRIS Imaging of Cuprite, Nevada <i>Image Courtesy Of NASA</i> . . . . .	32
3.2	Evolution time of a Fast Transient Event [9] . . . . .	34
3.3	Chromotomography Scenes as Time Progresses . . . . .	36
3.4	Lab Chromotomography Instrument Developed by AFIT [10] . . . . .	37
3.5	Field Chromotomography Instrument Developed by AFIT [11] . . . . .	38
3.6	Static Scene Images From O'Dell's Field Instrument [11] . . . . .	40
3.7	Series Of Unprocessed Images Taken During a 0.12 Second FTE Col- lection Test [11] . . . . .	40
3.8	Spectrum Captured by Field Instrument [11] . . . . .	41
4.1	Electrical Subsystem Overview . . . . .	43
4.2	Picture of e900 chassis . . . . .	45
4.3	Main Software Function Flowchart . . . . .	53

	Page
4.4	Flight Verification Test Function Flowchart . . . . . 58
4.5	Slewing Control Software Flowchart . . . . . 61
4.6	Camera Control Software Flowchart . . . . . 64
4.7	Prism Rotation Control Software Flow . . . . . 67
4.8	Potential AFIT Ground Station Layout . . . . . 72

## *List of Tables*

Table		Page
4.1	DCP-1201 Connections . . . . .	46
4.2	v710 External and Internal Memory Comparison . . . . .	49
4.3	Example Command Sequences . . . . .	69

# PRELIMINARY ELECTRICAL DESIGNS FOR CTEX AND AFIT SATELLITE GROUND STATION

## I. Introduction

THIS thesis details the initial concept design for the electrical and software systems of the Air Force Institute of Technology (AFIT) space-based Chromotomography Experiment (CTEx). CTEx is an engineering proof of concept experiment for a space-based high-speed chromotomographic hyperspectral imager. It will be a payload that is integrated onto the International Space Station's (ISS) Japanese Experimental Module - Exposed Facility (JEM-EF). Additionally, a ground station is needed at AFIT to interface with the National Aeronautics and Space Agency (NASA) to send commands to and download data from CTEx. This ground station will not be specific to the CTEx mission; it will also support future AFIT satellite programs.

### 1.1 *Motivation*

Air and space-borne spectral imagery has been used for years by scientists and military planners. Spatial imagery only allows the viewer to see a two dimensional visible light interpretation of the ground. With spectral imagery, data relating to the chemical makeup of different land features can be assessed and utilized for planning purposes and environmental impact studies. For military planners, the ability to easily discern friend from foe or the ability to see and reconnoiter the enemy is paramount and spectral imagery can provide this capability.

Over the years spectral imagery has been used to defeat enemy camouflage and hiding techniques to give military planners a better sense of the battlespace and the potential threat they are facing. Hyperspectral imaging, as described in this thesis, is the imaging of the spectral characteristics of light via two methods. The first is using a prism to split the light into its principle components (spectrum) by refraction. The second method uses a defraction grating to split the light into its spectrum using defraction. For more detail on spectroscopy please refer to Section 2.1 where this subject is developed

in more detail. Once the light has been split into its characteristic components, a sensor, CTE $x$  uses a charged-coupled device (CCD), is used to capture the spectrum. The more wavelengths of light a sensor can resolve the higher the resolution of the spectrum that can be obtained. This data has typically been taken from systems that were only capable of static scene reconnaissance. However, the battlespace is never truly static and new techniques to better ascertain the situation facing military planners are needed. [2]

Chromotomography is a method of spectral data acquisition that AFIT feels can provide military planners with the dynamic spectral data that is not available currently. Chromotomography, for AFIT's application, uses a spinning prism to break the incoming light from a scene into its spectrum. The CCD image of the captured scene spectrum then undergoes a mathematical reconstruction to build a pixel by pixel spectrum of the scene. This reconstruction occurs for each image captured by the imager allowing for the reconstruction of a spectral movie. A more detailed description of chromotomography can be found in Section 3.0.4. As envisioned by AFIT, high-speed chromotomography provides analysts with not only spectral data, but can also the temporal variation of the spectrum allowing for the characterization of muzzle flashes and ground explosions. Using this data analysts may be able to provide military planners with a more detailed characterization of the battlespace.

## **1.2 CTE $x$**

The CTE $x$  mission is a proof of concept experiment to demonstrate high-speed chromotomography. The main goal of the mission is to show that a chromotomographer on a space platform can ascertain the spectral characteristics of both static scenes and fast transient events. The actual system itself is composed of 3 main systems: the telescope, imager, and electrical control.

The telescope is a custom design developed by RC Optics that uses internal steerable mirrors that point the optics without slewing the entire instrument. The imaging system is composed of a high-speed camera from vision research and a motor/encoder assembly to spin a prism at high-speed to separate the incoming light. The last system is the electrical system. This system consists of a central computer and all of its periph-

erals that are needed to effectively control the entire experiment. These three systems need to work together seamlessly to allow the CTE<sub>x</sub> mission to meet its goals of accurate spectral data acquisition.

### **1.3 Purpose**

The purpose of this thesis is to provide a preliminary design concept for the CTE<sub>x</sub> electrical and software systems. Additionally, this thesis will provide a flight verification test plan to be performed during final integration and on-orbit check-out. Lastly, this thesis develops a preliminary design for the AFIT ground station to command and control CTE<sub>x</sub> and future AFIT spacecraft.

### **1.4 Scope**

This thesis is limited to initial concept designs for the CTE<sub>x</sub> electrical and software systems as well as the AFIT ground station. The electrical design is taken to the subsystem level of the computer and no internal electrical design of the Power Switching Unit (PSU) is attempted. The software section is a collection of top level flow charts showing the flow of commands and processes needed for the experiment to function properly. Lastly, the ground station is treated as a system design with needed components and cost.

### **1.5 Organization**

For all intents and purposes, this thesis attempts to document the development of the subject designs in a logical and chronological order. In general, each chapter is divided into sections that detail each of the main topics mentioned above.

Chapter II lays the foundation for the thesis. The first section covers the basic physics of light and spectral imagery needed to understand the experiment. The next section covers a couple of existing space-borne hyperspectral imagers. The Hyperspectral Imager for the Coastal Ocean (HICO) experiment is of special note because it is a spectral imager that is, as of this thesis writing, gathering data from the ISS JEM-EF. The third section talks about the Rigidized Inflatable Get-away special EXperiment (RIGEX) and

its software flow. Lastly, the fourth section describes existing ground stations that were used as jumping-off points for the AFIT ground station.

Chapter III discusses chromotomography, the basis for CTE<sub>x</sub>, and AFIT's work with chromotomography. The first details what chromotomography is and how it is different from other forms of hyperspectral imagery. The second section talks about AFIT's developments with chromotomography and briefly discusses the results of a field instrument built at AFIT.

Chapter IV gets into the design choices for the CTE<sub>x</sub> and its associated pieces. The first section walks through the electrical preliminary design with some component selections. The second section walks through logic flow diagrams for the software. Also included in this section is a discussion about the functional verification test that should be accomplished on the ground and during on orbit check out. The last section talks about the AFIT ground station and its associated components.

Chapter V lays the foundation for future work and talks about the challenges that need to be addressed in the future. Again the first section talks about the electrical design, the second discusses the software, and the last section lays out the future issues for the ground station.

## II. Background

EACH section of this research relies on many different bodies of work as foundational material. For CTE<sub>x</sub>, the main electrical designs looked at were the ISS experiment HICO and the Advanced Responsive Tactically Effective Military Imaging Spectrometer (ARTEMIS) sensor flying on TacSat-3. The software uses a foundation from the previous highly successful AFIT Shuttle Get Away Special (GAS) experiment, RIGEX, to build upon. Finally, the AFIT ground station is based upon the United States Air Force Academy’s (USAFA) ground station and the Naval Academy’s Midshipman Space Technologies Applications Research (MidSTAR) ground station. However, before any attempt at designing CTE<sub>x</sub> can be made, a basic understanding of spectral imaging needs to be developed.

### 2.1 Spectral Imaging Basics

*2.1.1 Spectroscopy.* Simply put, spectroscopy is the analysis of the light that is emitted or absorbed by substances [12]. Light is understood to have a dual nature, displaying characteristics of a particle or wave depending on the experiment being performed. For this thesis, light can be viewed as a wave of electromagnetic radiation, which is a combination of electrical and magnetic waves. Electromagnetic radiation covers a broad range of wavelengths and includes radio waves, X-rays, infrared, and ultraviolet to name a few. The full electromagnetic spectrum is shown in Fig. 2.1. As the figure

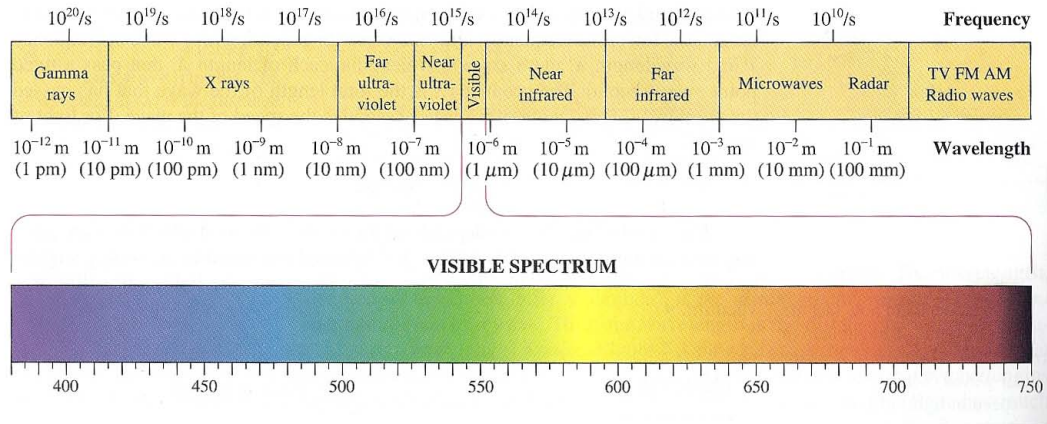


Figure 2.1: Electromagnetic Spectrum [1]



shows very little of the electromagnetic spectrum is visible light; however, it is in this region that spectroscopy is best applied and most widely used.

In order to separate visible light into its constituent wavelengths, a couple of different methods can be used. The first is a diffraction grating. As the name implies, it takes advantage of diffraction (spreading) of light when passing through or along a regular pattern of slits or grooves. The diffracted light is dispersed by the grating in differing amounts depending on its frequency. When this dispersion is viewed, the spectra of the light source can plainly be seen. The other method to separate light is with a prism. A prism uses the principle of refraction (turning) of light to separate the light. As light passes from one medium to a different medium it is turned. The amount of turning experienced by the light, similar to diffraction, depends on the frequency of light. So, as light enters the prism it is turned and then when it exits the prism it is turned again. When the exiting light is observed, a spectrum of light from the source can be seen. [2]

Using either of the methods above, two different types of spectrum can be observed. When light is emitted from a source and passes through a low density substance prior to going through a grating or prism, absorption or emission spectrum can be seen. Figure 2.2 shows a simplified depiction of this phenomenon. Looking at the diagram an absorption

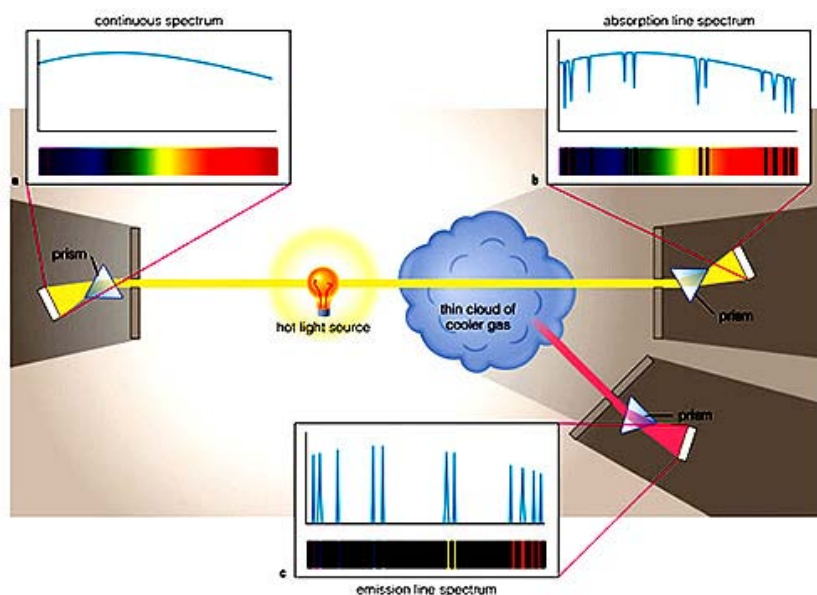
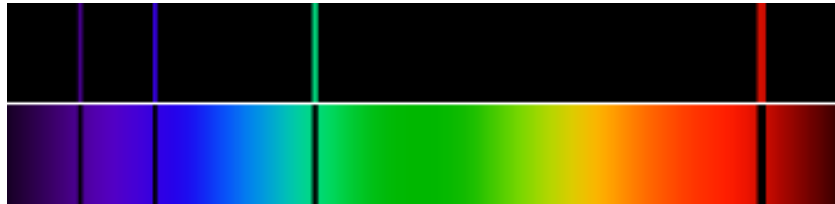


Figure 2.2: The Different Types of Spectra [2]

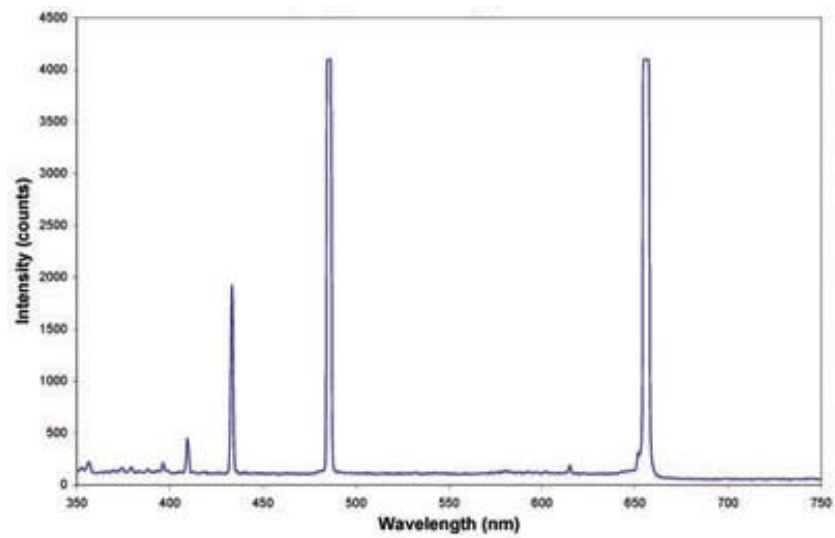
spectrum is created when you look at the source through an intermediate gas, top right image in Figure 2.2. This absorption is caused by the intermediate gas absorbing energy associated with certain wavelengths of light. An emission spectrum can be seen when you observe the intermediate gas without the the light source in our field of view, lower image in Figure 2.2. The gas cloud emits the energy that it is absorbing from the light and the resulting spectrograph shows bright lines on a dark field, the emission spectrum. Additionally, emission spectra are created when substances are burned or react to an applied electric current. Examples of these sources are gas-discharge lamps, neon signs, or putting different salt compounds into an open flame. Along with the colored diagrams shown in Figure 2.2, another way of displaying spectral data is through an intensity plot. These plots can be made from either emission or absorption data and show the relative intensity of light along the sensed spectrum. [2][12]

Every molecule utilizes the energy from different wavelengths of light as their electrons move back and forth between energy states. As the electrons move from one energy state to another, they release a photon of energy associated with the distance between the electron states. The amount of energy released within these photons is dependent on the molecule and therefore creates a unique spectral signature. This unique signature is evident whether you are looking at absorption or emission spectra, the only difference is that one is the “negative” of the other. Figure 2.3(a) shows the emission and absorption spectra of hydrogen. Figure 2.3(b) shows an emission spectrum of hydrogen, but rather than a color representation, it is an example of an intensity plot. This idea of unique signatures is the cornerstone to spectroscopy. Using a spectrometer, you can determine the chemical makeup of substances just by looking at the light that is either emitted, absorbed or reflected. [2][13]

*2.1.2 Hyperspectral Imaging.* Spectral imaging can be classified by the spectral resolutions of the imager. A sensor with a spectral resolution on the order of  $0.2 \mu\text{m}$  is considered a low-resolution spectrometer, while a sensor with a resolution on the order of  $0.01 \mu\text{m}$  is considered a high resolution spectrometer [2]. The latter is often referred to as narrow band or hyperspectral spectroscopy, while the former is multispectral. To further



(a) Hydrogen Emission and Absorption Lines [14]



(b) Hydrogen Emission Intensity Plot [15]

Figure 2.3: Emission and Absorption Spectra of Hydrogen

illustrate the difference, Figure 2.4 shows a relative comparison between the resolution capability of a multispectral imager to a hyperspectral imager. As can be seen from the

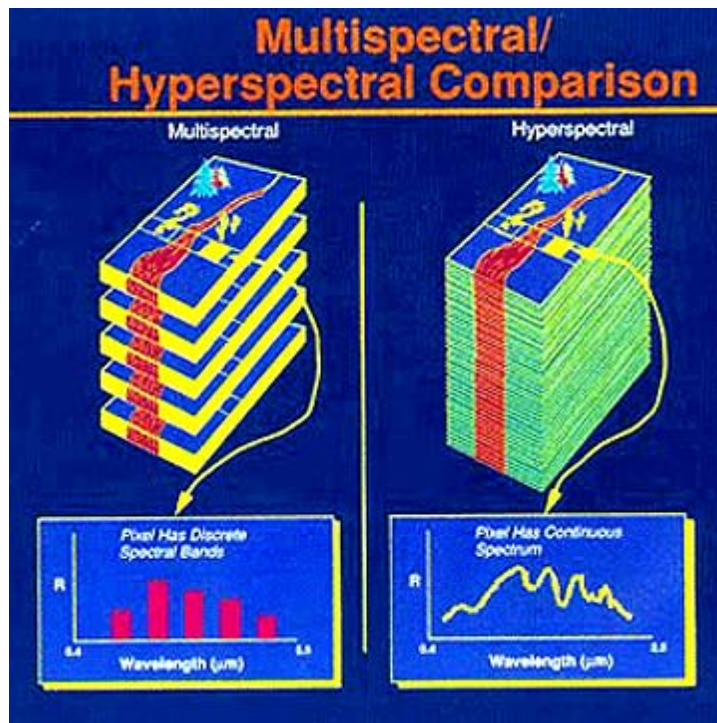


Figure 2.4: Comparison of Multi and Hyper spectral resolution [2]

plot, a hyperspectral imager allows for a relatively smooth intensity plot to be generated. Typically, a multispectral imager will, as seen in Figure 2.4, take data from a very select number bands of the spectrum. A hyperspectral imager, on the other hand, takes a virtually continuous spectrum throughout its spectral bands.

As a hyperspectral spectrometer flies over a target area it samples the target area throughout its spectral bands. Each sample is essentially an image of the target area taken in one wavelength of light. This sample is then added to other samples into a collection of data called a hyperspectral datacube. The datacube shows a complete scene of the target area and Figure 2.5 is an example of a hyperspectral data cube. The figure illustrates how each “slice” of the datacube represents the intensity of a single frequency of light. With this data, a pixel by pixel spectrum can be created and the process of determining the physical make up of that pixel can begin. Of course the drawback of the hyperspectral imager is the huge amount of data it can produce. Every

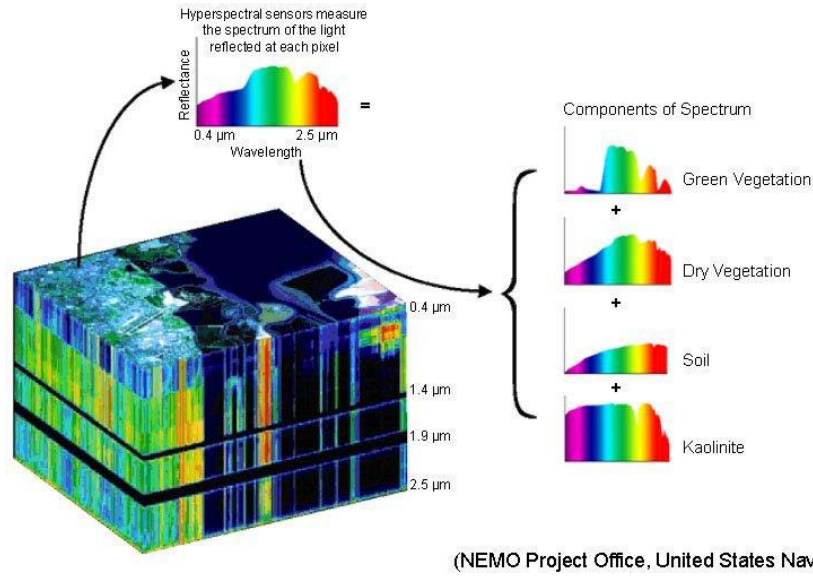


Figure 2.5: Hyperspectral Datacube. *Image courtesy of the NEMO project office*

frequency of light has its own image of relative intensity associated with it. When a hyperspectral imager develops the data cube the sheer number of images taken produces large data files.

## 2.2 Hyperspectral Imagers

**2.2.1 HICO.** The Naval Research Laboratory's (NRL) HICO experiment is currently flying on the ISS as a part of the larger HICO/RAIDS Experiment Payload (HREP). It was launched by the Japanese Aerospace Exploration Agency (JAXA) aboard the first flight of the H-II Transfer Vehicle (HTV) on 10 Sep 2009. The HREP was integrated on the JEM-EF in the Exposed Facility Unit 6 (EFU6) position [16]. The purpose of HICO is to rapidly develop and field a low cost very near infrared hyperspectral imager to characterize maritime coastal environments. As an example of a portion of HICO's capability, Figure 2.6 shows an image of Hong Kong taken by HICO on 25 Sep 2009. The FOV for this picture is 43 km wide by 109 km long [17], as a comparison the field of view as designed for CTEx is an estimated 700m [18].

The computer and control system of HREP was developed and manufactured by Silver Engineering and detailed in an unpublished presentation [3]. The main computer and control system for HREP is called the Payload Controller Unit (PCU) and is the



Figure 2.6: HICO Image of Hong Kong. *Image courtesy of NASA*

interface between the ISS and the HICO/RAIDS sensor suite. The HREP program was considered to be a Class D program. Due to this designation, the Electrical, Electronic, and Electromechanical (EEE) parts were able to be off the shelf components and did not have to be the more screened space rated parts. This allows the HREP computer system to use Commercial Off The Shelf (COTS) parts, greatly reducing schedule and monetary cost to the program.

The PCU was designed to function in several different modes of operation. The first being a survival mode where the 120V operational power is not applied, and all PCU and instrument functions are off except for the survival power subsystem. The second mode is a standby mode where full operational power is applied to the PCU; however, the HICO and RAIDS experiments are not powered. The last mode is an acquisition mode where all of the systems are powered up and fully functional.

The PCU is made up of several subsystems that control different aspects of HREP. Figure 2.7 shows the subsystems of the PCU, the instruments, and the electrical interfaces of HREP. Also, the figure shows how all of the subsystems are interconnected and the connections to the ISS. As can be seen the JEM-EF provides the HREP with 120V of DC power along with a 1553 connection and an ethernet connection. These connections will be the same connections that CTEx will take advantage of during on-orbit operations. Also the layout shows that subsystems are separated by function into the following, which are discussed in detail later in this section;

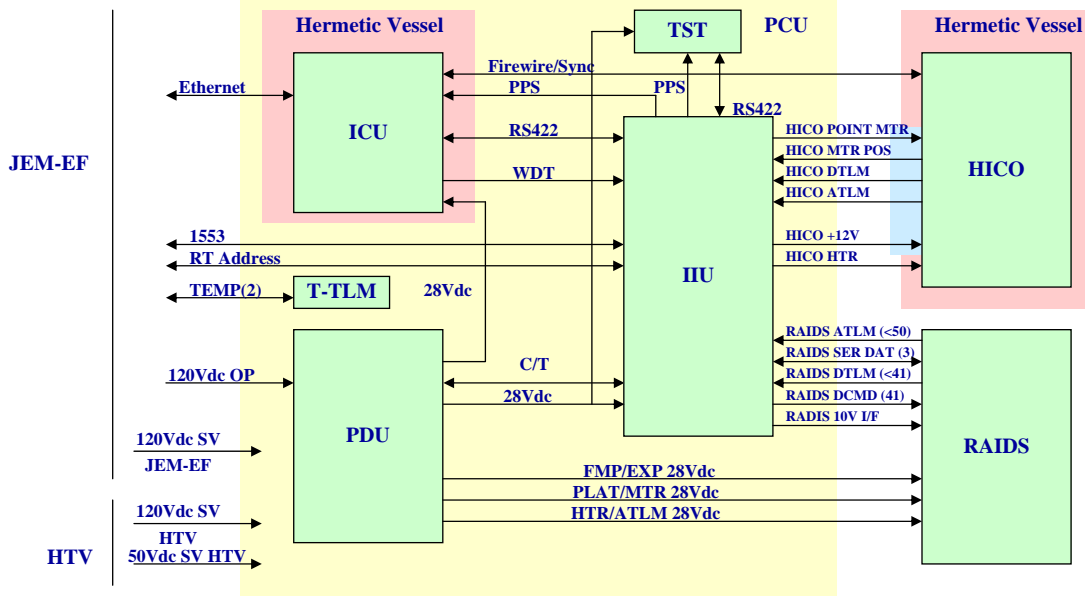


Figure 2.7: Subsystem overview of HREP [3]

- Instrument Interface Unit (IIU)
- Instrument Computer Unit (ICU)
- Power Distribution Unit (PDU)
- TERMA Star Tracker Unit (TST)

When power is applied to HREP the IIU and the star tracker are powered up. The IIU controls power to the ICU and RAIDS using discrete control signals to the PDU. The IIU directly controls power to the HICO instrument and its stepper motor. The 1553 bus is used to transmit the ISS timing, attitude, and position signals along with ancillary data to the IIU for distribution to the ICU and the TST. The ICU uses the data from the IIU for time stamping of images while the TST uses the data to correlate attitude. There is also an RS-422 connection between the ICU and IIU to relay information regarding the HICO instrument commands and telemetry sensed by the IIU.

*2.2.1.1 Instrument Interface Unit.* The IIU is a custom module design that is rated for space applications and is Single Event Upset/Single Event Latchup (SEU/SEL) tolerant. The main function of the IIU is to provide command and control



for the payload. Figure 2.8 shows a basic block diagram of the functions of the IIU. The IIU is based upon an Actel 8051 microcontroller in an Field Programmable Gate Array (FPGA) architecture. The diagram shows that the HICO motor encoder is connected to the onboard A/D converters and the motor driver is housed within the IIU.

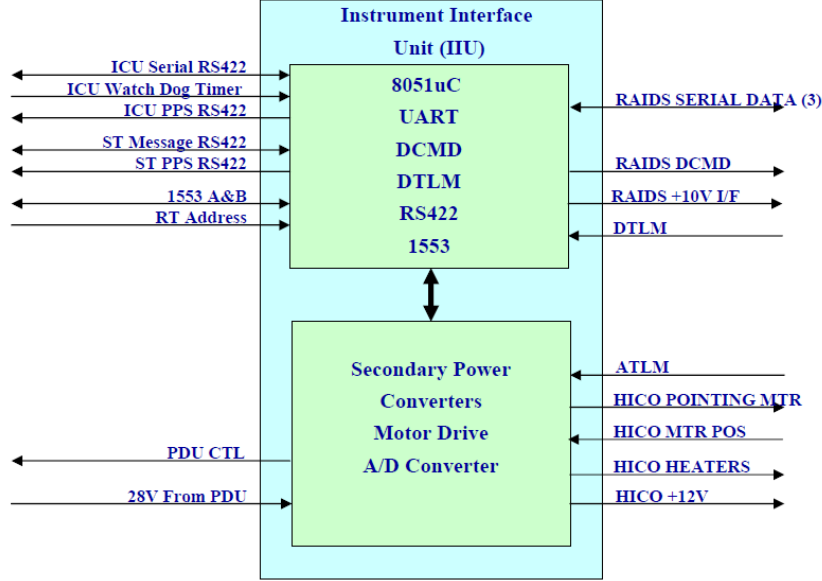


Figure 2.8: Instrument Interface Unit Diagram [3]

*2.2.1.2 Instrument Computer Unit.* The ICU is a COTS PC104+ stack. Figure 2.9 shows its functional block diagram. The ICU is the main data collection system for the HREP payload. HICO interfaces directly with ICU to save instrument data and to make use of the camera control interface. The stack has a Windows-based operating system in order to interface with the camera software and control of the camera. The ICU is connected to the ISS via an ethernet connection that is used to transfer data from the ICU to the ISS for downlink. Utilizing the RS-422 connection the IIU monitors the performance of the ICU and has the ability to power cycle the ICU to mitigate SEU/SEFI. The PC 104+ stack has the SEU/SEL performance that is comparable to an ISS laptop and as of the writing of this thesis, has not had a detected SEU. Because of the prolific COTS use, the ICU is contained within a pressurized hermetically sealed box with an internal fan to circulate air and allow for convection cooling of the stack.



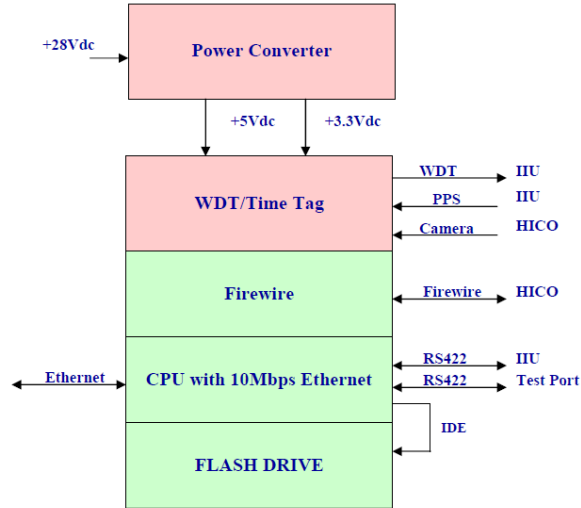


Figure 2.9: Instrument Control Unit [3]

*2.2.1.3 Power Distribution Unit.* The PDU takes the JEM-EF 120Vdc operational power and conditions the power to the 28Vdc level for distribution to the many electronics boxes within HREP. Figure 2.10 shows the functional block diagram of the PDU. As the diagram shows, conditioned 120Vdc is supplied to the individual power conditioners for voltage step down before being sent to the electronics. There is, however, an additional PDU control signal that comes from the IIU to switch power to the different HREP electronics. The only exception to the switched power is the IIU, the TST, and 3 RAIDS telemetry points. These are always powered on when the ISS operational power is applied.

*2.2.1.4 TERMA Star Tracker.* The TST is a commercially available star tracker from TERMA that has flown on MiTEx and TacSat-1. Figure 2.11 shows a picture of the TERMA star tracker and its associated control box. The addition of a star tracker allows the system to have precise knowledge of its attitude and facilitates accurate pointing of the instrument. The ISS provides attitude data through the 1553 connection; however, the station trusses flex and the station data may not be accurate enough of precise pointing of instruments on the JEM-EF. The TST has an accuracy of  $<1$  arcsec RMS in pitch and yaw and a  $<5$  arcsec in roll [4]. According to the TERMA brochure the components are screened per military standards and a full space class part

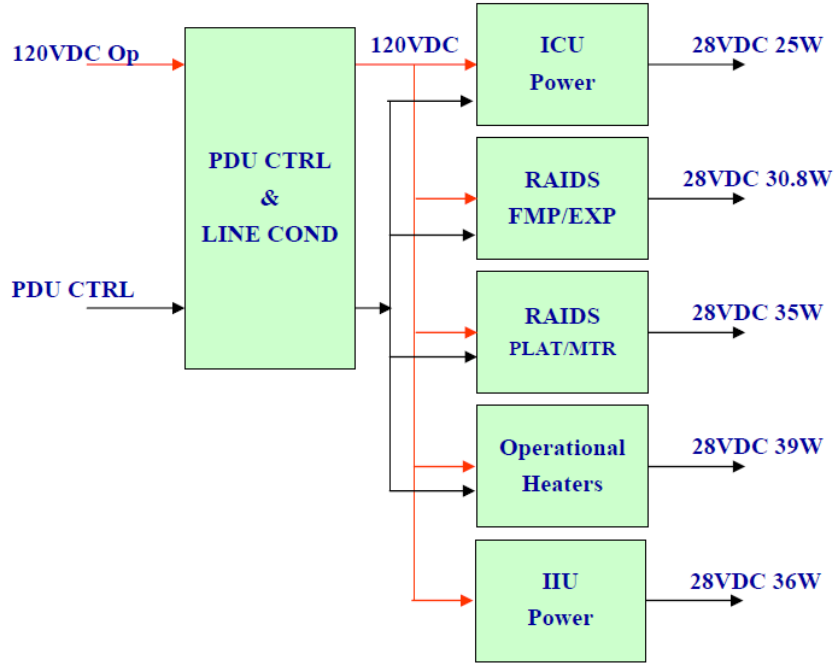


Figure 2.10: Power Distribution Unit [3]

selection is available if desired. The parts also meet an EEE hardening level of 100 kRad. The interface to the tracker is via a standard RS-422 connection to the IIU.

*2.2.2 ARTEMIS.* The ARTEMIS sensor on board the TacSat-3 is in response to a desire by the Air Force Research Lab Responsive Space Initiatives to develop inexpensive but high quality sensors to integrate onto small satellites with a “plug and play capability”. This integration technique will in theory allow satellites to be built similar to a personal computer where peripheral instruments can be added to enhance capability. It is the focus of the initiative to develop and deploy space technologies to support military operations while containing costs and producing tactically relevant data products. [5]. TacSat-3 was successfully launched on an Orbital Sciences Minotaur 1 from Wallops Island on 19 May 2009.

The design and fabrication of the electrical system for the ARTEMIS sensor was performed by SEAKR Engineering and published in the paper “Achieving Multipurpose Space Imaging with the ARTEMIS Reconfigurable Payload Processor” at the Aerospace Conference in March 2008 [5]. SEAKR Engineering produces commercially available



Figure 2.11: TERMA Star Tracker [4]

ruggedized computer components for military and space applications. The central computer architecture for the payload is called the ARTEMIS Payload Processor. The Payload processor is built upon an independent processing architecture by utilizing FPGAs coupled with a central Power PC-based general-purpose processor. Some of the key system objectives for the ARTEMIS Payload Processor are: on-orbit reconfigurability, incorporation of open standards, and Single Event Effects(SEE) and Total Ionization Dose (TID) tolerance. Figure 2.12 shows a breakdown of the ARTEMIS processor system architecture with its key components. As shown in the diagram there are four main components to the ARTEMIS payload processor;

- G4-Single Board Computer (G4-SBC)
- Responsive Avionics ReConfigurable Computer (RA-RCC)
- Power Supply
- Universal Power Switch (UPS)

All of the cards in the payload processor conform to the cPCI formfactor and are either a 3U (100mm x 160mm) or 6U (160mm x 233mm) size card [19]. cPCI is a standard computer system that is used for embedded and industrial applications. As a part of this form factor, there is a built-in back plane connection that can be customized. In

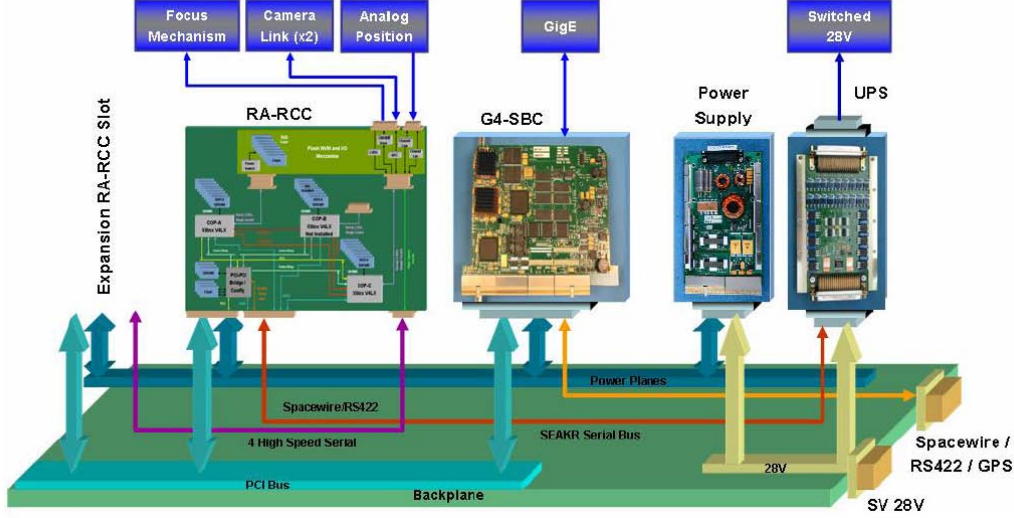


Figure 2.12: ARTEMIS Payload Processor Configuration [5]

the case of ARTEMIS, as Figure 2.12 shows, the 28V spacecraft power supply is on a different plane than the instrument power plane. There is also a spacewire/RS-422 bus, a high-speed serial bus, and the basic PCI Bus allowing the cards to communicate with each other via different methods.

*2.2.2.1 G4-Single Board Computer.* The G4-SBC is a COTS 6U cPCI Power-PC based single board computer. Figure 2.13 shows a block diagram of the G4-SBC and the interfaces used on ARTEMIS. The G4-SBC manages external interfaces to TacSat-3's up/down links, controls the system configuration and orchestrates the data processing. As Figure 2.13 shows, the G4-SBC has connections for the cPCI plane, Spacewire/RS-422 connections, and a Gigabit Ethernet connection. Additionally there is a support FPGA that provides Error Detection And Correction (EDAC) protected interfaces to the mainboard memory.

*2.2.2.2 Responsive Avionics ReConfigurable Computer.* The RA-RCC is a COTS 6U cPCI ReConfigurable Computer. The RA-RCC is reconfigurable because of its use of programmable FPGAs and mezzanine expansion cards for sensor interfaces. This combination allows for the mezzanine cards to be changed and the associated FPGAs then reprogrammed to take full advantage of the new capability. Additionally, the

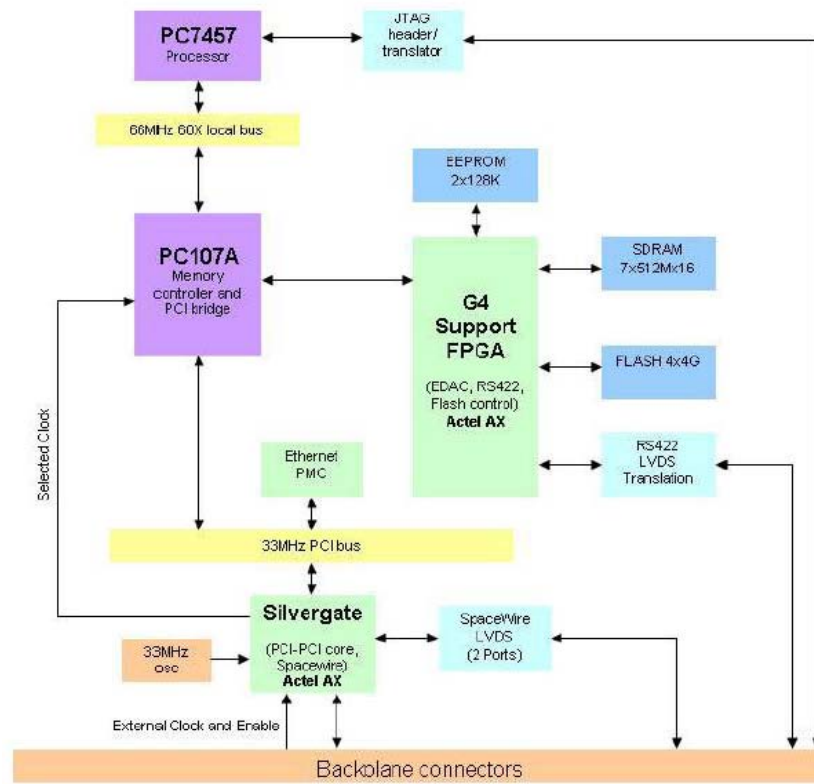


Figure 2.13: Functional Block Diagram of the G4-SBC 6U Single Board Computer [5]

FPGAs can be flashed with a new program if the instrument connected to the mezzanine card is changed. With these capabilities the RA-RCC is a very versatile and powerful card. Figure 2.14 shows a functional block diagram of the RA-RCC used on ARTEMIS. The RCC's main function is to control sensor functionality, perform on-board data pro-

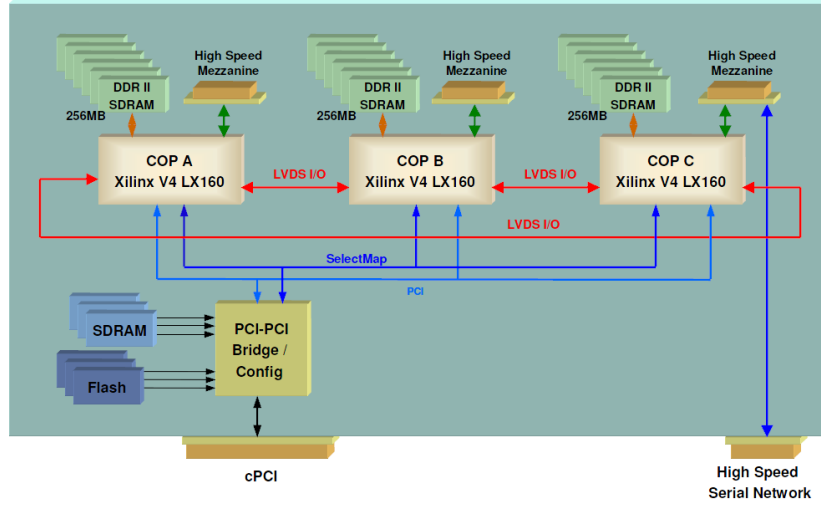


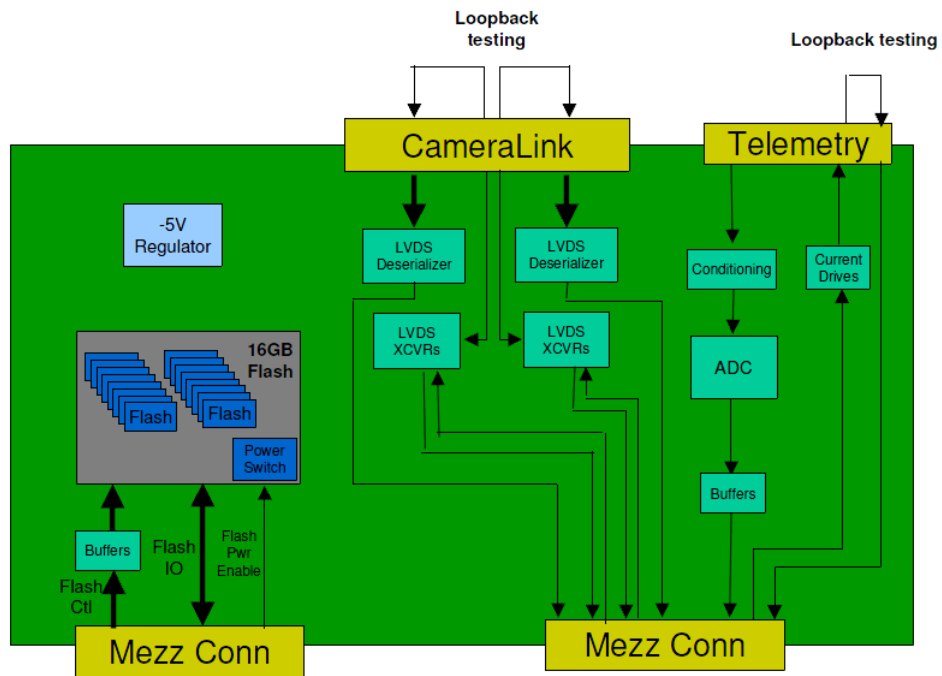
Figure 2.14: Functional Block Diagram of the Reconfigurable Computer [6]

cessing, and control the power switching of the sensors and nonvolatile mass storage. The RA-RCC utilizes four FPGAs. One Actel RTAX2000 provides a rad hardened PCI to PCI bridge between the cPCI bus and the local board PCI bus. The Actel FPGA also handles configuration management by accessing a triple redundant bank of SDRAM to scrub the COPs as needed. Additionally the Actel also interfaces with the UPS and controls the power state of the payload sensors.

The other three FPGAs are Xilinx Virtex-4 LX160 coprocessors (COPs). The COPs interface with the mezzanine cards and control access to a 256MB bank of EDAC protected RAM. The Mezzanine cards offer a flexible interface to payload sensors. Each mezzanine card can be tailored to the specific application and connections needed by the system. Figure 15(a) shows a camera and telemetry interface mezzanine card used on ARTEMIS. The mezzanine cards used on ARTEMIS have camera link connections for high-speed image capturing and an analog control and telemetry connection. An additional mezzanine card houses the 16GB flash drive. Figure 15(b) shows the mezzanine card configurations used on ARTEMIS and diagrams their connections.



(a) ARTEMIS Mezzanine Card



(b) Functional Diagram of ARTEMIS Mezzanines

Figure 2.15: ARTEMIS Mezzanine Cards [6]

*2.2.2.3 Power Supply & Universal Power Switch.* The power supply simply takes the 28V power from the TacSat-3 power bus and conditions it for the +3.3V, +5V, +15V, and -15V power planes. The UPS uses the same 28V and applies power to the redundant power planes and individual payload sensor components using internal switches. Power switching commands are sent from the G4-SBC to the RA-RCC via the cPCI bus. The RA-RCC then relays the commands to the UPS via a high-speed serial bus.

## **2.3 CTE<sub>x</sub> Software Foundation**

*2.3.1 RIGEX.* RIGEX was a highly successful AFIT experiment launched in March 2007 on the STS-123 mission. RIGEX was initially a part of NASA’s Get Away Special (GAS) program but eventually transitioned to a Cannister for All Payload Ejections (CAPE) experiment. RIGEX’s main goal was to test the inflation characteristics of carbon fiber rigidized tubes. Initially the tubes were not inflated and folded down in a compact stowed position. When power was applied to the experiment a heating element was turned on to soften the carbon and allowed for the inflation of the tube. After a full inflation height of 20 inches was achieved, the heating elements were turned off and the carbon began to cool down and rigidize in the fully extended position. The computer system of RIGEX was a PC104 stack using commercial off the shelf components.

Figure 2.16 shows the software process flow for the RIGEX experiment developed by the Master’s student David Moody [7]. Looking at the figure you can see that the process is very straightforward and logical. It is the intention of this thesis to develop a similar straightforward logical flow for the CTE<sub>x</sub> experiment. It is important to note that the RIGEX software had fail-safe points so that it could be shutdown in the event of an emergency. These fail-safe points allowed the RIGEX experiment to return to the last successful command sequence executed once power was restored.

*2.3.1.1 Initialization.* The initialization process for the RIGEX software begins with the aptly named “Begin” step and ends with the fail-safe check. The begin step occurs during launch. Once an altitude of 50,000 ft is reached, a barometric switch is



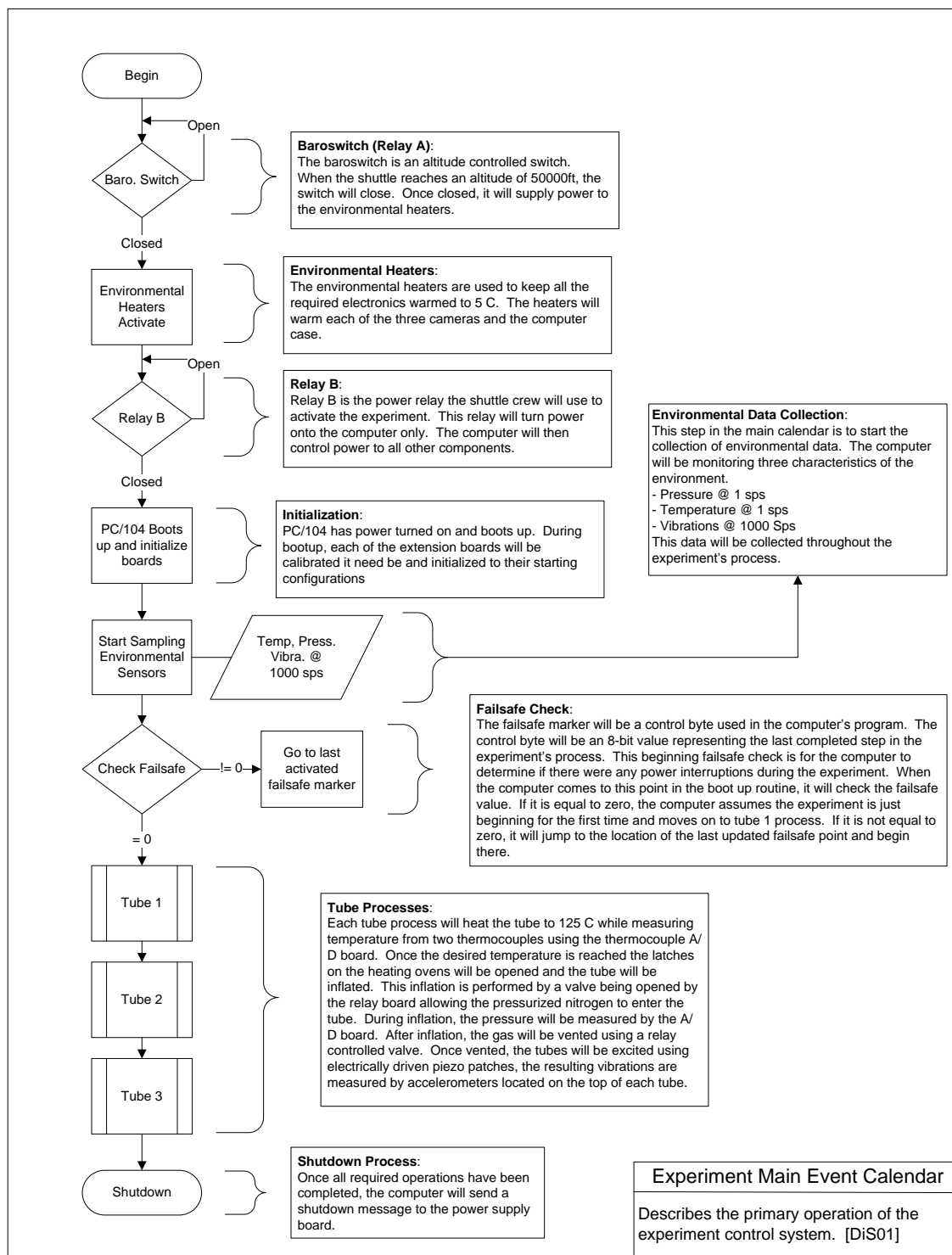


Figure 2.16: RIGEX Schedule of Events [7]

activated and turns on RIGEX's environmental heaters. This altitude switch is standard on all GAS experiments. The heaters are controlled by a temperature sensor and are set to keep the electronics of RIGEX at 5°C. Once the altitude switch is turned on, RIGEX is in a stand by mode until the switch internal to the shuttle is activated.

When the internal switch is activated, power is applied to the PC104 buses and they begin the boot up process. During the boot up process the PC104 application boards are calibrated, control registers for the A/D boards are set, and variables are created for future processing. Once the boot up process completes, RIGEX begins environmental sampling. This data is stored for use during post processing to help separate the shuttle steady state vibration environment from the vibration induced by tube inflation. Finally the fail-safe check is performed to check the progress of the experiment. If the check returns a 0 value, then the experiment begins as planned. If the check returns something other than 0, the computer determines where the experiment stopped and returns to that step for test completion.

*2.3.1.2 Tube Inflation.* Each tube goes through the same inflation process separately and is listed here;

- Mark fail-safe Point
- Activate Thermocouple A/D ports
- Activate Heater and Lights
- Test Temperature vs. Threshold Temperature of  $\geq 125^{\circ}\text{C}$
- Start Inflation Timer
- Activate A/D Board Channels
- Begin Triggering Camera
- Open Heater Box and Inflation Valve
- Wait For Inflation Timer Time-Out
- Open Vent Valve
- Halt Data Collection

- Mark fail-safe Point

*2.3.1.3 Excitation.* The RIGEX experiment was designed to not only test the inflation of rigidized tubes in space, but to also determine the vibration transformation function associated with a space inflatable tube. Again each tube undergoes the same process independently and the steps are listed here;

- Trigger Camera For a Single Frame Picture
- Mark fail-safe Point
- Activate A/D Channels for Vibration
- Transmit Excitation Waveform for 25 secs
- Halt Vibration Data Collection
- Mark fail-safe Point
- Trigger Camera For a Single Frame Picture
- Mark fail-safe Point

Once the excitation process is complete for each tube, the shutdown process begins. The environmental data collected is saved to storage and then a command is sent to a relay that effectively disconnects the power supply.

## **2.4 AFIT Ground Station Foundation**

*2.4.1 United States Air Force Academy.* The USAFA has recently built a robust student satellite program, FalconSAT. The FalconSAT program allows cadets to design and fabricate a satellite and then operate the satellite after launch. The first FalconSAT, Falcon Gold, was launched in 25 Oct 1997. Falcon Gold was hard mounted to a centaur upper stage and showed that GPS navigation was possible outside the orbit of the GPS constellation. The most recent, FalconSAT-3, was launched as a part of the STP-1 mission on 9 Mar 2007. FalconSAT-3 is a three axis stabilized spacecraft and carries three experiments [20]. Over the years the academy has built a ground station to allow the cadets to interact with and track the FalconSAT program satellites. The

FalconSAT program typically uses amateur radio frequencies for its uplink and downlink. FalconSAT-3 uses a Very High Frequency (VHF) uplink and a Ultra High Frequency (UHF) downlink while the yet to be launched FalconSAT-5 uses a UHF uplink and a S-band downlink. This frequency scheme is opposite from common practices. Usually, the downlink frequency is less than the uplink frequency because of power requirements. It is easier and more efficient to produce the higher power needed for higher frequency on the ground than trying to produce the same power on the resource limited satellite [21].

The current ground station at the academy is the main basis for the design at AFIT. Figure 2.17 shows the current setup at the academy and Appendix A has a detailed list of components. The USAFA ground station consists of separate uplink and downlink antenna systems. The downlink data is received by a S-band dish or Yagi, while the uplink data is routed through two Yagi antennas. To track the satellite during a pass, a tracking computer is connected directly to the downlink dish M2 rotator controller and to the south Yagi antenna mast.

*2.4.1.1 Downlink.* The left side of Figure 2.17 details most of the downlink setup for the USAFA ground station which is simplified in Figure 2.18. The data is received via the S-band dish and VHF and UHF antennas. The signals are then routed to a lightning arrestor system before passing to the ICOM 910 receiver. The receiver passes the data to the SYMEK TNC series modems. After the modems, the data is sent to a “A” and “B” rack selector for distribution. Once either the “A” or “B” rack has been selected, the data is sent to a 3-way command switch for distribution to separate Telemetry, Command, and SOE computers for analysis by the cadets.

*2.4.1.2 Uplink.* The right side of Figure 2.17 details the uplink setup with a simplified diagram in Figure 2.19. The command, telemetry, and SOE computers send data to be uploaded back to the 3-way command switch. The switch then relays the data to the SYMEK TNC series modems. The modems then route the signals to a modulator for uplink signal conditioning. These signals are then routed to the ICOM 910 transceiver. The ICOM sends the data through linear amplifiers before being sent

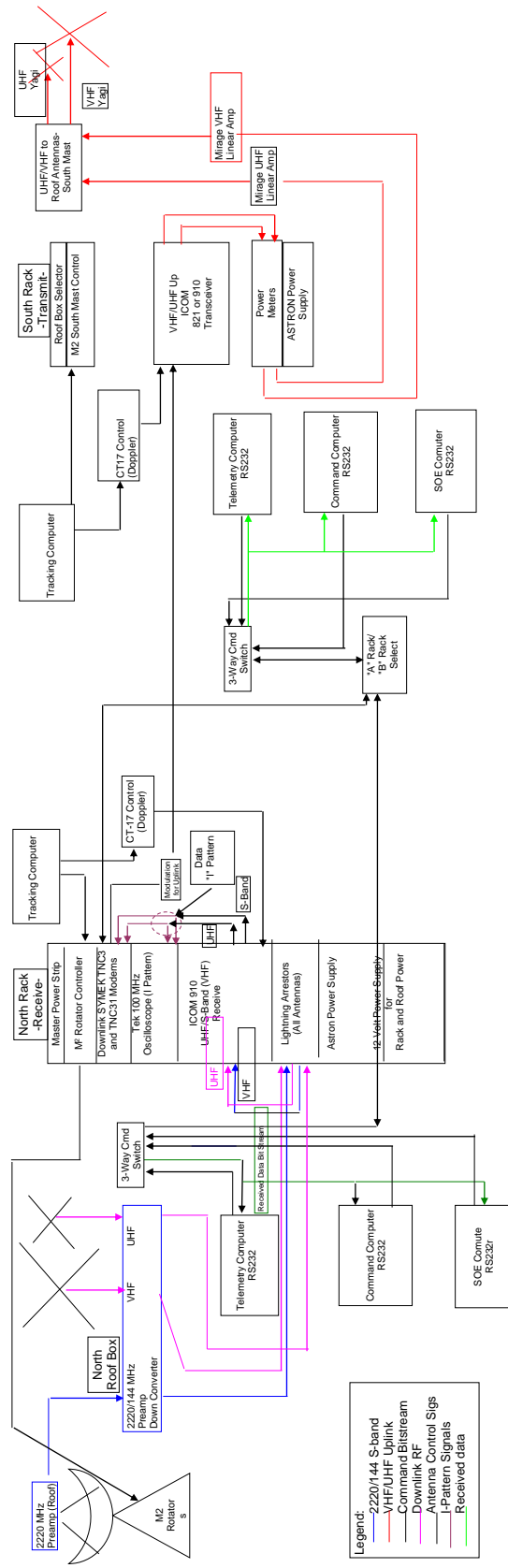
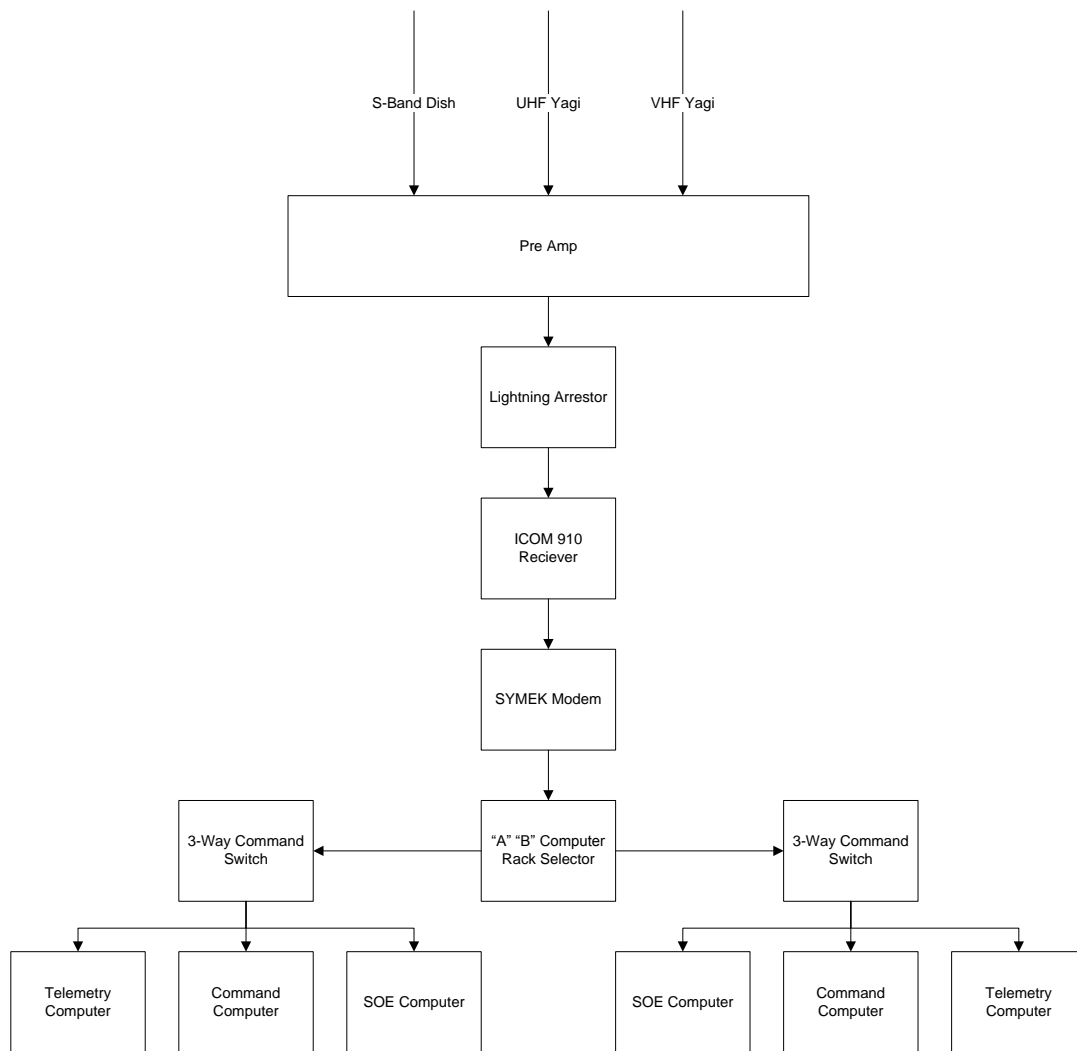


Figure 2.17: USAFA Ground Station Schematic Diagram Courtesy of USAFA



USAFA Ground Station Simplified Downlink

Figure 2.18: Simplified USAFA Ground Station Downlink Schematic

to the Yagi antennas mounted on the roof for transmission. If an antenna is used for a frequency range that is outside of its tuned range, its efficiency is reduced. The farther from the tuned range it is used the more the efficiency is reduced until the antenna ceases to function. For this reason the ground station uses two Yagi antennas that allow the use of multiple frequency ranges.

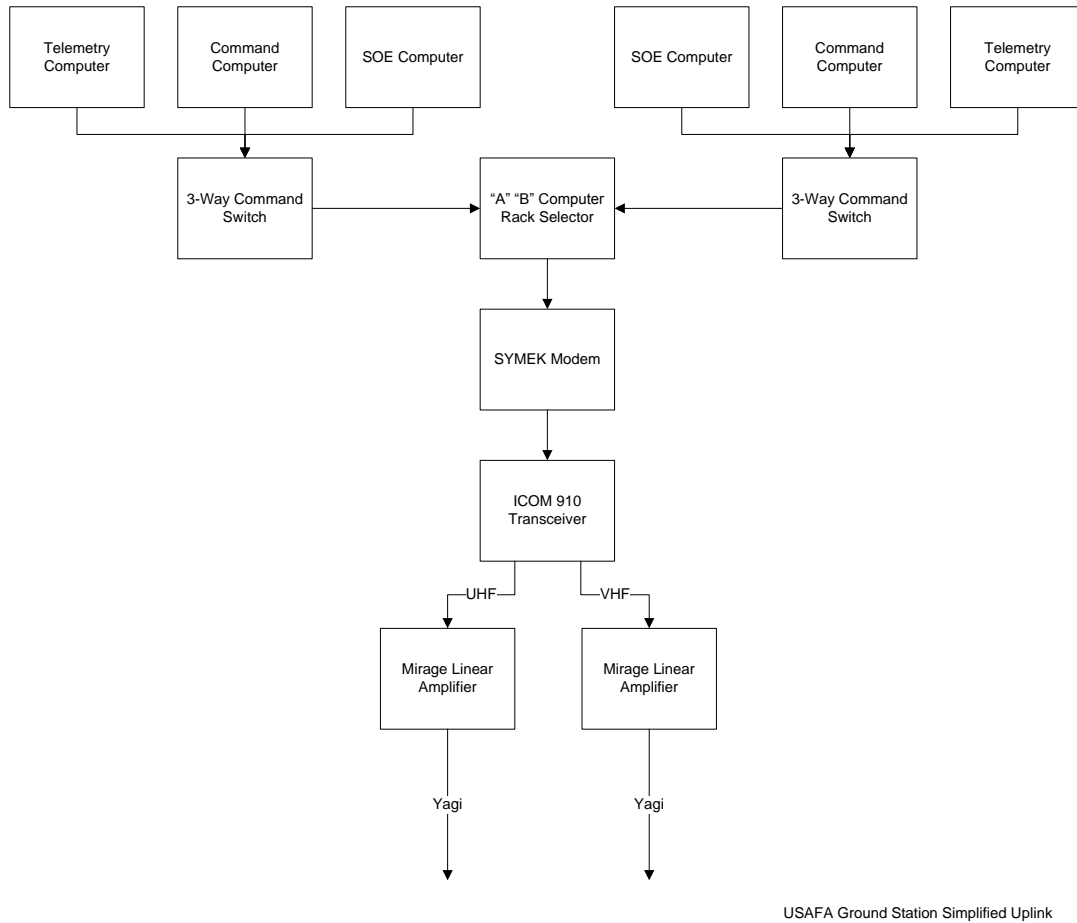


Figure 2.19: Simplified USAFA Ground Station Uplink Schematic

*2.4.2 United States Naval Academy.* Recently, the USNA launched their first general-purpose satellite bus experiment satellite, similar to FalconSAT, as a part of the STP-1 mission on 9 March 2007. MidSTAR-1 carried four experimental payloads for users from the USNA, NASA, and the Naval Post Graduate School (NPS) [8]. For command and data communications, MidSTAR-1 operates both the uplink and downlink

in the S-Band frequencies. Figure 2.20 shows a basic block diagram of the ground station for MidSTAR-1, a list of components for the ground station can be found in Appendix A.

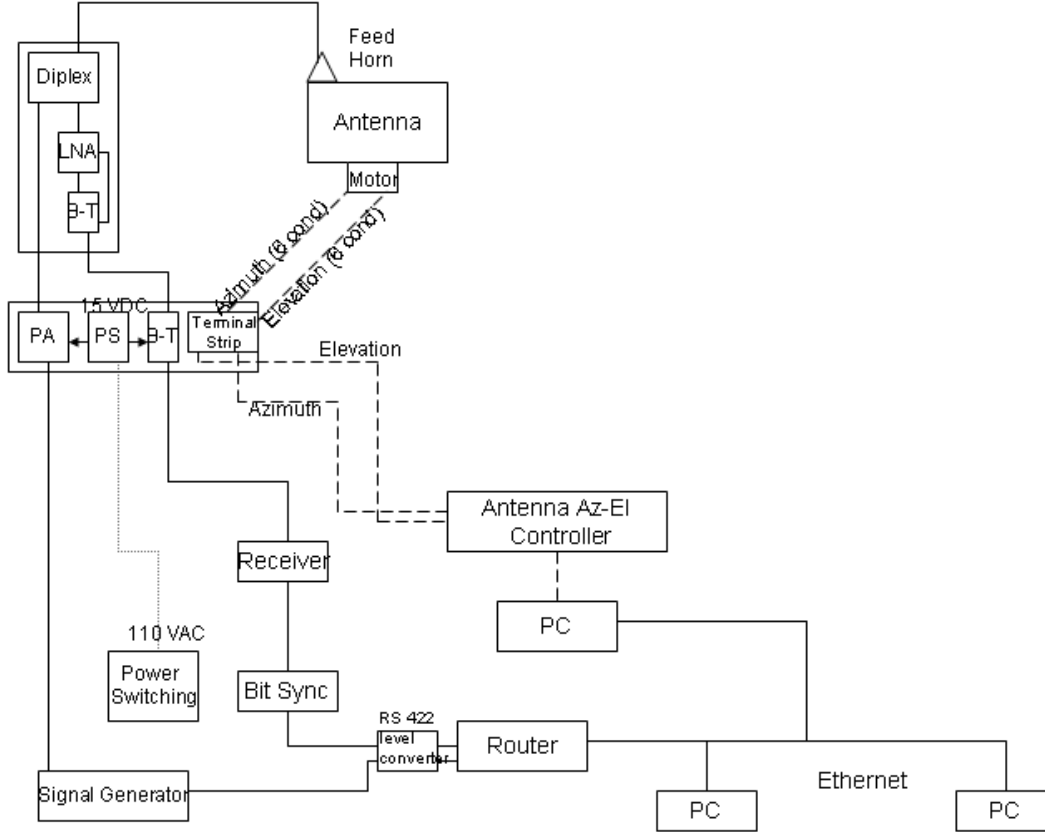


Figure 2.20: USNA MidSTAR Ground Station Schematic [8]

The USNA's ground station is more simplified than the USAFA station. The most noticeable simplification is the single dish used for both up and downlink. This simplification leads to the obvious need for only one motor and controller and less potential for failure; however, if a failure does occur than the failure is catastrophic in nature. Similar to the USAFA ground station, a tracking computer is connected directly to the antenna motor controller for azimuth and elevation tracking of satellites.

*2.4.2.1 Downlink.* The antenna receives the 2.22 GHz signal from the tracked MidSTAR-1 satellite and pass the signal to a diplexer. The diplexer routes the signal at the uplink frequency from the antenna to the receiver leg of the system and



likewise routes the signal at the downlink frequency from the transmitter leg to the antenna. From the diplexer the modulated downlink signal passes through a Low Noise Amplifier (LNA) and two Bias Tees to reduce noise and strip away everything from the signal except for the desired 2.22 GHz. Once the signal conditioners strip away the unwanted portion of the signal it progresses to the receiver. The receiver demodulates the data and passes the digital data stream to a bit synchronizer. The bit synchronizer checks the incoming data stream for a predetermined digital preamble in order to packetize each frame of data and create a serial data stream for distribution. The bit synchronizer then funnels the serialized data to a standard blade router for distribution to networked PCs.

*2.4.2.2 Uplink.* The networked computers first send data streams over the network to the signal generator. The signal generator, then takes the data streams and modulates them onto the 1.767 GHz uplink carrier frequency. From the signal generator the information is sent to a signal amplifier. The signal amplifier boosts the signal and sends it to the diplexer. The diplexer sends the signal to the antenna for transmission.

## **2.5 CTEX Application**

*2.5.1 Electrical.* The HICO system is a great system to help lay the foundation for the CTEX electrical systems. As was discussed earlier both systems will be flown on the same experimental platform so interfaces will be identical. The CTEX system will take advantage of the 120V DC power from the JEM-EF as well as the 1553 communications port and the ethernet data connection similar to HICO. Also, HICO's division of subsystems is very logical and simple. The CTEX design will try and take advantage of this design feature to develop a logical subsystem architecture.

The CTEX design also uses some of the design features of ARTEMIS as design cues. The ARTEMIS payload processor uses the industry standard cPCI form factor as the basis for its computer design. Use of the cPCI form factor facilitates the use of readily available COTS hardware. The use of COTS hardware allows for CTEX's computer system to be rapidly developed and the cost of the system to be relatively low. Also, the use of a SBC as the experiment controller will be used by the CTEX space experiment.

*2.5.2 Software.* The RIGEX software is a straight forward and logical design. Granted the self starting and autonomous nature of RIGEX does not apply to CTE<sub>x</sub>, the software will try and emulate the logical flow of RIGEX's software. CTE<sub>x</sub> will attempt to do this by using function calls from the main software function to group commands that have a similar function.

*2.5.3 Ground Station.* The ground station at USAFA will be the main driver for AFIT's ground station. One of the initial goals for the AFIT ground station is to communicate with FalconSAT 3. To do this AFIT will need to use similar, if not identical equipment, to that used at USAFA. However, the USAFA ground station appears to be overly complicated for AFIT's need. Therefore the very simple design used at USNA will also be taken into account during the design phase of the AFIT ground station.

### III. CTE<sub>x</sub> Overview

**H**YPERSPECTRAL imaging is a valuable tool for military and civilian planners alike. A visible light picture can only convey spatial characteristics of a target scene and can provide basic information to plan activities. In many instances more information about the chemical make up of the scene would greatly affect the plans made by the interested parties. A good example is a group of pictures of hyperspectral data from Cuprite Nevada showing different iron bearing substances. Figure 3.1 shows a false color picture of the area on the left and then images from different portions of the spectrum showing the mineral data. As you can see, very little information can be discerned

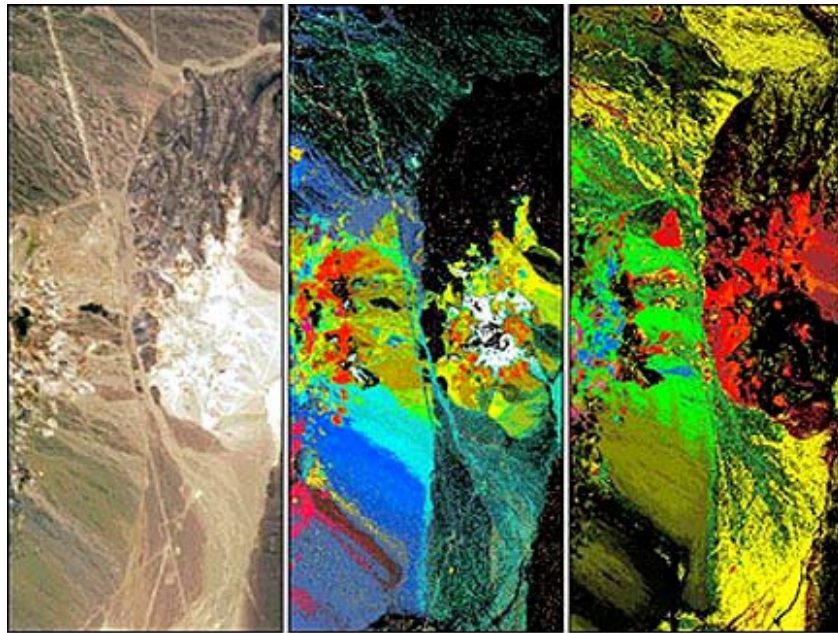


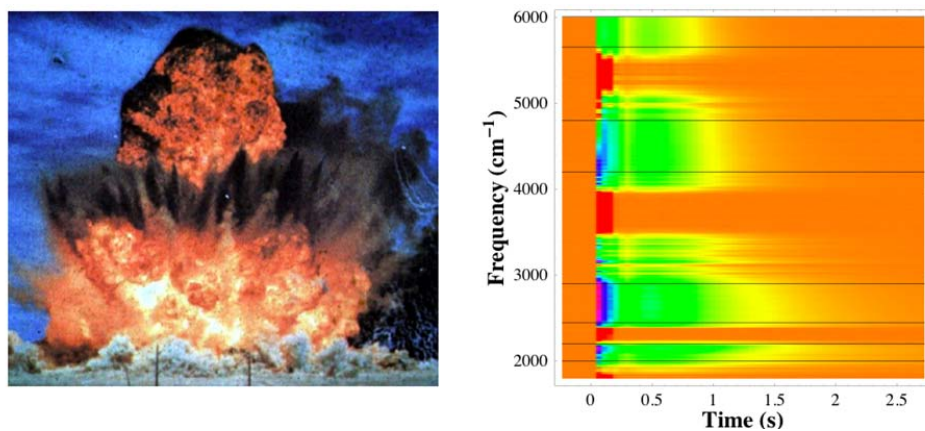
Figure 3.1: AVRIS Imaging of Cuprite, Nevada *Image Courtesy Of NASA*

looking at the false color image. The basic layout of the area and some assumptions about the terrain can be made. However, the middle image is an image created from AVRIS data in the 2,000-2,500 nm range. This range is known to contain peak emissions for some silicates, carbonates, and sulphates [2]. Looking at the data, the sensor is able to distinguish between differing types of material and each color is associated with a different type of material. Similarly, the image on the far right is created from AVRIS data in the 400-1,200 nm range. This band is known to contain peaks for Hematites, Geothites and other iron bearing minerals [2]. Looking at this data and being able

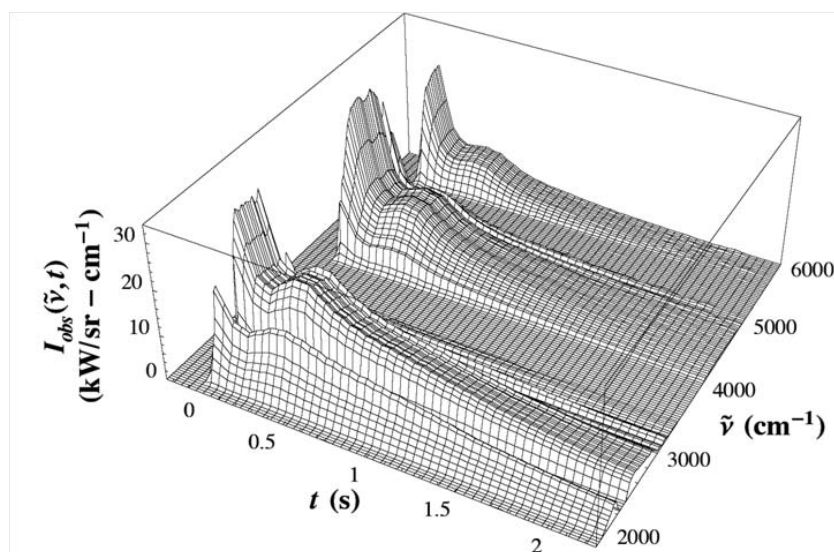
to determine the mineral types is extremely valuable to planners looking to develop potential mines in the area. Typically developers would need to send survey teams to the area covering the area by foot to map out the chemical composition of the area at a large expense of time and manpower. Using this data, the size and time needed to survey the area can be greatly decreased. Some surveys would still need to be done to verify the hyperspectral data; however, this verification would take less time and manpower to perform. Once verification is made, the interested parties can move out with their development plans quicker than they could without this data.

For the military planner, hyperspectral images are an invaluable tool to plan operations and assess impacts of current operations. Many important factors about troop movement and operations, industrial base spin up, and hidden assets can be discovered. The information from a spectral imager can tell you what industries are up and running and how they are being utilized, and potentially whether there is a massive around the clock operation or a normal level of operation. Hidden objects are very important in military applications. If you can detect your enemies use of deception techniques to hide troop strength and resources, you gain the advantage of surprise by seeing through the deception techniques of the enemy. Likewise, if you have an understanding of these techniques, you can be more effective in camouflaging your own assets and troop strength. Rudimentary camouflage material will help hide objects from a visible light image; however, their properties can be very different in portions of the spectrum outside of visible light. A trained analyst who knows what to look for in the above examples can provide knowledge to the decision maker that can give him a large advantage over the enemy.

With the potential huge advantage that can be obtained by hyperspectral imaging it still cannot provide reliable data about dynamic sources. If hyperspectral imaging could be performed reliably and fast enough; muzzle flashes, detonations, and other Fast Transient Events (FTEs) could be observed and classified. Unfortunately, as Figure 3.2 shows, the speed at which these events occur can make it nearly impossible to capture and classify an FTE. The important pieces of spectral data from a detonation, according to Figure 3.2, occurs in less than a tenth of a second. In order to reliably capture this data you must be able to sample the entire spectrum of a scene on the order of 10



(a) Fast Transient Events



(b) 3-D Spectrum of Fast Transient Event

Figure 3.2: Evolution time of a Fast Transient Event [9]

if not 100 times faster than that. An added difficulty is the unpredictable nature of conflicts and when and where these FTEs will take place. For this reason, AFIT has been working and developing hyperspectral imaging using chromotomography with the aim to help remedy this capability gap.

*3.0.4 Chromotomography.* Chromotomography is a hyperspectral technique that uses medical imaging algorithms to reconstruct a hyperspectral data cube. Several methods have been used to capture the data needed for the chromotomographic algorithms to build the hyperspectral data cube. Johnathan Mooney at the Air Force Research Labs pioneered the use of a spinning prism as the dispersion source [22]. The benefit of the spinning prism is the increase of light that is able to pass through the instrument and onto the sensor array. The papers he published discuss their use of the prism and lays the foundation for AFIT's work in chromotomography [22] [23].

The unique operational method associated with chromotomography makes it ideal for remote sensing of real-time events. Traditional sensors must sacrifice either full-frame observation or complete spectral wavelength observation to image a scene. The sacrifice of full-frame resolution leads to the opportunity of an event occurring in an area or pixel of the full-frame that the sensor is not currently looking, an interferometer is a good example of this type of sensor. Because the interferometer sacrifices full-frame resolution, the sensor might be collecting data in the lower right of the frame while the detonation has occurred in the upper half of the frame. In this instance the hyperspectral data cube that is constructed will not show this important information.

In trading off spectral wavelength observation, using filter wheels as an example, the hyperspectral imager is still susceptible to missing important data about the scene. This type of method images the entire scene; however, it must step through a set of individual wavelengths of light to develop the data cube. The drawback of the method is that even though the imager can see the full-frame, an event can occur in one wavelength while the sensor is recording data in another. Again, potentially important spectral data may be lost.

Chromotomography, as used in CTE<sub>x</sub>, has the ability to both record full-frame data and the complete spectrum simultaneously. As the prism rotates it disperses each individual wavelength of light a consistent distance from its source depending on the wavelength. The complexity inherent with this technique is that you have multiple wavelengths of light from different sources overlaying on top of each other on a single pixel. So a single image is insufficient to develop the hyperspectral data cube because you can't decipher what wavelength is associated with its source. However, if a sequence of images are taken as the prism spins, you can begin to construct the hyperspectral datacube. Figure 3.3 illustrates why the sequential images are so important. Figure

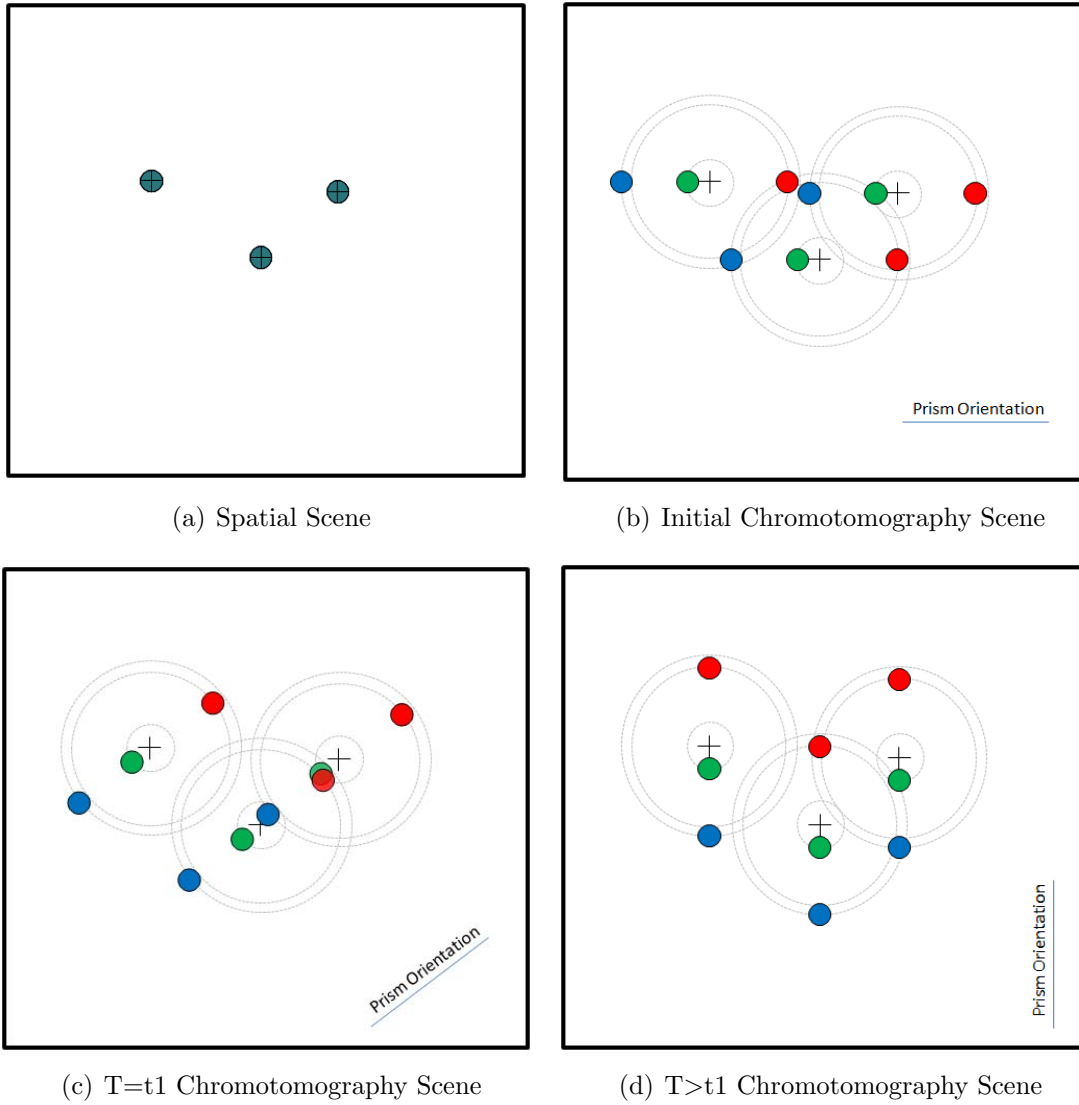


Figure 3.3: Chromotomography Scenes as Time Progresses

3.3(a) shows an example of a color scene viewed without a prism. The rest of the figures show the same scene with the spectra of each point source refracted by the prism with Figure 3.3(c), showing an example of overlying spectral points. However, as the figure shows, the refracted light rotates around the originating pixel as the prism rotates. Using this phenomenon, the chromotomography algorithms use complex transforms to discern what wavelengths of light are associated with which pixels and thus, building a full-frame hyperspectral data cube for each moment in time that an image was taken. The potential of this technology is the ability to see a movie of a dynamic scene in any desired wavelength. Additionally this technique may allow the spectral data of potential explosions and muzzle flashes to be analyzed and classified for use in planning future course of actions.

*3.0.5 AFIT Chromotomography.* AFIT's initial work into chromotomography began around 2003 with the work done by Dearing [24] and Gustke [25]. Dearing's work involved using optics fundamentals and wave propagation theory to develop a computer simulation of data created from a chromotomographic imager. Gustke's work compared reconstruction techniques using simulated data as the test data set. AFIT Master's student LeMaster [10] conceptually designed a spinning prism chromotomographer for AFIT and began the process of building a near infrared sensor. Figure 3.4 shows an initial diagram of the instrument and its main parts. As the diagram shows,

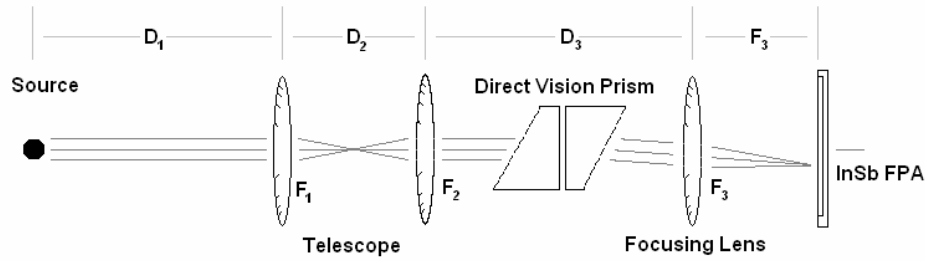


Figure 3.4: Lab Chromotomography Instrument Developed by AFIT [10]

light enters the telescope optics and then enters the prism. The prism refracts the light and then a focusing lens focuses the light onto a collector. The collector for the initial imager is a simple Focal Plane Array (FPA) imager.



AFIT PhD candidate Randy Bostick's research first built a fully characterized chromotomography instrument using the same layout as Figure 3.4. However, Bostick's real contribution lay in the evolution of the algorithms used for data reconstruction. As stated in Section 3.0.4 the algorithms in use relied on highly complex mathematical transformations and the movement of spectral lines to determine the source pixel. Bostick, leveraging knowledge of some medical tomographic techniques, simplified the algorithm using back projection [26]. With the knowledge of the prism angle and the characteristics of how the prism refracts light, Bostick was able to start at a source pixel and begin to pull spectral data back to the source by shifting the intensity data along the prism's line of refraction. This simplifies the transforms immensely due to the fact that the distance that a wavelength of light is diffracted is constant, and as long as you know the exact angle of the prism you can shift the data by the appropriate distance back to the source pixel.

Concurrent with this thesis, another Master's student, O'Dell [11], is taking the design and algorithms developed by Bostick and building a mobile spinning prism chromotomographer for field use. The optical path is identical to Figure 3.4 above; however, it is not a linear optics path as shown in Bostick's instrument. Figure 3.5 shows both an optical diagram and the instrument developed by O'Dell with the structural design engineered by Master's student Book [27]. As you can see, a Newtonian type of tele-

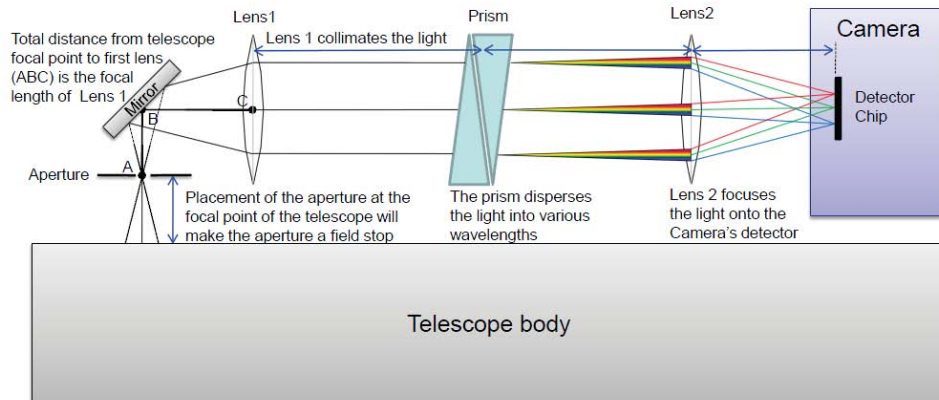


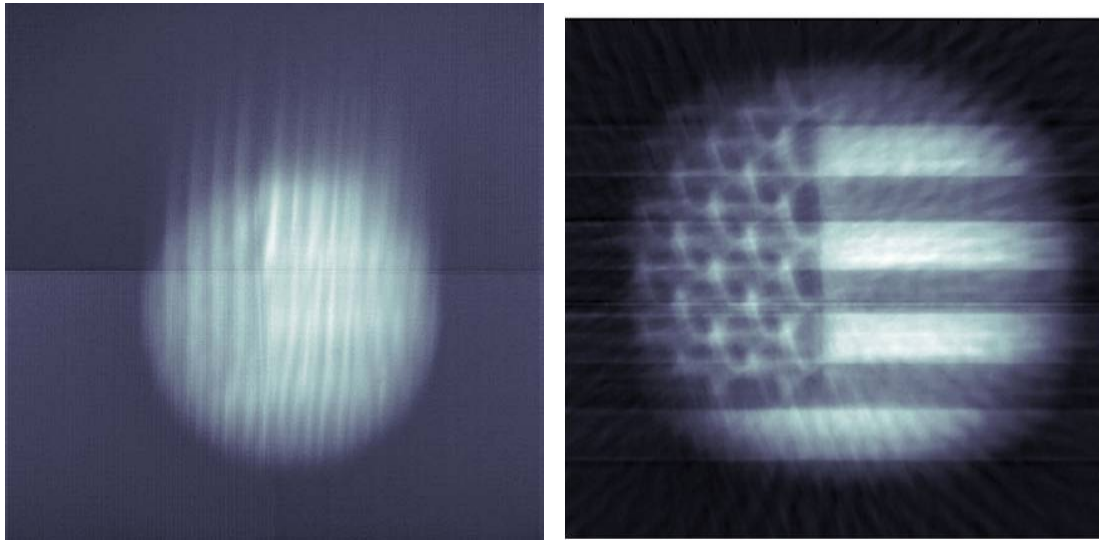
Figure 3.5: Field Chromotomography Instrument Developed by AFIT [11]

scope is used as the foreoptic with the light turned back parallel to the telescope's optical

path before passing into the spinning prism. A high-speed CCD camera is used for the imaging of the data. Using this instrument, O'Dell was able to capture the spectral data with the prism spinning at 10 Hz and imaging the scene at 1,000 fps. Figure 3.6 shows a sample of the images O'Dell was able to capture. Figure 3.6(a) shows an unprocessed image of an American flag taken outside, while Figure 3.6(b) shows the processed image where you can make out the star field and the stripes. Figure 3.6 demonstrates that the field instrument and the AFIT developed algorithm can function outside of a pure lab environment. However, a key milestone for the space-based system is the ability to image and classify FTEs. Figures 3.7 and 3.8 show some very encouraging images of the field instrument's ability to capture and classify explosions.

As Figure 3.7 shows, the flash from a firecracker was imaged during a collection sequence and the elapsed time between Figures 3.7(a) and 3.7(c) is less than 0.12 seconds [11]. Figure 3.7(b) shows the actual flash from the firecracker. When you carefully examine Figure 3.7(b) you can make out the spectrum from the flash being spread out in the frame. A couple of tests using firecrackers were performed with the field instrument. Figure 3.8 shows the spectrum captured during one of those tests. Further refinement of the instrument is needed to improve prism angle fidelity; however, there is a potential potassium line shown in the spectrum around 795nm. Potassium is a common component found in explosives and has an emission line at 766nm [11]. Also, sodium is a common component in explosives and the bump seen at 600nm can potentially be the 589nm sodium spectral line. Unfortunately, due to the offset, O'Dell cannot claim that the lines seen are in fact potassium and sodium [11].

The potential that these figures point to is very exciting. The static scene image, Figure 3.6, shows the potential of this instrument to image a static scene and reconstruct a spatial image from the spectral data. Even though the reconstructed image is not as sharp as possible, the image quality should increase as the algorithm is perfected and the prism angle is known more precisely. The figures showing the explosion, Figure 3.7, demonstrate the ability of the ground instrument to image and capture a fast transient event. This is one of the main goals of the CTEx space experiment and the demonstration of this ability with the field instrument is encouraging. Lastly, Figure



(a) Unprocessed American Flag Image

(b) Processed American Flag Image

Figure 3.6: Static Scene Images From O'Dell's Field Instrument [11]



(a) Scene Prior To FTE

(b) Scene During FTE

(c) Scene After FTE

Figure 3.7: Series Of Unprocessed Images Taken During a 0.12 Second FTE Collection Test [11]

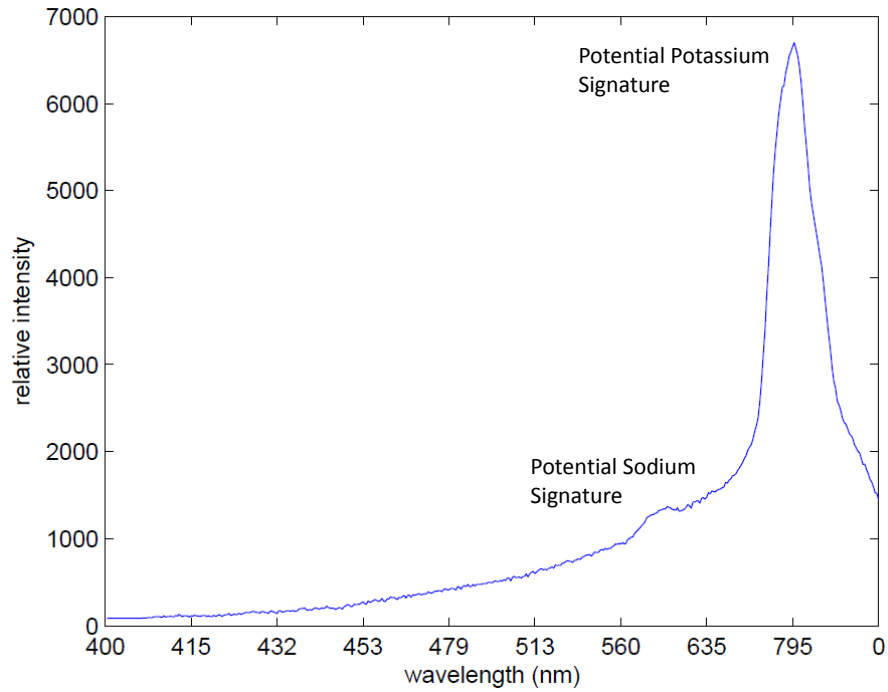


Figure 3.8: Spectrum Captured by Field Instrument [11]

3.8 shows the ability of the field instrument and the algorithm to construct a spectrum for an explosion. This again is a main goal of the CTE<sub>x</sub> space system and verification of this ability by the field instrument is paramount. These tests, when taken together, show that the technology behind high-speed chromotomography is potentially ready to be demonstrated in a relevant environment.

## IV. Designs

WITH the basics of spectroscopy, a survey of existing systems and their designs, and finally a brief discussion about the AFIT chromotomography systems understood, we can now discuss the different subsystem designs for the CTE<sub>x</sub> space experiment. This chapter details these designs and aims to provide the information needed to proceed into a prototype or final design phase.

### 4.1 CTE<sub>x</sub> Electrical Subsystem

The CTE<sub>x</sub> electrical subsystem uses design cues from the systems produced for HICO and ARTEMIS as discussed in Sections 2.2.1 and 2.2.2. CTE<sub>x</sub> is a proof of concept experiment that will take chromotomography out of the laboratory and field and demonstrate the ability to image from a space-based platform. This proof of concept experiment allows risks to be taken with CTE<sub>x</sub> that would otherwise not be considered. In this vein, the CTE<sub>x</sub> electrical system utilizes COTS hardware, many of which are not space qualified. This was done because of the performance hit normally associated with space qualified computer systems and to allow for quick procurement at a lower overall cost. To help mitigate the space environment, shielded enclosures are used where possible.

The basic architecture of the design uses a central cPCI computer subsystem with external connections to the various components. Figure 4.1 shows the basic layout of the design. As the figure shows there are five main assemblies: the Data Collection and Control Unit (DCCU), Power Switching Unit (PSU), CTE<sub>x</sub> Imaging System (CIS), Attitude Determination System (ADS), and the Telescope Assembly (TA). Each of these systems is discussed in more detail in the following sections.

The overall architecture of the system can be seen as a spoke and hub. The hub of the entire electrical system is the DCCU. The DCCU houses the processor, communication interfaces, and system memory cPCI boards. The figure also shows which subsystem is connected to which card within the DCCU and the connection type. All of the connectors to the DCCU are customizable to fit any form factor that is chosen during final design. Each of the other subsystems sit at the end of their respective spoke with no

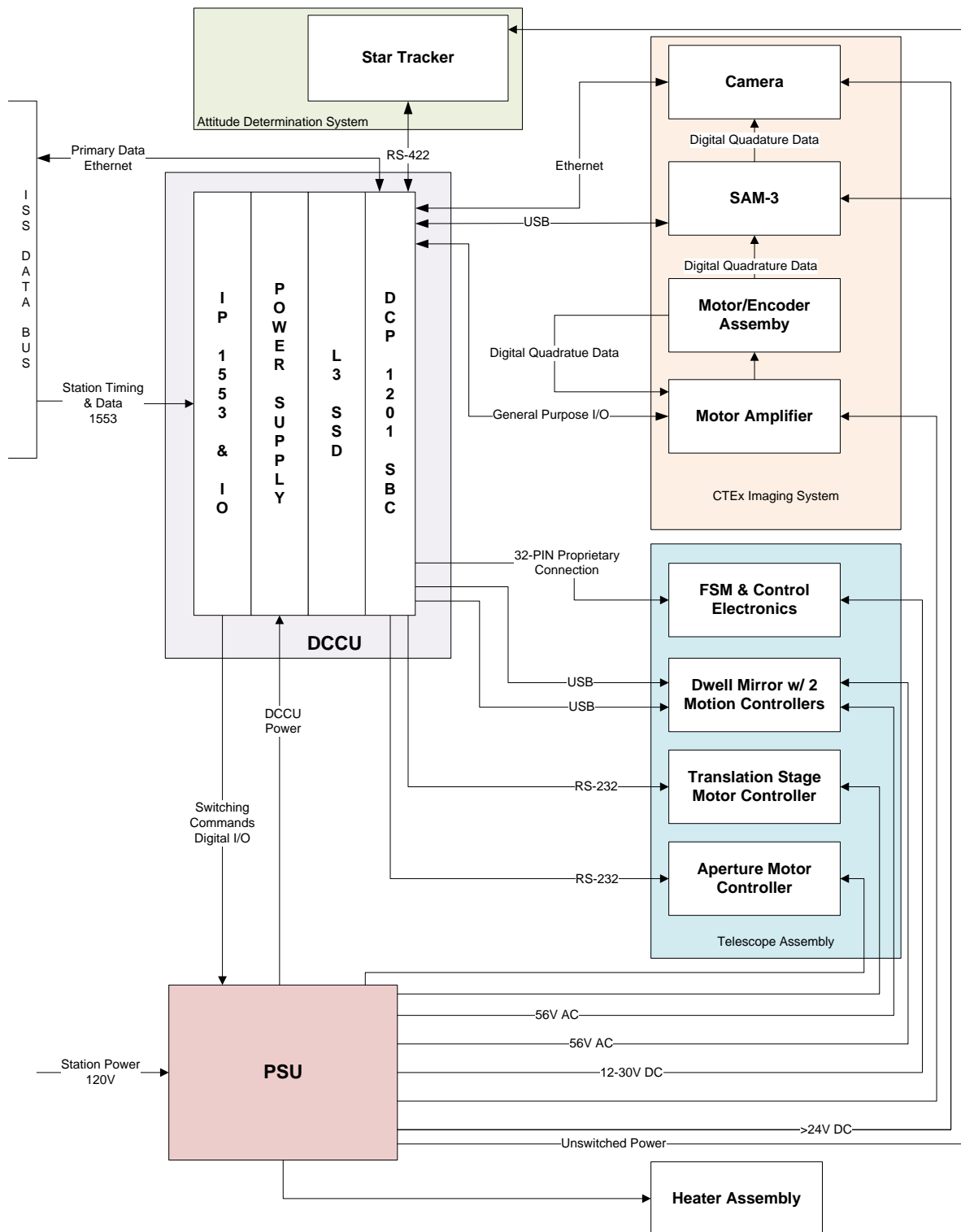


Figure 4.1: Electrical Subsystem Overview

interconnection between them, with the exception of the PSU. As the name implies the PSU is the central power conditioner and distributor for the CTE<sub>x</sub> space system. The only systems that are not switched by the PSU are the DCCU and the ADS. Having the DCCU on unswitched power allows it to always be connected to station power and therefore always powered up and transmitting telemetry data. With the ADS on unswitched power, the DCCU will always know its current position and attitude. The next sections discuss the function and interfaces for each of the subsystems in Figure 4.1. Information about all of the components named in the following sections can be found in Appendix B - E.

*4.1.1 Data Collection and Command Unit.* The DCCU is the central computer for the CTE<sub>x</sub> mission, component datasheets can be found in Appendix B. It is based upon the same standard cPCI bus architecture of the ARTEMIS Payload Processor. However, the proposed DCCU takes advantage of more COTS equipment similar to the HICO system. The cPCI standard was created for industrial computer use and is electrically a superset of the common personal computer PCI standard only in a more compact system [19]. Typically, in the PC, a motherboard contains the processor and a basic set of interface connectors. Some of these interfaces are PCI connectors that allow expansion boards to be connected to the motherboard that will increase the capability of the computer. Commonly the boards that are connected to the motherboard to increase capability in PCs are a graphics card and sound card. This is essentially what the cPCI form factor does. The SBC can be looked at as the motherboard in your PC and the other expansion cards add to functionality of the system that the SBC can not provide.

The chassis chosen for the DCCU is the E900 from Aitech. This chassis fits 3U cPCI cards and has a ruggedized power supply built in. The E900 has the ability to house the cPCI standard maximum eight cards. The front panel of the E900 is customizable to meet the connector needs of our DCCU design. Figure 4.2 shows the rear and front of the e900 to illustrate how the cPCI cards are inserted into the chassis. The rear of the e900 is shown in the left picture. cPCI cards are slid into place, connector first, into the slots that can be seen in the lower left of the box. The front panel is shown in the right



Figure 4.2: Picture of e900 chassis

picture and the customized connections can be readily seen. When the cards are placed into the chassis they connect with the cPCI backplane. The customized connection on the front panel of the chassis interface with the backplane and allow for the any type of connector to be used for integration. This allows for the connections from the cards to the subsystems to be customized to meet the unique space and launch environments.

The system controller board is the main CPU and controller for the DCCU. The system controller is a DCP-1201 single board computer (SBC) produced by Curtis Wright Controls Embedded Computing. The DCP-1201 is an Intel duo core processor and the 3u card is conduction cooled. If the data is captured, as discussed in section 4.1.3, with minimal usage of DCCU resources, this processor should be sufficient to control the experiment. The main board has three RS-422 connections, three USB connections, two ethernet connections, two RS-232 connections, and five GP I/O lanes. The uses for each connection are shown in Table 4.1.

In addition to the connections to the single board computer, the DCCU needs to communicate with the ISS over a 1553 connection and to the PSU. To accomplish these connections, the DCCU contains an adapter card that allows IndustryPack (IP) cards



Table 4.1: DCP-1201 Connections

Processor Board Connections			
Type	Number Avail/Used	System Use	Reference Section
RS-422	3/1	Star Tracker	4.1.4
RS-232	2/2	Filter Translation Stage	4.1.5
		Instrument Cover	4.1.5
USB	3/3	Dwell Mirror Controller	4.1.5
		Dwell Mirror Controller	4.1.5
		Data Acquisition Module	4.1.3
Ethernet	2/2	ISS Communications	
		Camera	4.1.3
GPIO	5/5	Prism Motor Control	4.1.3

to be placed into a cPCI form factor. To adapt the IP cards to the cPCI architecture, the AcPC8635E carrier card was chosen from Acromag. This card was chosen because of its ability to accept two IP cards and thus, save space. To communicate with the ISS via a 1553 connection the dual redundant IP-1553 card from Dynamic Engineering was chosen. Through this connection the system receives timing and basic position data from the ISS. To control the PSU, a digital I/O connection is needed to switch the internal relays that apply power to the other subsystems. To make this connection a IP409E Digital I/O card from Acromag was chosen. This card has 24 digital I/O channels and should be sufficient to control the PSU relays.

Lastly, the main system memory for the unit is the CPCI325 128GB Solid State Disk (SSD), produced by L-3 Targa Systems. The CPCI325 connects to the DCP-1201's SATA connector and acts as the main data storage device for the system. As with all of the above components, the operating temperature is -40°C to 70°C.

There are issues with this design that need to be addressed. The controller for the fast steering mirror has a proprietary 32-pin connector. Due to time constraints the interface between the DCCU and the controller was not explored. Additionally, the components listed above are not rad tolerant. However, the shielding provided by aluminium enclosures will help limit their exposure. Future work looking at the possibility of adding a radiation tolerant SBC to the system should be considered. This radiation tolerant SBC will not be a part of the experiment but will be evaluating the health of the DCP-

1201 through an available RS-422 connection. If it detects a fault in the DCP-1201, it should have the ability to power cycle the DCP-1201 to hopefully clear any errors. Also, a small radiation tolerant SSD should be used for a system OS secure back-up in case a flash of the OS is needed in the event of memory corruption from bugged software or environmental effects.

*4.1.2 Power Switching Unit.* The PSU is the central power distribution unit and this section will outline the basic functionality of the PSU, but will not attempt to design it. Its main function is to take in the 120V station power and distribute conditioned power at the correct levels to the other components of the instrument. The DCCU controls the power distribution with a simple digital signal that will either put a relay into an on or off state. The only components that will always receive power when station power is connected is the DCCU and the ADS. The ADS is always powered on to allow the DCCU to initialize its system time and the experiment's attitude and position after boot up. For the safety of the instrument and the components from reverse current conditions, all of the conditioned output power connections should be zener diode protected.

The zener diode should be used because it provides a non-destructive means to turn off the circuit should an over-current condition occur. The zener accomplishes this by breaking the connection when the back voltage reaches what is called the breakdown voltage, thus protecting electrical equipment from potential overstress. The diode will stay in this open circuit mode until the back voltage is within a tolerable level, at which point the zener closes the circuit which allows current to flow again, that is, unless the destructive voltage limit of the zener has been exceeded. A good analogy for the zener diode is a self healing circuit breaker.

*4.1.3 CTE<sub>x</sub> Imaging System.* The CIS is not just an imager. The CIS must gather all of the data for scene reconstruction. The CIS contains components to collect the position data from the encoder. The position data from the encoder is very valuable and will allow proper reconstruction of the spectral data during post-processing. Datasheets about these components can be found in Appendix C. This system is based

around products from Vision Research who specialize in high-speed cameras. As seen in Figure 4.1, the imaging subsystem consists of the camera, data acquisition unit, and prism rotation motor/encoder. One of the main goals of the CIS is to image a scene at 10,000 fps with a threshold of 1,000 fps.

The prism rotational angle data is extremely important for the post-processing of the chromotomography images. As Section 3.0.5 pointed out, if the angular position data is not known very precisely, then the reconstructed data will be blurry and any useful data will be difficult to discern from the image. Vision Research offers a Signal Acquisition Module (SAM-3) that is capable of acquiring a maximum of 32 analog or 16 digital signals at a 100k samples per second rate. The SAM-3 samples these signals continuously and sends them to the camera for placement into the header of the captured images. For our application, the digital data coming from the prism position encoder in the telescope assembly, will be sent to the camera for placement into the header of the image. This proposed architecture should provide the most seamless integration of the digital position data and the images captured by the camera. Additionally, this architecture simplifies computer operation because only one file will need to be saved, transmitted, and processed.

The main imager proposed for use on the CTE<sub>x</sub> experiment is the Phantom v710 camera which has the ability to image at over 1 million frames per second and has a maximum resolution of 1280x800 pixels. The resolution and speed of the camera are user selectable so that the a trade-off can be made between the two. The v710 also is available with 32GB of on board volatile RAM that can be used to save video files. This internal memory is capable of saving data at very fast data rates; however, it is constantly overwritten whenever a new image capture event is triggered.

To avoid using the camera's internal memory, an external CineMag can be used for data storage. The external CineMag is available in 128 GB, 256 GB and 512 GB sizes. Unfortunately, the use of the CineMag comes with a performance hit. Due to the nature of offboard vs. onboard memory, the CineMag is slower and not capable of saving data at the same speed as internal memory and thus limits the speed of the camera. Using estimation software provided by Vision Research, Table 4.2 shows the estimated

maximum fps of the camera and maximum capture time for different resolutions and internal or external memory use. As you can see, the performance hit taken by saving

Table 4.2: v710 External and Internal Memory Comparison

<b>v710 Memory Capability</b>					
<b>Resolution</b>		<b>Internal 32GB</b>		<b>CineMag 256GB</b>	
		<b>Max FPS</b>	<b>Time (sec)</b>	<b>Max FPS</b>	<b>Time (sec)</b>
1280 x 800	8-bit	7585	4.41	700	383.37
	12-bit	7585	2.94	700	255.58
1280 x 720 (720p)	8-bit	8425	4.42	778	383.26
	12-bit	8425	2.94	778	255.129
1024 x 768	8-bit	9622	4.53	912	383.14
	12-bit	9622	3.02	912	255.43
1024 x 512	8-bit	14405	4.54	1368	383.14
	12-bit	14405	3.026	1368	255.43
800 x 600	8-bit	13813	4.59	1334	381.00
	12-bit	13813	3.08	1334	255.29

directly to the external memory can be substantial. If AFIT can work with Vision research to double the internal memory of the v710 for our purposes, then the camera would be able to image for 9 secs at 9622 fps and a resolution of 1024 x 768.

To handle instrument data, this thesis proposes to use the internal memory of the camera to capture the data. This will allow for the full use of the camera at the best possible resolution and speed while making trades with the small collection times available. As will be discussed in the software portion of this thesis, Section 4.2, it is proposed that immediately after any capture event occurs, the software automatically transfers the data to the main CTE<sub>x</sub> system memory. Unless directly saving to offboard storage becomes near equivalent to using the onboard memory, this proposed solution appears to be the best way of handling the instrument data.

The motor and encoder assembly proposed was developed by the Kolmorgen company and assembled by the Mike Kilroy Corporation. The motor is a RBE(H) series and is capable of rotating at 100Hz and has a three inch bore in the shaft to accommodate the prism. The encoder is delivered as a part of the assembly by Kilroy Corporation and has a resolution of 1024 lines per revolution, which translates into an accuracy of 6.14 milliradians.

Once all of the components of the imaging system are procured, ground characterization of the instrument is critical. This characterization will determine the latency in the system between the camera and the SAM-3. Only with this characterization will the precise angle of the prism be known and proper reconstruction during post-processing can occur. In setting up the characterization, it is critical that all wiring be the same length to match the expected impedance levels of the integrated system. The characterization is performed by setting up the imaging system with the camera focused on the encoder. The encoder does not need to be setup in the exact location as the final experiment, because, instead of looking through the prism, the camera is focused upon a florescent dot on the encoder shaft. The encoder is then swept through its range of expected rpms while the camera images the encoder shaft. When the data has been collected the actual prism angle, as observed by the florescent dot in the image, is compared to the sensed angle located in the image's header data. The angle offset between the observed and sensed data can then be calculated and tabulated for use by the chromotomographic algorithm.

*4.1.4 Attitude Determination System.* One of the main challenges for the CTEx experiment is pointing accuracy. Datasheets for the following components can be found in Appendix D. With a 700m field of view, which corresponds to an instrument half-angle of  $0.05^\circ$ , the experiment must know exactly where it is pointing, otherwise the target may be missed. The ISS provides position and attitude data through the 1553 bus connection; However, the data only has an accuracy of 70m for position and  $\pm 3^\circ$  for attitude [28]. This level of accuracy pushes the limits of the mirrors actuators because of the high angle accuracy needed.

To address the inadequacy of the attitude data, the HE-5AS star tracker from TERMA is proposed for use. The HE-5AS has a space flight heritage and provides  $<1$  arc-second RMS accuracy for pitch and yaw and  $<5$  arc-seconds RMS accuracy for roll. The thesis performed by Starr [18] details the pointing accuracy of the HE-5AS and should be consulted if more information is desired. The attitude data provided by

the HE-5AS is sent to the DCCU using a RS-422 connection, also called an EIA-422 connection.

The 70m accuracy of the ISS's position data would still allow us to potentially acquire our target. However, according to Starr [18], this accuracy occupies a large portion of our pointing budget. If future work determines that a more accurate position is needed, Surrey Satellite Technology Ltd, produces a space GPS receiver with space flight heritage. The SGR-07 is a single antenna GPS system that provides 10m positional accuracy and 15cm/s velocity accuracy. Similar to the star tracker, the SGR-07 interfaces with the computer using a RS-422 connection.

*4.1.5 Telescope Assembly Control.* The telescope of the CTE<sub>x</sub> experiment was designed by RC Optical Systems and datasheets for all of the following components can be found in Appendix E. The details of its design and optical functions can be found in the thesis performed by Book [27]. In lieu of using large actuators to slew the entire instrument for targeting purposes, the internal mirrors of the telescope are used to point and track objects on the ground. There are two internal mirrors that are used: the dwell mirror and the fast steering mirror. The dwell mirror is also referred to as the slow steering mirror and is the first mirror that the incoming light encounters. This mirror is the primary mirror used for pointing the optics. The fast steering mirror is positioned close to the field stop and is used primarily to counteract jitter in the system.

The dwell mirror is attached to two ADRS-200 wedge rotary stages manufactured by Aerotech. In order to control the dwell mirror assembly, two Ensemble CL controllers are used. The Ensemble CL controllers can interface with the DCCU either using ethernet or USB connections. For the proposed design of the DCCU, the USB connections will be utilized. The integration of the Ensemble CL has its own unique challenge mainly its use of AC power. Unless an alternative controller can be found, the PSU will need to have an integrated power inverter to adequately supply the Ensemble CL.

For control of the fast steering mirror, a Physik Instrumente (PI) S-340 high-speed piezo tip/tilt platform is used. Control of the S-340 will be accomplished by the PI E-616. The E-616 is available in a bench-top model or a self contained OEM 3U module. The

bench-top model utilizes a SubMiniature B coaxial connection for analog input and a 15-pin D-sub connector for sensor monitor output. The OEM module uses a proprietary 32-pin connection. To reduce the number of connections and possibly reduce internal footprint, the OEM module is proposed for use.

To enable on orbit camera calibration, filters attached to a translation stage are moved in and out of the optical path during specific portions of the flight. The chosen translation stage for the filters is the PI M-122 linear translation stage controlled by a PI C-863 controller. Additionally, for actuating the telescope cover, a linear actuator connected to a lever arm will swing the cover open. To accomplish this, a PI M-227 linear actuator and another C-863 are proposed for this design. The C-863 can be connected to the computer via a USB or RS-232 connection. For this application, the RS-232 connections are being proposed for interface to the DCCU.

## 4.2 *CTEx Software*

Because of the fast calculations that will be done and the accuracy needed, an operating system that has a small footprint, and real-time operations should be used as the command and control software. UNIX, its LINUX variants, and VxWorks are all operating systems that can be used effectively on systems with limited resources such as CTEx. VxWorks is intriguing because it is a real-time operating system and, according to the Wind River website, its purpose built to optimize performance of real-time operations [29]. The components listed above in Section 4.1 have available Dynamic-Link Library (DLL) files that will allow the system programmer to build the interface between the components and the DCCU operating system. No matter which of the above operating system is chosen, the following software flowcharts show a proposed set of functions that allow for maximum flexibility.

*4.2.1 Main Software Function.* Figure 4.3 Shows a flowchart for the control software of the CTEx experiment. In the diagram, any item that is underlined is an item that links to a separate flowchart for the associated software function. As an example, the Functional Verification Test (FVT) block is underlined and therefore has its own

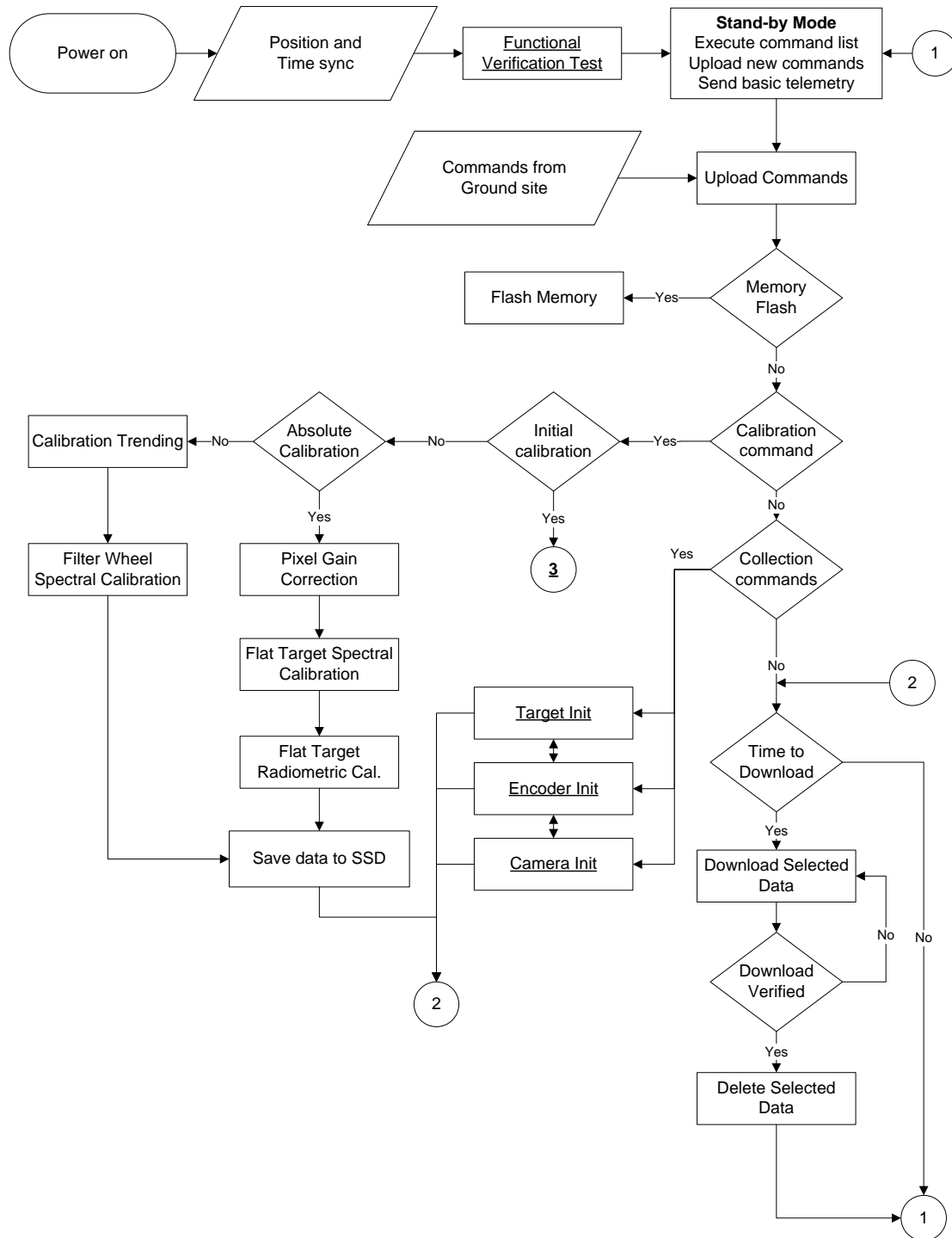


Figure 4.3: Main Software Function Flowchart



flowchart associated with it, Section 4.2.2. Also, a circular block is a link to an entry point of a flowchart that is not the main entry point.

Figure 4.3 is the main software function for the entire CTE<sub>x</sub> space experiment. This function handles the overall processing of incoming commands and calls the necessary functions to execute those commands. Starting with the bootup portion, the function initializes its state and performs a verification test. After initialization, the function begins to check for an incoming command list and executes those commands once received. Based on the commands received from stand-by the main function will call either maintenance or data acquisition functions. These functions are subroutines that interface with the CTE<sub>x</sub> subsystems and operates the experiment. Each of the following subsections talks briefly about a block shown in Figure 4.3 starting with synchronization.

*4.2.1.1 Position & Time Synchronization.* Once power is applied to experiment after installation onto the JEM-EF, the computer boots up. During the boot up phase the computer interrogates the ISS 1553 position data coming in, the star tracker, and possibly the GPS unit. Once the internal clock and position are synced with the incoming signals, the computer begins to send telemetry down to the ground station with its current position and attitude state. The system clock sync to either the GPS receiver or ISS time is used for future time stamping functions. With the computer synced to the outside timing and position sensors, a Functional Verification Test begins.

*4.2.1.2 Functional Verification Test.* The Functional Verification Test is performed on the ground during final assembly and integration as well as during on-orbit check-out. The FVT is a general health status check and subsystem initialization of the CTE<sub>x</sub> space system. During this test, the translation stages and position motors are aligned, the camera is initially calibrated, and currents of motors and electrical components are logged to verify nominal functionality. Hopefully the diagnostics that are completed during FVT will allow the ground crew to troubleshoot and potentially solve or work around any off nominal results observed. The FVT has its own flow associated with it and a full description can be found in Section 4.2.2. When the software returns to the main software function from the FVT, the system is put into a stand-by mode.

*4.2.1.3 Stand-by Mode & Upload Commands.* This step is a general placeholder for when the system is not actively acquiring data or transferring data. During this step the system is sending basic telemetry, position, voltage states, and instrument health. This basic telemetry stream is always broadcast for monitoring by the ground crew. If commands have been loaded into the system, it will immediately begin to process those commands. If no commands have been pre-loaded or the system has exhausted the list of uploaded commands, the system begins checking the incoming data stream for new command sequences. Once the system sees that new command sequences are available, it captures these sequences and places them into memory for execution.

*4.2.1.4 Memory Flash.* After receiving commands the system begins to execute those commands. The memory flash block is the first command block in the software flow. When the system works through the command sequences, if there is a command to flash the memory, then the computer executes this command prior to proceeding any further. The flash memory command essentially wipes the old command software from the system and replaces it with the new command software. This prevents the system from executing potentially bugged or corrupted control sequences that may have detrimental effects or to update the software to provide enhanced capability.

*4.2.1.5 Calibration Command.* If there is no flash command, the next command block in the software flow is imager calibration. This command sequence will put the system into one of three imager calibration modes: Initial (Section 4.2.1.6), Absolute (Section 4.2.1.7), and Trending (Section 4.2.1.8). For more detailed explanation of the calibration steps and procedures, please refer to the Master's thesis performed by Book [27].

*4.2.1.6 Initial Calibration.* If, after a period of on-orbit ops, it is determined that the imager needs to be fully recalibrated, the system enters into this initial calibration mode. This mode is a subset of the functional verification test software flow, Section 4.2.2. In this instance the calibration proceeds into the functional verification test at the point labeled "3" and performs the entire camera calibration sequence. This

is accomplished if the imager is observed to be producing images that are very distorted in some fashion. Proper image capturing of the incoming scene is paramount to accurate scene reconstruction.

*4.2.1.7 Absolute Calibration.* This calibration step is typically performed monthly or whenever it is determined to be necessary by calibration trending. In this calibration mode the system performs a set of calibration steps that are a subset of the initial calibration process. These include: Pixel Gain Correction, Flat Target Spectral Calibration, and Flat Target Radiometric Calibration. These calibration steps are important to keep the images produced by the CTEx imager as true to incoming light as possible. The the image begins to capture off nominal images, the chromotomographic reconstruction algorithms will not produce correct results. When these tests are completed the software reenters the flow at “2” and the data sets are saved to the main memory for download and analysis.

*4.2.1.8 Calibration Trending.* This level of calibration is the simplest of the calibration modes and is typically performed weekly [27]. With this data trends in the calibration can be observed and if the trends show that the images are beginning to become too off nominal, a more involved calibration step can be commanded to correct the issues. While in this mode, a series of filters are placed into the optical path and images are collected. After the filter data sets have been saved, they are placed onto the onboard system memory for future download and analysis.

*4.2.1.9 Collection Commands.* After the calibration commands the next set of commands the software executes is the data collection commands which place the system into the data acquisition flow. The functions, and their associated software descriptions, that make up the data acquisition mode are: Target Init (Section 4.2.3), Camera Init (Section 4.2.4), and Encoder Init (Section 4.2.5). Even though these functions are listed in a sequential order, they are executed by the system in a simultaneous nature. Each function has a time or position trigger within the function that waits for the initial conditions to be met before performing its main function. Similar to the cali-

bration modes, once the data acquisition functions are complete the system moves into the download sequence beginning at the “2” entry point.

*4.2.1.10 Time To Download.* NASA will provide the CTE<sub>x</sub> experiment a predetermined time designated for instrument data downlink. This time is uploaded to the CTE<sub>x</sub> system and is flagged by the system to trigger data download. Once the system triggers the download sequence, data is sent via the ISS downlink to the ground for analysis. The downloaded data is not deleted from the system memory until after verification that the data was successfully received. Once the data can be verified, a system flag is uplinked to the CTE<sub>x</sub> experiment to delete the data. To prevent accidental deletion of data because of an erroneous command, it is recommended that this delete command be composed of two separate command sequences similar to the “Are you sure?” question found within Windows applications. Once the data has been verified and deleted, the system is then placed into the stand-by mode that waits for further command sequences.

*4.2.2 Flight Verification Test Software Function.* As mentioned in Section 4.2.1, the flight verification test is performed both on the ground and on orbit to ensure system functionality. Figure 4.4 shows the software flowchart associated with the functional verification test. This flowchart has two start points, the first is the functional verification test entry point that puts the system through the entire function verification test sequence. The second is denoted as “3” and is used for full calibration of the instrument. The camera calibration cannot be performed without the telescope cover closed. The telescope cover is therefore closed right after the system enters into the full calibration system flow. The end point for this software flow is identical no matter which entry point is used.

*4.2.2.1 Continuous Voltage Logging.* When the functional verification test begins the system goes into a diagnostics mode. This diagnostics mode monitors and logs the current draws of the instruments and subsystems. The complete logged data is downloaded to the ground station once the test is complete. During the test

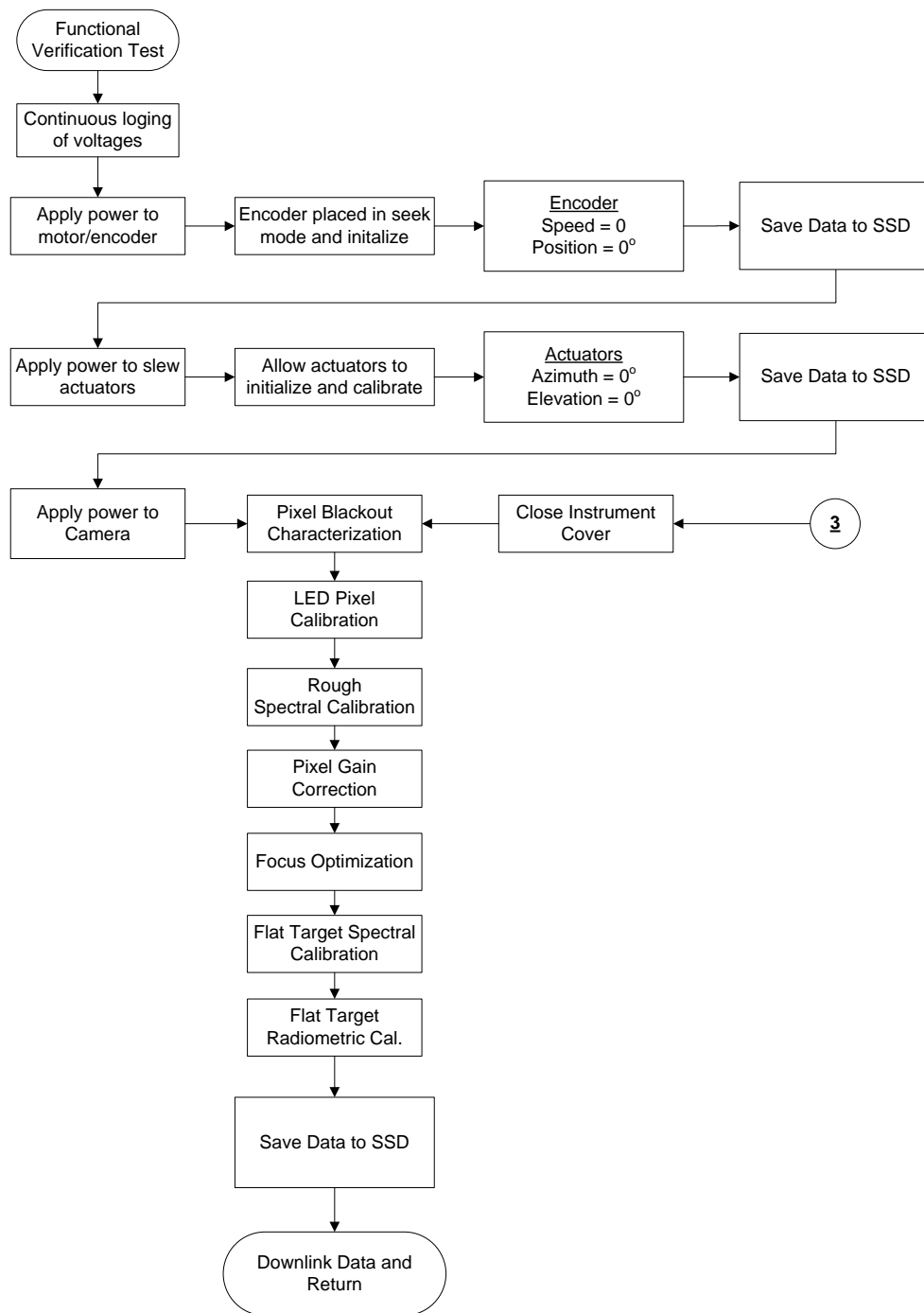


Figure 4.4: Flight Verification Test Function Flowchart

however, the currents pertinent to the subsystem being tested are sent via the telemetry data stream for monitoring. This data will help the team on the ground ascertain the preliminary functionality of the system while performing commands.

*4.2.2.2 Apply Power to Motor/Encoder.* The first subsystem that the functional verification test checks out is the spinning prism motor/encoder. Once power is applied to the motor/encoder assembly, a search sequence is executed to find the  $0^\circ$  angle point. The encoder has a single counter mark on the encoder disk, as the disk rotates the mark indicates that the disk has made a complete revolution. Once the encoder initializes and finds the zero angle point, a zero state command is given: speed = 0 rpm and position =  $0^\circ$ . After the zero state command is given the motor/encoder assembly is ready for operation.

*4.2.2.3 Apply Power to Slew Actuators.* The slow and fast steering mirror actuators, discussed in Section 4.1.5, on the CTE<sub>x</sub> experiment function similarly to the motor/encoder assembly. When power is applied to them they begin to search for the zero point and initialize. After the initialization is complete, a zero state command is applied: Azimuth =  $0^\circ$  and Elevation =  $0^\circ$ . With the actuators ready to be commanded, the camera is powered on next.

*4.2.2.4 Apply Power to Camera.* Camera initialization is more complicated than the previous initialization steps. Once the camera is powered on and its own internal initialization steps have been performed, the camera needs to be calibrated. For an in depth discussion about the calibration steps please refer the thesis by Book [27]. Once the camera has completed its internal initialization, it performs a pixel calibration with the telescope cover closed. The telescope cover remains closed during this step of calibration and during the Algorithm Spectral Cal and Pixel Gain Correction. After these steps the telescope cover is opened to allow the camera to finish calibration. The next steps involve a Urban Site Focus Optimization and Flat Target spectral and Radiometric Calibrations [27]. Once these steps are complete all data is saved to the SSD

and prepared for downlink. The camera calibration is the last step in the functional verification test, now lets talk about data acquisition.

*4.2.3 Slewing Control Software (Target Init).* The slewing control software is the most complicated of the acquisition processes. Figure 4.5 shows how the system will handle the targeting of the optics. This function is complicated and is broken down into three separate modes of operation: stationary, manual, and tracked targeting. The stationary targeting is the simplest targeting method allowing for the sensor to stare at a constant azimuth and elevation on the slow steering mirror. A more complicated mode of operation is the manual control targeting mode. During manual mode operation, a data file containing times and set angles is uploaded to the system. When the system reaches one of the times listed in the file, it slews the mirror to the angle associated with the time gate. The most complicated mode of operation is the tracked target. In this mode the system first calculates an orbital collection window that tells the system it is in range of the target. Once the system knows that it is in range it begins to constantly calculate the mirror angles needed to track a target as it passes under the ISS.

*4.2.3.1 Slewing Control Input.* No matter which targeting method is used, the software needs to read in the global and local variables. The global variables used are global in the sense that they are available to the other data acquisition processes. The global variables needed by this software function are bold in Figure 4.5 and include: longitude and latitude of the target, the start and end time for the data acquisition, and the name of the manual angle control data file. The local variables needed are the targeting methodology flag and the Azimuth and Elevation angles if a stationary tracking methodology is desired.

*4.2.3.2 Stationary Targeting: Dwell Mirror Control.* The stationary targeting is the simplest of the targeting methods. When the software receives the stationary targeting flag it begins to evaluate the system time vs the experiment start time. Once the times match up the system begins to articulate the mirrors and send a trigger command to the prism control software. Using the local azimuth and elevation

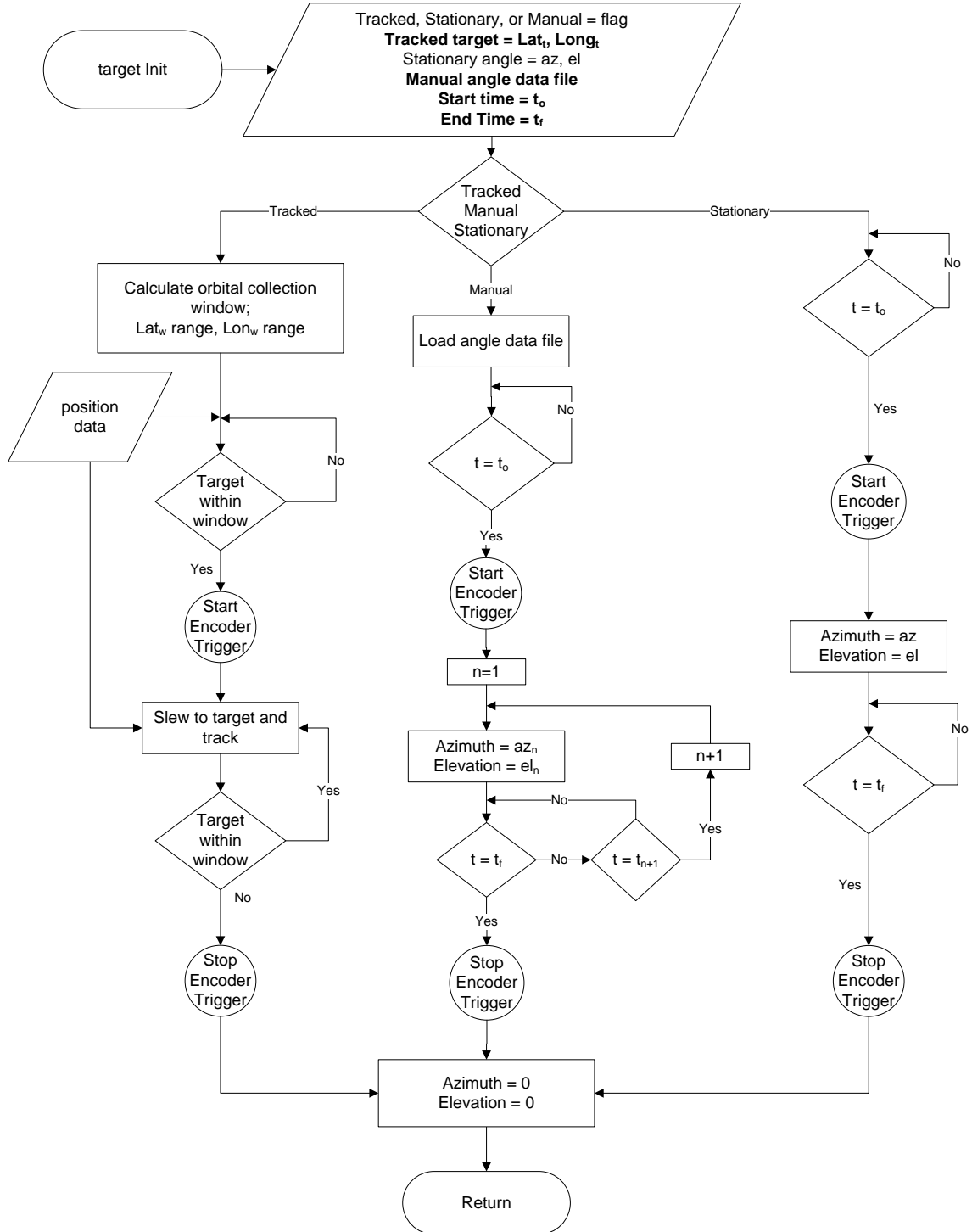


Figure 4.5: Slewing Control Software Flowchart



variables, the system sends the appropriate commands to the mirror controllers to the appropriate angles. After the angle commands have been sent the system begins to evaluate the system time versus the experiment end time. Once the times are equal then the system leaves the command loop, sends the stop trigger to the prism control software, and it returns the mirrors to an angle of  $0^\circ$  azimuth and elevation.

*4.2.3.3 Manual Targeting: Load Data File & Initial Angle.* The first step in manual targeting is to load the angle data file. This data file contains a tabulated list of times and azimuth and elevation angles that the system will follow. With the angle program loaded into memory the system begins to evaluate the system time to the initial angle time. When these times coincide, the function triggers the prism control software and slews the dwell mirror to the first angle and begins to reevaluate the time.

*4.2.3.4 Manual Targeting: Time Evaluation & Control.* The time evaluation step encompasses the time evaluation boxes in the flowchart and effectively controls the angle of the dwell mirror. After the first angles have been set the system checks the current time versus the end time of the acquisition process. If it is not time to end the acquisition sequence the system evaluates the time to see if its time to set the dwell mirror at the next angle. The function continues to evaluate these two time milestones until one of them is true. When the function determines that it is time to move the mirror to the next set-point, it goes back picks the next set angles and moves the mirror to the appropriate angles. The system then begins to evaluate the time milestones again. Once the function evaluates that the data acquisition process is complete, the stop trigger is transmitted to the prism control software and the dwell mirror is reset and the software returns to the main function.

*4.2.3.5 Tracked Targeting: ISS Orbital Collection Window Development.* After the Slewing Control Software has received the tracked target flag, the ISS orbital collection window is calculated. The collection window is calculated by using the target's latitude and longitude and applying the slewing limits of the mirrors along with a range expected ISS altitudes. The result of this calculation is a collection window that is a

3-D along the ISS's orbital path where the target is within visual contact of the instrument. This collection window's limits are evaluated vs the actual position of the ISS and determines if the experiment is within visual sight of the target. This window needs to be conservative to allow the system to slew the mirrors to their limits for immediate acquisition of the target when it comes within visible range. Special care should be taken to not confuse the ISS orbital collection window with the more non-conservative imaging acquisition window discussed in Section 4.2.4.2.

*4.2.3.6 Tracked Targeting: Tracking Sequence.* Once the collection window has been calculated by the software, it begins to evaluate its current position. Once the position of the ISS is within the collection window, the system begins slewing the mirrors and sends a start trigger command to prism control function. Using the incoming position data, the system calculates the required mirror angles to steer the optical beam to the target area. This angle calculation is performed in real-time with the system sending the appropriate voltages to the motor controllers to track the target.

As the tracking algorithm is active, the ISS position is being evaluated against the collection window. When the software has determined that the ISS has passed outside of the collection window, the system sends a  $0^\circ$  azimuth and elevation command to the mirrors, and a stop trigger to the prism control software. Once the reset position commands have been sent to the mirrors, the slewing control software returns to the main software function.

*4.2.4 Camera Control Software (Camera Init).* Figure 4.6 shows the basic flowchart of the camera data acquisition process. As stated in Section 4.1.3, the camera's resolution and speed can be adjusted by the user. Taking full advantage of these abilities, this software function allows for a wide range of testing possibilities.

*4.2.4.1 Camera Control Input.* This block is a generic control input block. It is in this block that the variable associated with the camera commands are read. As in the Slewing Control Software, the variables read into the camera control block are both global and local in nature. The global variables listed in bold in Figure

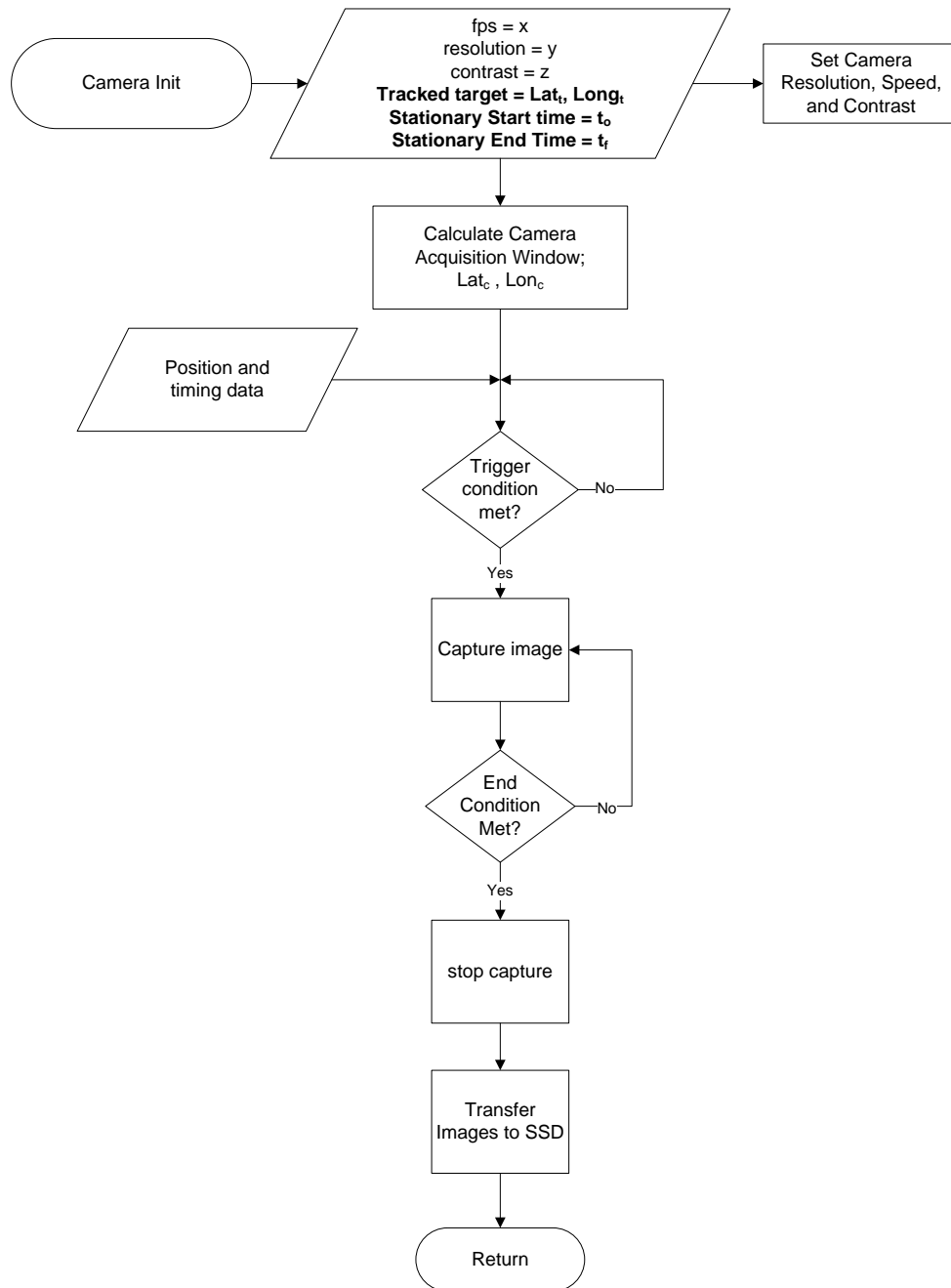


Figure 4.6: Camera Control Software Flowchart

4.6. The global variables tell the camera whether the experiment is in a tracking or stationary targeting mode. This distinction determines the trigger condition that will occur later in the function.

The local variables that are read in are shutter speed and resolution. Shutter speed is given in frames per second and, depending on the resolution used, can be set at a maximum of 1,400,000 fps. Additionally, resolution is software selectable and can be assigned in increments of 128 x 8 pixels.

Once the variables have been read into the system they are used to initialize the camera. The fps and resolution variables are passed to the camera and the camera is placed into “stand-by” mode. Once the camera is in this “stand-by” mode the software begins to evaluate the trigger condition.

*4.2.4.2 Camera Acquisition Window Development.* If the system is in a tracked target mode, the software calculates a camera acquisition window. This window is different than the ISS orbital collection window calculated in Section 4.2.3.5 flow because it is not as conservative. The camera acquisition window is developed using the same method as the ISS orbital collection window, but uses the exact limits of the mirror actuators instead of a conservative limit. This non-conservative method is used to ensure that the camera will begin to acquire data at the exact time that the target comes into view and not waste valuable memory assets on images without the target.

*4.2.4.3 Trigger Condition.* This decision block is essentially the block that begins the capture sequence. The actual trigger condition is determined by whether the targeting method is time based or position based. This block constantly checks the systems position and timing data against the trigger condition and once the software has determined that the ISS has satisfied the trigger condition, the capture sequence begins.

*4.2.4.4 Capture Sequence.* Once the software has determined that the trigger condition was met, the camera is commanded to capture images. With the camera in stand-by, a simple command using the supplied camera DLL files triggers the camera to begin image capture. Once the camera trigger command has been sent, the software

begins to evaluate the system time and position versus the trigger condition. Once the software determines that the sequence is complete, either by the target being out of view or elapsed time, a stop image capture trigger is sent to the camera via the same method as the begin capture command.

*4.2.4.5 Data Transfer.* Because of the volatile nature of the camera's internal memory, after every capture event, the data needs to be transferred to the CTE<sub>x</sub> mass storage device. This mass storage device may be an attached CineMag, a CineStation docked Cinemag, or a system level Solid State Drive (SSD). The files can be offloaded to mass storage using the existing ethernet port on the camera or through a direct connection to an attached Cinemag.

*4.2.5 Prism Control Software (Encoder Init).* The prism control software is the basic software function that controls the motor/encoder assembly. This function has two branches, one that sets the prism at predetermined angles at certain times, and another that spins the prism at a constant rate. Figure 4.7 shows the prism control software flowchart. No matter if the encoder is commanded to hold a specific angle or to constantly rotate the prism, there are three main portions to this function: input control variables, controlled rotation sequence, and finally shutdown.

*4.2.5.1 Encoder Control Input.* The first step in either mode of operation is the input of the control variables. Similar to other functions, there are both global and local variable read-in to the prism control function. There is only one global variable read in and it is the manual angle data file. This data file is the same as the slewing control function and contains angle data pertaining to the prism. The local variables utilized by the prism control function are a manual or velocity mode flag, and the RPM desired for the velocity mode. The RPM input has an associated voltage value determined during integration testing that is used for the actual controlling of the motor/encoder assembly.

*4.2.5.2 Velocity Mode: Rotational Control Sequence.* Spinning the prism at a constant rate allows the camera to image the scene a desired number of times per revolution of the prism. The first part of the rotational sequence is the trigger

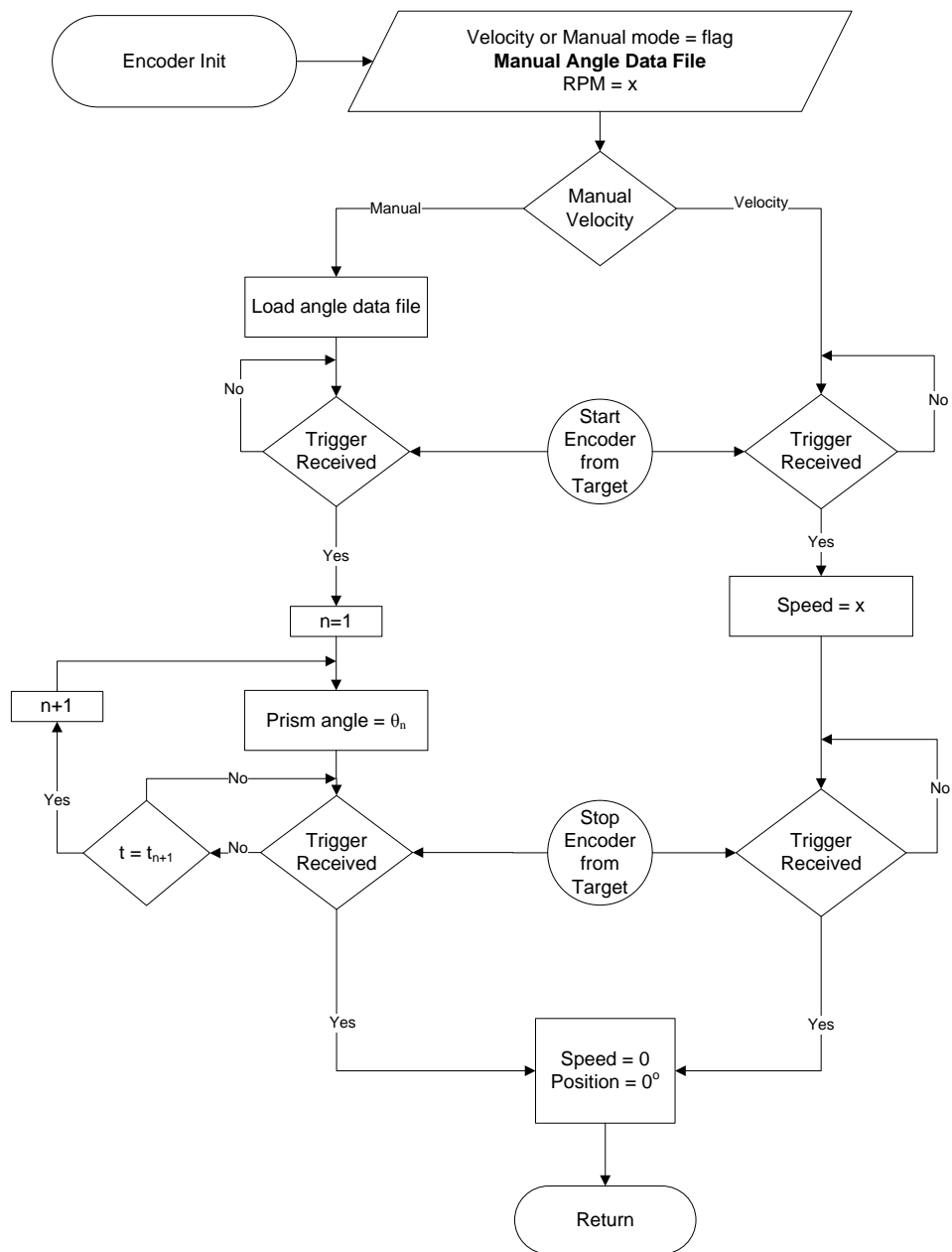


Figure 4.7: Prism Rotation Control Software Flow

evaluation. In this decision block a trigger command from the slew control software function is expected. Once the trigger is received, the software begins to control the motor by taking the rpm input and sending the associated voltage level to the motor controller for constant speed operation. The controller has an internal feedback loop that uses the quadrature data to maintain the commanded rotational velocity. While the prism is spinning at the designated rate, the software continues to monitor the trigger, waiting for a stop command to be received. Once the system receives the stop trigger, the software begins to shutdown the encoder.

*4.2.5.3 Manual Mode: Load Data File & Trigger Evaluation.* Similar to the manual portion of the slewing control function, the first step in manual mode operation is to load the data file. The data file contains the angle control sequence and their associated times. This data file can contain data pertaining to the dwell mirror; however, this sequence ignores any angular data that may be present associated with the dwell mirror. After the data file has been loaded into the system, the system begins to evaluate the start trigger from the slewing control function. Once the trigger command is received the system proceeds to the prism angle sequence.

*4.2.5.4 Manual Mode: Prism Angle Sequence.* Once the system receives the start trigger from the slewing control function, the prism is set to the first angle prescribed in the data file. Once the angle has been set the system begins to look for a stop trigger from the slewing control function. If the system determines that there is no stop trigger then it evaluates the system time versus the next commanded prism angle time. If it is not time to rotate the prism to another angle, the system reevaluates the trigger condition and continues to evaluate these values until one is true. If the system determines that it is time to change the prism angle it picks out the next angle from the data file and sets the prism to the appropriate angle and begins to evaluate the same milestones as before. If a stop trigger command is received from the slewing control function, the function leaves the prism angle sequence and proceeds to the shutdown portion of the function.

*4.2.5.5 End Rotational Control.* Once the software comes out of the rotational control sequence the encoder is shutdown. The software commands the encoder to stop and maintain a position of  $0^\circ$ . Once the command has been transmitted and the motor controller verifies the position, the prism control software function returns to the main sequence.

*4.2.6 Data Collection Example Sequence.* As an example of a data collection sequence the following scenario for the CTE<sub>x</sub> system is provided. The scenario consists of a collection pass over Dayton, Ohio to image a target at Wright-Patterson AFB while the ISS is overhead on March 16, 2013 at an estimated time of 1430 GMT. The camera is to image at 9000 fps with a resolution of 1280x800 and the prism spinning at 40 Hz. It is assumed that the CTE<sub>x</sub> space system has already completed initial calibration but has gone a couple of months without calibration trending. Commands will be uploaded on 3 Mar.

*4.2.6.1 Command Sequence.* The AFIT ground team develops the command sequence to be uploaded to CTE<sub>x</sub> for the needed collection event. The develops the following command sequences in Table 4.3. These commands start by commanding a

Table 4.3: Example Command Sequences

Date	Command
5 Mar 2013	caltrend,1200;
6 Mar 2013	downlink,cal.dat,0800;
16 Mar 2013	target,t,39.823056,-84.049444; camera,9000,1280,800; encoder,v,2400;
17 Mar 2013	downlink,targ.dat,0800;

calibration trending acquisition at 1200 GMT on 5 Mar. The data from this calibration will be downloaded the next day during the designated 0800 time slot. After the calibration we have an acquisition sequence on Mar 16. This acquisition is a tracked target acquisition using the details from the scenario.



*4.2.6.2 CTE<sub>x</sub> Operations.* On 3 March the commands are transmitted to CTE<sub>x</sub>. CTE<sub>x</sub> recognizes the commands and places them in its memory in a tasking order file. On 5 March CTE<sub>x</sub> evaluates the system time vs the calibration command time and executes calibration trending by sliding filters in and out of the optical path while imaging. Once the calibration function is complete the data is saved to system memory. The next day, at the allotted downlink time, CTE<sub>x</sub> begins to transmit the calibration data file to the ground station. The AFIT team evaluates the data and determines that the imaging system is still within calibration limits.

CTE<sub>x</sub> now begins to evaluate the next sequence, the acquisition commands. The first action in the acquisition process is the identification by CTE<sub>x</sub> of “t” flag. The target’s coordinates are then used to calculate the orbital collection window and the camera acquisition window. Using the algorithm’s in the slewing control function and the camera control function respectively the windows are calculated and the system begins to evaluate the system time and position against the calculated windows and date. Additionally, the imaging presets are sent to the camera for system load.

On 16 March during trigger condition evaluation, the software determines that the ISS is within the orbital collection window. A trigger is sent to the encoder which then begins to spin at the commanded 2400 rpm. Concurrently, the system begins to send angle commands to the dwell mirror and it begins to slew to its actuation limits. The system continues to update the dwell mirror with new angles as it calculates the position of the instrument and the target in real-time. Now the system identifies that the ISS is within the less conservative camera acquisition window and the camera control function triggers the camera. While the camera is imaging the SAM-3 is autonomously interrogating the encoder quadrature data and providing that data to the camera for placement in the header of each image.

Finally, the system determines that the ISS has passed outside of the camera acquisition window and sends the stop trigger to the camera. The camera control function, after receiving the stop trigger, transfers the data from the camera to the main system memory. While the transfer is taking place, the system recognizes that the ISS is now outside of the orbital collection window. A stop trigger is sent to the encoder control

function which issues the shutdown command to the encoder and resets the encoder to a zero state. The slew control function then resets the dwell mirror to a zero state. With the data acquisition functions complete they end and return to the main control function.

The next day, the main control function determines that it is time to downlink the acquired data and begins to transmit the data. The AFIT ground team takes control of the data from CTE<sub>x</sub> and runs the chromotomographic algorithm on the data to reconstruct the hyperspectral data cube from the image data.

With the end of the scenario we can see how the different functions work together to accomplish a data acquisition event. Even though there are many steps involved, it is a relatively straight forward and effective initial software design.

### ***4.3 AFIT Ground Station***

The AFIT ground station is a very straight forward and simple design. An initial quote from Front Range Aerospace is attached in Appendix F. Front Range Aerospace has experience in building ground stations, namely the ground station currently at the USAFA. One of the initial goals of the ground station is to be able to communicate with USAFA's FalconSAT 3 currently on orbit. This will allow AFIT to gain valuable experience about ground station operations that will enable future AFIT missions to effectively use this capability. The following description is a basic understanding of the ground station and requires more work with the contractor to flesh out the design. Figure 4.8 shows an initial diagram of how the main components from Front Range Engineering will potentially be connected.

*4.3.0.3 Tracking.* To allow the AFIT ground station to communicate with FalconSAT 3, two roof mounted Yagi antennas are used. These antennas are attached to an antenna tower with a thrust bearing. Yagi antennas are directional antennas and need to be pointed at the satellite to ensure a strong communication link. A tracking computer with NOVA Software for Tracking and Control is used to point the Yagis at the satellite

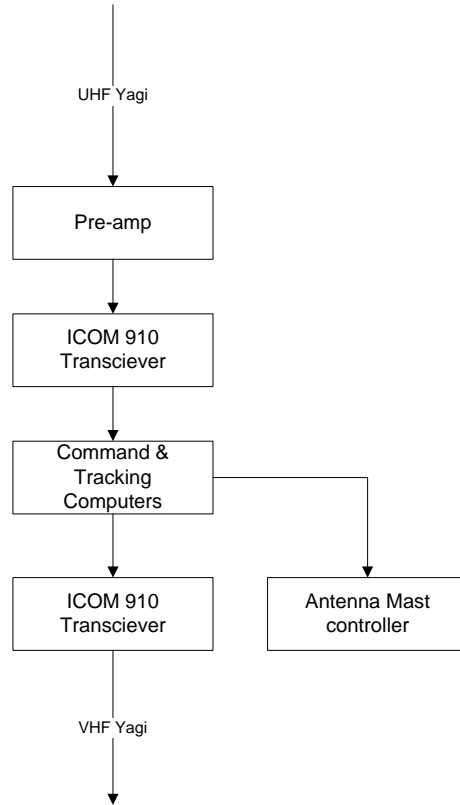


Figure 4.8: Potential AFIT Ground Station Layout

flying overhead. The computer sends commands to an antenna controller which then sweeps the antennas along the path of the satellite.

*4.3.0.4 Downlink.* For downlink, the system uses a Yagi antenna tuned to the UHF frequency range. The signal from the Yagi is conditioned by a preamplifier prior to being received by an ICOM 910 H transceiver. This transceiver demodulates the data and then passes the data to the tracking and command computers for display and data logging.

*4.3.0.5 Uplink.* The uplink leg is just as straight forward and simple as the downlink. The commands are sent via the command computers to the ICOM 910 H transceiver for modulation. From the transceiver the modulated signal is sent through a power meter prior to be sent to the VHF Yagi for transmission.

## V. Conclusions

THIS thesis has investigated preliminary designs of the computer and software for CTE<sub>x</sub>. A brief analysis of the design for a permanent satellite ground station based at AFIT was presented. These designs, though preliminary, lay the foundation for the CTE<sub>x</sub> system and the future detailed design work.

### 5.1 Overview of Designs

*5.1.0.6 Electrical Design.* The computer hardware design presented in the thesis builds upon the HICO and ARTEMIS systems and attempts to take lessons learned from each. HICO uses the PC104 form factor for its system and combines several cards with specific tasks together to perform the mission. ARTEMIS utilizes the cPCI form factor and relies on a modified COTS single board computer with a FPGA card and focused mezzanine cards for data acquisition. The recommended preliminary design for CTE<sub>x</sub> utilizes the cPCI form factor and a COTS single board computer with expansion cards to fulfill the needs of the system.

The DCCU is the computer subsystem for the CTE<sub>x</sub> mission and is housed within a single aluminum chassis engineered by Aitech. The DCCU's processor is the DCP-1201 SBC, manufactured by Curtiss Wright Controls, and it governs all of the activities of the experiment. In order to interface with the other control electronics that the DCP cannot, expansion IP cards are used. These cards provide 1553 and I/O connections for communication with the ISS and the PSU of the CTE<sub>x</sub> system. The last DCCU component is a 128 GB solid state disk from L-3 Targa Systems that provides system memory and non-volatile data storage.

The attitude and determination subsystem consists of a star tracker from Terma and, if needed, a SGR-07 GPS receiver from Surrey Satellite. These components communicate via RS-422 connections to the SBC of the DCCU. Additionally, the control of the telescope internals are performed by numerous actuators that are controlled by their manufacturer suggested controllers, more information about the actuators is available in Section 4.1.5.

The PSU box contains a bank of power conditioning transformers and relays that distribute power throughout CTE<sub>x</sub>. The PSU is connected to the DCCU through a simple digital I/O connection that is used to control the internal relays.

The last subsystem, and probably the most demanding subsystem, is the imaging subsystem. Saving the movie files and correlating the prism angle data is the most taxing event for the system. To help alleviate this, the imaging subsystem utilizes camera equipment from Vision Research and its integrated data acquisition module. The camera selected is the v710 because of its speed and on board memory capacity. To simplify data acquisition the SAM-3 data acquisition system from Vision Research places analog or digital data acquired into the header of the images themselves. This allows for the simplest of hookups and eliminates the need for individually timestamped data files.

*5.1.0.7 Software Design.* The software design is a logical flow that provides flexibility for the execution of experiments. When the system is initialized, it begins to transmit basic telemetry data and goes through a checkout phase. During checkout, the mirror actuators and the motor/encoder assembly are initialized and a lengthy calibration process of the camera occurs. After calibration, the main software function begins and goes into a stand-by mode waiting for transmitted commands.

The main software function then steps through differing paths depending on the commands it receives. If the proper commands are given it can flash the internal memory, effectively performing a reset. The software can also perform calibration of differing complexities on the camera as needed. Lastly, given the correct commands, the software will go into the data acquisition software functions.

In the data acquisition software functions, care is taken to allow flexibility in commanding the experiment. Both global and local variables are used in the three simultaneous data acquisition software functions. The first data acquisition software function discussed is the slewing control function where either a fixed angle or targeting slewing is commanded to the internal telescope mirrors. Either targeting methods triggers the prism control software function to begin spinning the prism. The next function, the camera control software function, sets the camera's resolution and frame rate. The camera

function also transfers the image data from the camera's internal memory to the system's main memory for downlink later. The last software function is probably the simplest function and sets the rotational velocity of the prism. After the data acquisition software functions are complete, the software moves back into stand-by mode.

The last portion of the main software function is the downlink of the data. The system checks its system time versus the designated downlink time. If the times match, the system downlinks the data via the ISS ethernet connection and waits for confirmation from the ground before deleting the data from the system's memory. Just like after the data acquisition, once the main software function completes downlink, the system moves to the stand-by mode and waits for commands.

*5.1.0.8 Ground Station.* The AFIT ground station is heavily based upon the design of the ground station at USAFA. This design is setup to communicate with USAFA's FalconSAT 3 initially but will be connected into NASA for telemetry data from the CTE<sub>x</sub> mission aboard the ISS. The initial design of the ground station consists of Yagi antennas on the roof connected to a LNA then progressing to a receiver. From the receiver the signal is distributed to the control computers. For the uplink, the control computers send the signal to a function generator which places the data onto the carrier frequency and then the data is sent to the antennas for transmission.

## **5.2 Future Work**

This thesis has laid the foundation for future final design tasks for CTE<sub>x</sub>. There are items that need to be addressed in future efforts to ensure that the final design of the CTE<sub>x</sub> system is optimal.

The suitability of Vision Research's SAM-3 for space operations needs to be more fully understood. There is a concern that the current package of the SAM-3 is not rugged enough for use on the ISS. A protoflight test can be performed on the unit to assess worthiness. Another option is working with Vision Research to understand how the SAM-3 inserts the information into the header of the images. This may allow AFIT to develop a more suitable unit for space applications.

Another area of concern that needs to be evaluated is the controllers for the dwell mirror. The dwell mirror requires two actuators, each of which need their own controller. The controller suggested by RC Optics and the actuator manufacturer is powered by AC. While the PSA can condition the DC ISS power to the appropriate AC level it would be a simpler set-up if a DC controller could be found to replace the proposed AC controller.

The interconnections between the electrical subsystems and the DCCU also need to be evaluated for the space and, more importantly, the launch environment. Currently, many of the control boxes utilize USB connectors common to those used on personal computers. This type of has been shown to be sensitive to the harsh launch environment and will almost certainly need to be ruggedized. The trade space about whether the connection needs to be changed to a more standard multi-pin screw on connector or other techniques of locking it in place, still needs to be accomplished.

A special area of need is component survivability with respect to the space environment. Currently the sun is in a period of solar minimum. When the CTE<sub>x</sub> mission is ready for launch the sun should be at or near a peak of solar activity. This peak of solar activity leads to an increase in the number of energetic particles in the Earth's magnetosphere. Aluminium housings can provide shielding versus highly energetic particles and the thicker the aluminium the better shielding it provides. In the low Earth orbit of the ISS, energetic particles are less prevalent than in higher orbits; however, the ISS flies through the south Atlantic anomaly. The south Atlantic anomaly is caused by the offset of the Earth's magnetic field and is an area with less magnetic field strength. The lessening of the magnetic field allows for energetic particles to penetrate closer to the Earth's surface than any other portion of the ISS's orbit. Most of the components listed in this thesis are constructed of commercial electrical components and thus are not hardened against the radiation environment. The system is already partially shielded because the electrical system is contained within a large aluminum experiment "crate" that attaches to the JEM-EF structure. Adding an aluminium enclosure around all of the components would help shield the commercial electrical components and is highly recommended. Additionally, the use of a rad tolerant SBC and SSD should be evaluated.

These two components can act as a system health monitor and a safe system restore if necessary

In general, there is still a lot of design work left to be done on the electrical system. The internal design of the PSU needs to be completed and an evaluation of the backplane of the cPCI DCCU needs to be done. At a minimum it is recommended that a computer or electrical engineer be brought on board the project for complete final design of the electrical systems of the CTE<sub>x</sub> mission.

For the software side, there is also still a lot of work that needs to be done. This thesis only provided basic flow charts for the overall software design but did not provide any code or pseudocode. The next step for the software design is to procure the actual computer components and begin to build the executable code. Additionally, the DLL files associated with the telescope, camera, and attitude determination systems need to be obtained to complete the software coding.

Future work needed on the AFIT ground station is more easily completed. First and foremost, the integration of a network server blade to allow for the connection to the NASA network needs to be completed. The ground station currently being used by the HICO system should be used as foundational material for the AFIT ground station connection. Additionally, prior to the final assembly of the system, antennas need to be placed on the roof and cable runs made to the room containing the ground station equipment.

### **5.3 *Conclusions***

The main goal for this thesis was to lay a foundation for final systems designs of the noted systems for the CTE<sub>x</sub> space experiment. The electrical design shown gives the CTE<sub>x</sub> space experiment the ability to accomplish the task of integrating all of the subsystems and controlling the experiment. Additionally, the cPCI architecture chosen allows the system to be as compact as possible for integration into the limited space available. For the Software design, this thesis presented a flow that maximizes the flexibility in the control of the experiment. The software functions have multiple execution paths that allow the system to react to any desired scenario. Additionally, the software



flowcharts developed can be shown to a code developer and allow them to quickly begin to generate code. Lastly the satellite ground station is an entirely brand new capability that will be available for AFIT. Initially, it will have a meager capability; however, the foundation has been laid that will allow it to be upgraded in the future as AFIT pursues a small satellite program. The design is simple enough that accommodating new capabilities should be easy. All of the preliminary designs that have been discussed, provides foundation that will enable a logical path toward final designs. There is still optimization that needs to be done with these systems; however, the foundation has been created.

## *Appendix A. Satellite Ground Station Parts List*

THE following is a list of parts identified by USAFA and USNA that make up their ground stations.

# USAFA Ground Station

<b>Quantity</b>	<b>Description</b>	<b>Application</b>
1	M2 VHF Yagi Antenna (2MCP14)	VHF Uplink Antenna
1	M2 UHF Yagi Antenna (436CP42 U/G)	VHF Uplink Antenna
1	M2 UHF Yagi Antenna (436CP42 U/G)	UHF Downlink Antenna
2	RC2800PRKX Antenna Controller	Control of Antenna Positioners
1	MT-3000A Elevation Positioner	Elevation Control for VHF/UHF Transmit
1	OR2800P-DC Azimuth Positioner	Azimuth Control for VHF/UHF Transmit
1	AzEI 1000 AzEI Mount Positioner	Az/EI Control for VHF/UHF/S-band Receive
1	7 foot Rohn Mast for Transmit Mount (25G7)	Mounts all Transmit Antennas/Positioners
1	Thrust Bearing for vertical shaft on Transmit tower	65mm thrust bearing to support Xmit vertical shaft
1	7 foot vertical shaft for AzEI1000 Support	7 inch tube reduced to 3" OD to match AzEI1000
2	3 inch x 14 foot Fiberglass through shaft for Tx/Rx	Horizontal shaft for VHF/UHF antenna mounts
1	10 foot parabolic S-band dish (Skyvision 1512015)	Receives down link signals in S-band
1	Antenna mounting yoke for S-band Dish	Couples AzEI1000 to S-band dish and VHF/UHF Receive ant
2	420-450MHz Preamps (P432VDG)	UHF Receive Preamps (hooked in series)
2	144-148MHz Preamps (P144VDG)	VHF Receive Preamps (hooked in series)
1	S-band down converter (2220MHz to 144MHz)	Converts S-band signals to 144 Mhz input to ICOM 910
1	S-band Preamplifier (2442LNAHC)	Preamplifier for S-band downlink
2	ICOM 910H Transceivers (1 Xmit/ 1 Receive)	1 910 used for VHF/UHF/S-band receive; 1 for VHF/UHF Xmit
1	Symek TNC31 Terminal Node Controller	9.6KBs up/down link modem
1	Symek TNC3S (9.6KBS up/76K8/38K4KBs Down)	High Speed S-band Down Link Modem
1	IFD Demodulator for ICOM910 (F-IFD)	IFD board for internal mounting in ICOM 910 (High Speed Data)
1	Rack Mount Astron Power Supply (RM60M)	Power supply for rack radios and antenna preamps
1	Tectronix 40 MHz rack mount scope (TDS1001B)	Observe bit sync of "I" pattern
1	Rack Mount Kit for Oscilloscope	Mounts Oscilloscope in rack
2	Daiwa Power meters (CN-103L)	Monitors output power level and SWR
1	Mirage B-1018G 144MHz Linear Amplifier	High Power output linear amplifier for Uplink VHF
1	Mirage D-1010-N 430MHz Linear Amplifier	High Power output linear amplifier for Uplink UHF
2	12 volt 100 cfm fans (273-243)	mounted on top of Mirage Amps for cooling
1	Windows Radio (WR-G315i)	PCI Bus Windows Radio used as downlink spectrum analyzer
3	Desktop PCs w/PCI bus and RS232 port	Windows XP Pro operating system
2	Nova Software for Antenna Control	Windows software for satellite tracking and antenna control
1	6 foot x 19 inch rack cabinet (WRKSA-4432)	Rack Mount Cabinet
1	Switch panel (3U rack)	Switching receive signals to Winradio Spectrum Analyzer
1	3 x 1 - 25 pin 3 way switch	Switches from one computer/downlink data to all

**USNA Ground Station**

<b>Description</b>	<b>Component</b>	<b>Manufacturer</b>	<b>Quantity</b>
Receiver	700 MRB	L3 Communications	1
IF Filters	720-I(3)	L3	2
Bit Synchronizer	Model 7715	Decom	1
Cisco Router	2600 series	Cisco Systems	1
Az-EI Controller	RC-2800-PRK	M2	1
HP 8648 Transmitter		Hewlett-Packard	1
Rack Mounted Computer	Pentium II	Industrial Computer	1
Power Supply (rack)	120 V	N/A	
Diplexer	D0421601	Microwave Circuits, Inc.	1
Power Amp	AM-178238-30	Comtech PST	1
Low Noise Amplifier	04dBNF	Miteq	1
Power Supply (antenna)	SP-500	Mean Well	1
Helix Cable	N/A		1
Power supply cable			
Antenna Control Cable			
Cable Trays			
Feed Horn for Antenna		N/A	1
Bias-Tees		Mini-Circuits	2
Thin coaxial cable		Pasternack	
Linux software for Rack-Mounted Computer		Linux	1
Windows based NOVA software to track MIDSTAR		NLSA	1
Configuration program for ground station software		N/A	1
Graphical Interface Software		N/A	1

*Appendix B. Data Collection & Command Unit Component Datasheets*



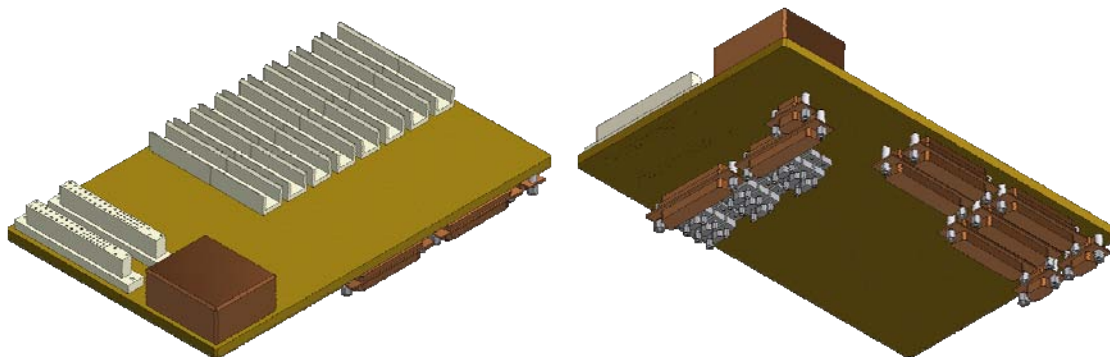
# E900

## 3U CompactPCI Enclosure

---



- ***Rugged Chassis Specially Designed for High Reliability Space Applications***
- ***Dual 28 V/140 W Radiation Tolerant and Latch-up Immune Power Supplies***
- ***8-Slot 3U CompactPCI Compliant Backplane***
- ***Cold Plate Conduction Cooling***
- ***Faraday Cage Design for Enhanced EMI/RFI Performance***
- ***Complete EMI/RFI Power Line Filtering***
- ***Can Accommodate Up to 9 High-Speed I/O Interfaces (Tested to 400Mbps)***
- ***No Wire Harnessing between the Backplane and Front Panel to Increase Overall System Reliability***



---

### Aitech Defense Systems Inc.

A member of the Aitech Rugged Group

9301 Oakdale Ave, Chatsworth, CA 91311

Tel: (888) AITECH-8 (888-248-3248) Fax: (818) 350-6888 e-mail: [sales@rugged.com](mailto:sales@rugged.com) web: [www.rugged.com](http://www.rugged.com)



## **Overview**

The Aitech E900 is a cold plate cooled 8-slot 3U CompactPCI compliant rugged computer enclosure, specially designed for space applications. The power supplies provide standard CompactPCI bus voltages and additional outputs in +15VDC, -15VDC and a dedicated +12VDC to power external equipment.

## **Sturdy Mechanical Design**

The design of the E900 has been optimized to provide maximum strength with minimum weight. Constructed of durable CNC machined 6061-T6 aluminum, the chassis is assembled using stainless steel fasteners to prevent corrosion. Often-used threads have self-locking stainless steel helicoils to withstand severe vibration and shock. All connectors are located on the front panel of the enclosure for easy access. All external surfaces, with the exception of the cold plate interface, are hard anodized coated for excellent corrosion resistance. The cold plate-mating surface is precision machined to ensure excellent heat transfer to the cold plate, and it is configurable to meet any customer-mounting requirements.

## **Board Capacity**

The E900 accommodates 8 standard 3U CompactPCI boards with 0.8 inch pitch per VITA 30.1-2002.

## **CompactPCI Backplane**

The backplane is 3U CompactPCI compliant with J1 and J2 connectors in all slots. By eliminating an intermediate wire harness, all the signals are routed within the backplane to the corresponding front panel I/O connectors.

## **Front Panel**

The chassis front panel is fully customizable to meet customer I/O connector requirements. The middle section of the front panel is available for up to 9 high-speed I/O connectors.

## **Thermally Efficient**

The E900 is conduction cooled through the specially designed sidewalls. Heat is channeled from the power supplies and CompactPCI boards to the cold plate, resulting in a highly efficient

thermal design. The chassis can dissipate more than 75 W of heat to a 55°C cold plate with 15°C  $\Delta T$  to card rails.

## **Electro-Magnetic Compatibility**

Aitech's E900 minimizes EMI/RFI emissions and susceptibility with these features:

- Metal-to-metal clamping with conductive surfaces and fasteners
- Shielded power supply boards
- Shielded power cabling
- Metallic partition between the power supply and VME sections
- Faraday cage input power line filter mounted to the backplane
- Isolated chassis ground and optional connection between chassis GND and signal GND

## **Corrosion Resistant Finish**

External surfaces of the E900 are hard anodize coated for excellent corrosion resistance. As an option, epoxy paint is available with nonstandard colors upon request.

Internal surfaces are chemical conversion coated for corrosion resistance and electrical conductivity. All finishes and components are fungus resistant.

## **High Performance Power Supplies**

The removable power supplies provide continuous high current, high efficiency operation, under the most adverse conditions. The power supplies are designed to meet Low Earth Orbit radiation requirements using radiation tolerant, latch-up immune DC-DC converters.

Major power supply features include:

- Radiation tolerant, latch-up immune, ES screened DC-DC converters
- Extensive input filtering
- Under-voltage input lockout circuit
- Fully isolated inputs and outputs, eliminating the possibility of ground loops
- Monolithic heatsink for efficient power supply cooling and EMI shielding

- Health status output signal routed to backplane I/O connectors
- Outputs protected against
  - Short circuits
  - Thermal breakdown
  - Over-voltage transients
  - Overshoot
- Input protected against
  - Reverse polarity
  - Over-voltage transients

### Power Supply Specifications

- **Input Power**  
Voltage Range (DC) 20 V to 36 V (28 V nominal)
- **Isolation Resistance**  
500 V to output or enclosure
- **Total Output Power** 140 W
- **Efficiency** > 80%
- **Total Ionization Dose** > 25 krad (Si)
- **Latch-up Immune** LET of 37 MeV·cm<sup>2</sup>/mg
- **Output Power:**

### Environmental Specifications

- **Operating Cold Plate Temp.** -55 °C to +70 °C
- **Non-operating Temp.** -55 °C to +125 °C
- **Humidity**  
0%-95% non- condensing
- **Vibration** 16 G<sub>rms</sub> at 20-2000Hz
- **Shock** 40 g terminal sawtooth/11 ms or half SINE
- **Bench Handling**  
4-in unpackaged drop at a 45° angle to simulate conditions during servicing
- **Pressure** Ground to space vacuum
- **EMI/RFI**  
Meets emanation and susceptibility limits

### MTBF

- **S<sub>F</sub>** > 693,088 hours @ 50° C
- **M<sub>L</sub>** > 113,892 hours @ 50° C

Power Supply Output Voltages and Currents				
Nominal (V)	Minimum (V)	Maximum (V)	Current (Amp)	Noise (mVpp)
+3.30V	3.23	3.37	9.1	50mVpp to 10MHz
+5.00V	4.8	5.2	8.0	50mVpp to 10MHz
+12.00V	11.40	12.60	3.3	External Device Dependent
+15.00V	+14.25	+15.75	0.75@ 15V	50mVpp to 10MHz
-15.00V	-14.25	-15.75	0.75@-15V	50mVpp to 10MHz
+12.00V	11.52	12.48	0.25	50mVpp to 10MHz
-12.00V	-11.52	12.48	0.25	50mVpp to 10MHz







## ***General Specifications***

- **Dimensions**

Maximum external dimensions:  
12.0 x 9.2 x 8.0 in (L x W x H)

- **Weight**

Less than 17.5 lbs without boards

- **Power Dissipation Capability**

Exceeds 75 W with CompactPCI boards  
using a 55 °C cold plate (maximum  $\Delta T$  of  
15 °C at card edge).

## ***Accessories***

Aitech offers a wide range of custom mounting  
options and cable sets.

For more information about Aitech's rugged and  
military VME enclosures or any Aitech product,  
please contact your local sales representative or  
our sales office.

For more information about the E900 or any Aitech product,  
please contact Aitech Defense Systems sales department at (888) AITECH-8 (888-248-3248).

All names, products, and/or services mentioned are trademarks or registered trademarks of their respective holders.  
All information contained herein is subject to change without notice.

E900T0110R14

### **Aitech Defense Systems Inc.**

A member of the Aitech Rugged Group

9301 Oakdale Ave, Chatsworth, CA 91311

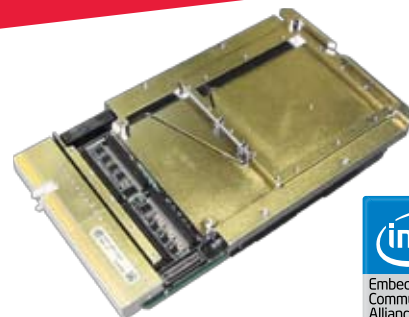
Tel: (888) AITECH-8 (888-248-3248) Fax: (818) 350-6888 e-mail: [sales@rugged.com](mailto:sales@rugged.com) web: [www.rugged.com](http://www.rugged.com)



# SCP/DCP-1201

## Dual Core™ Intel® CompactPCI

### Single Board Computer



#### Features

- ◆ Intel® Core™2 Duo
  - 1.5GHz @ 17W (ultra low voltage)
  - 667MHz (5.3GB/s) FSB
  - 64KB L1 cache per core
  - 4MB shared L2 advanced transfer cache
  - 1GB of DDR2 SDRAM with ECC
  - 3.2GB/s memory bandwidth
  - Intel MMX, SSE, SSE2, and SSE3 SIMD instruction support
- ◆ High-performance Intel 7520 MCH
- ◆ 6300 ESB ICH
- ◆ 16Mb (2MB) Firmware hub
  - Hardware FLASH write protection jumper
- ◆ 1GB on-board FLASH drive
- ◆ Two 10/100/1000 Ethernet interfaces
- ◆ 3U CompactPCI 33/66MHz interface
- ◆ Two RS-232 Async COM ports
- ◆ Three RS-422 Async COM ports
- ◆ One PMC site, 64-bit/66MHz PCIX
- ◆ Optimized for conduction-cooled PMCs
- ◆ Capacitor backed real time clock
- ◆ Additional I/O Options include:
  - 3x USB ports
  - 3x RS-422 COM ports
  - 1x SATA port
  - 5x GPIO lines
- ◆ State-of-the-art EFI BIOS
- ◆ Window®, Linux®, VxWorks® 6.x BSPs, LynxOS SE, Solaris 10 and WindRiver™ GPP Linux® 2.6
- ◆ World class Longevity of Supply and Longevity or Repair supplied by the Life Cycle support group
- ◆ On-board temperature sensors
- ◆ Basecard uses 3.3/5V from backplane 3.3V, 5V, and +/-12V are routed to the PMC sites
- ◆ Occupies dual 1.6" slot in air-cooled configurations
- ◆ Occupies single .8" pitch slot in air- and conduction-cooled configurations
- ◆ Optimized conduction cooling with TherMax™ thermal frame and direct processor shunts
- ◆ EFI BIOS supports Ethernet and USB storage devices
  - Debug monitor with system exerciser functions in BIOS
  - Power-up BIT (PBIT)
  - Embedded non-volatile memory programmer (NVMP) for BIOS updates
- ◆ VxWorks® /Tornado™ integration:
  - Tornado 2.2.x and Workbench 2.0
  - Full suite of drivers for hardware features
  - Run-time BIT libraries for Initiated and Continuous BIT
- ◆ Intel supplied DSP libraries for Windows and Linux
- ◆ Available in a range of ruggedization levels, both air- and conduction-cooled

Please note:

All hardware features may not be supported by all operating systems. Contact Curtiss-Wright for details and release schedules.

#### Learn More

Web / [cwcembedded.com](http://cwcembedded.com)

Email / [sales@cwcembedded.com](mailto:sales@cwcembedded.com)

**CURTISS  
WRIGHT** Controls  
Embedded Computing

Innovation In Motion.  
[cwcembedded.com](http://cwcembedded.com)



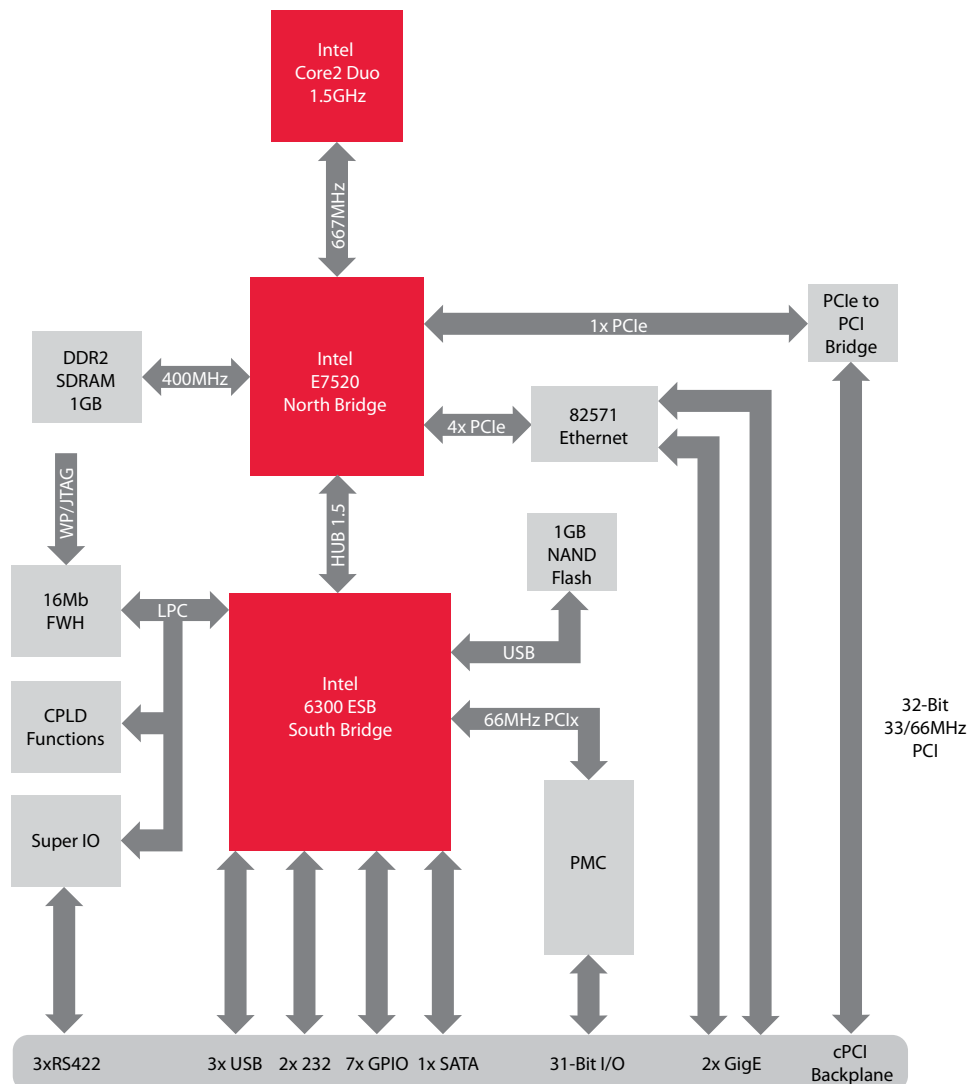
## Overview

The S/DCP-1201 from Curtiss-Wright Controls supports one Intel® Core™2 Duo. With a Core2 Duo processor the 1201 acts as a dual CPU 3U CompactPCI (cPCI) Single Board Computer (SBC) built to meet the diverse needs of the evolving embedded community. With the addition of a SATA or USB hard drive, the SCP-1201 becomes a full-featured computing platform. In addition to running Windows XPe™, the SCP-1201 runs Linux 2.6™ operating system. Support for VxWorks 6.x™ for real-time applications is in development.

The 1201 is designed for rugged and benign air-cooled and conduction-cooled systems. It has support for a clock calendar and NVRAM from a system supplied battery backup and/or on-board capacitor. A user programmable operating frequency allows dynamic, user controlled power consumption adjustment.

The 1201 supports several rear I/O configurations. The 1201 is designed for embedded systems concerned with performance per watt. It also supports those users that desire the Windows XPe™ operating system for legacy, driver, or development reasons.

Figure 1: SCP/DCP-1201 Flow-through Architecture





## Powerful Intel Server Architecture

The SCP/DCP-1201 was designed around Intel's state-of-the-art Core2 Duo processors and the high-performance 7520 Northbridge Memory Controller (MCH) and the Intel 6300ESB Southbridge (ICH). These components were specifically designed for server class applications and provide the ultimate in performance. The 7520 Northbridge supports the following features:

- ♦ 667MHz Front Side Bus (FSB) which provides 5.3GB/s of data transfer performance between the memory controller and CPUs
- ♦ Single 400MHz DDR2 memory bus provides 3.2GB/s of memory bandwidth
- ♦ Two PCI Express® (PCIe) links provide high full-duplex I/O bandwidth (up to 1GB/s in each direction)

Careful attention was paid to the flow-through I/O design in the 1201 architecture. Data can be input from the PMC, written to memory, processed by the Dual Core CPU and output to other boards in the chassis, maximizing the I/O and memory bandwidth of all components involved.

Hardware enforced cache coherency, read prefetching, write posting and many other features built into the Intel 7520 MCH provide world class throughput for I/O and processor intensive applications. Applications requiring maximum sustained throughput are ideally suited to this single board computer.

The SCP/DCP-1201 has a rich set of I/O capabilities as well. An Intel 6300ESB Southbridge combined with a dual channel GigaBit Ethernet controller, and a super I/O chip are all present in the design. Various I/O modes provide access to the following capabilities:

- ♦ 1x Serial ATA port (1.0)
- ♦ 2x RS-232 Async Ports
- ♦ 5x GPIO
- ♦ 2x GigaBit Ethernet ports
- ♦ 3x RS-422 Async ports
- ♦ 1x PMC Site
- ♦ 3x USB ports
- ♦ 1x On-board USB FLASH

## Power Consumption and CPU Tuning

For applications requiring ultra low power consumption, the SCP/DCP-1201 comes with a configurable BIOS capable of turning off one of the processing cores and providing the ability to adjust the processor core speed. In low power consumption modes, the 1201 draws less than 20W.

Aside from the ability of parking one processor core, the BIOS for the SCP/DCP-1201 is capable of setting the processor clock speed at slower frequencies to save power. The default setting is full speed at 1.5GHz, however the 1201 processor can also be set to a medium speed of 1.33GHz or a slow speed of 1.0GHz. The following table summarizes the power requirements of the Core2 Duo in different speed settings and parked CPU core modes.

Table 1: Power requirements of the Core2 Duo

S1201 with Intel Core2Duo running @ 1.5GHz (+/-12V rails - no power draw)	5V Rail Current (A)	3.3V Rail Current (A)	Power (W)
Dual Core / 1.5GHz / TDP, 2xGbE 500Mbps xfer	6.2	0.6	33.7
Single Core / 1.5GHz / TDP, 2xGbE 500Mbps xfer	5.0	0.6	27.5
Dual Core / 1.33GHz / TDP, 2xGbE 500Mbps xfer	5.7	0.6	31.3
Single Core / 1.33GHz / TDP, 2xGbE 500Mbps xfer	4.8	0.6	26.5
Dual Core / 1.0GHz / TDP, 2xGbE 500Mbps xfer	5.0	0.6	27.5
Single Core / 1.0GHz / TDP, 2xGbE 500Mbps xfer	4.4	0.6	24.7

Notes:

1. TDP: Thermal Design Power – Set by Intel at 85%



## High Performance PMC support

One PMC site complements the flow-through architecture of the SCP/DCP-1201. The PMC site shown in the 1201 block diagram (Figure 1) supports PCIe @ 64-bits/66MHz with 3.3V signaling only.

Due to the component density and connector placement on the SCP/DCP-1201 there are some potential issues with the PMC keep-out area of the single PMC site. These issues are only likely to arise for air-cooled PMCs. Memory components on the top side of the board may interfere with PMC front I/O connectors that require the full keep-out area. The interfering memory components are approximately .5mm thick. All versions of the SCP/DCP-1201 have memory parts mounted in the keep-out area of the PMC site.

Figure 2: SCP-1201-4223 Air-cooled 2-slot

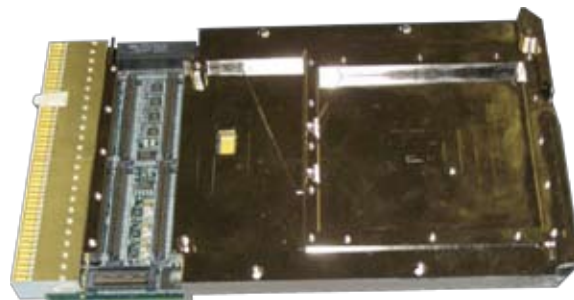


## Designed for Harsh Environments

To cost-effectively address a diverse range of military/aerospace applications, the SCP/DCP-1201 is available in a range of ruggedization levels, both air- and conduction-cooled.

All versions are functionally identical, with air-cooled versions (SCP) available in Curtiss-Wright ruggedization levels 0 and 100, and a conduction-cooled version (DCP) in level 200. Air-cooled level 200 is available on a special order basis. Curtiss-Wright's standard ruggedization guidelines define the environmental tolerance of each ruggedization level (see Curtiss-Wright's Ruggedization Guidelines fact sheet for more information).

Figure 3: DCP-1201-2223 Conduction-cooled 1-slot



## Enhanced Thermal Management for Conduction-Cooled Applications

For those demanding application environments that require conduction-cooling, the 1201 uses a combination of thermal management layers within the Printed Wiring Board (PWB) and an aluminum thermal frame that provides a cooling path for the PMC site and for high-power components such as the processors, caches, and bridge devices. The 1201 thermal frame employs a number of innovative design techniques to keep the temperature rise of the electronic components to a minimum, thus increasing the long-term reliability of the product:

- ◆ Direct processor thermal shunts
- ◆ Provision of both primary and secondary thermal interfaces on PMC sites
- ◆ Mid-plane thermal shunts for PMC site
- ◆ TherMax design approach
- ◆ Full-width thermal interface to back-side slot wall

## Mid-plane thermal shunts for PMCs

To optimize the conduction-cooling of high performance, high power PMC modules such as graphics or networking PMCs, the 1201 thermal frame incorporates mid-plane thermal shunts for the PMC site. High power PMCs can include a mating cooling surface on the PMC module to contact the mid-plane thermal shunt. By taking advantage of the thermal shunt, suitably designed PMC modules can significantly lower the heat rise from the 1201 card edge to the PMC components. The mid-plane thermal shunt does not impinge on the VITA-20 allowed component height.

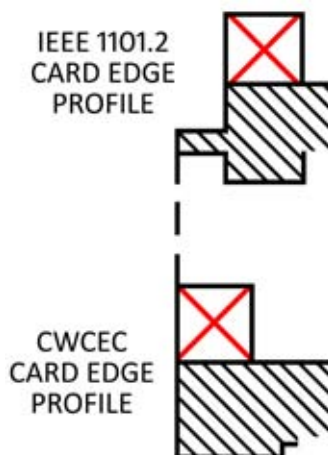




## TherMax-style thermal frame

A TherMax™ thermal frame provides an unbroken metallic path from the PMC sites and shunted components to the back-side cooling surface of the card therefore minimizing the temperature rise to these devices. In comparison, a typical thermal frame simply sits on top of the PWB and forces heat to flow through the PWB which has a high thermal resistance compared to aluminum.

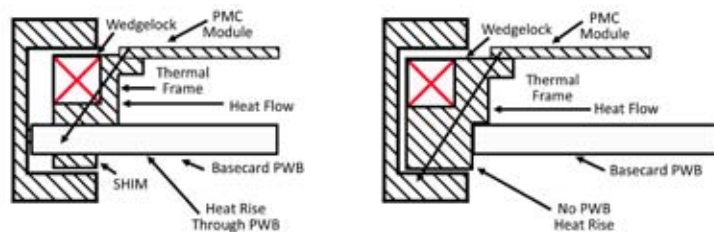
Figure 4: Deviation from 1101.2 Standard



## Full-width thermal interface to back-side slot wall

To minimize the temperature rise from the mating slot wall of conduction-cooled enclosures to the back-side thermal interface region of the 1201, the 1201 thermal frame maximizes the thermal interface area by extending the frame to the full width of the card, as illustrated in Figure 5. This deviation from the IEEE 1101.2 standard, which calls for the thermal frame to be notched for compatibility with card guides in standard air-cooled chassis, has the benefit of lower card operating temperatures and increased long-term reliability. During test and integration activities where it may be desirable to install a conduction-cooled 1201 into an air-cooled card-cage, this can normally be accomplished simply by removing the card guides

Figure 5: TherMax Style Thermal Frame



## Built in Self Test (BIT)

Curtiss-Wright's COTS Continuum Initiative defines common software and user interfaces for all Curtiss-Wright products. The SCP/DCP-1201 is designed with a rich set of Built-In-Test (BIT) functions both at the BIOS and operating system levels.

## Ordering Information

The SCP/DCP-1201 is available in both air- and conduction-cooled variants. There are two air-cooled ruggedization levels (L0, and L100) and one conduction-cooled ruggedization level (L200). All ruggedization levels greater than L0 have an acrylic conformal coating. The SCP/DCP-1201 adheres to the standard Curtiss-Wright ruggedization standards below:



Table 2: Ruggedization

	Air-cooled		Conduction-cooled
	Level 0	Level 100	Level 200
Operating Temperature	0°C - 50°C (Note 4)	-40°C - 71°C (Note 4)	-40°C - 85°C (Note 6)
Non-Operating Temperature (Storage)	-40°C - 85°C	-55°C - 125°C	-55°C - 125°C
Operating Humidity (Non-condensing)	0 - 95%	0 - 100%	0 - 100%
Non-Operating Humidity (Storage, condensing)	0 - 95%	0 - 100%	0 - 100%
Vibration Sine (Note 1)	2g peak 15-2k Hz	10g peak 15-2k Hz	10g peak 15-2k Hz
Vibration Random (Note 2)	0.01g <sup>2</sup> /Hz 15-2k Hz	0.04g <sup>2</sup> /Hz 15-2k Hz	0.1g <sup>2</sup> /Hz 15-2k Hz
Shock (Note 3)	20g peak	30g peak	40g peak
Conformal Coat (Note 5)	No	Yes	Yes
2 Level Maintenance Ready	-	-	No

Notes:

1. Sine vibration based on a sine sweep duration of 10 minutes per axis in each of three mutually perpendicular axes.
2. May be displacement limited from 15 to 44Hz, depending on specific test equipment.
3. Random vibration 60 minutes per axis, in each of three mutually perpendicular axes.
4. Three hits in each axis, both directions, 1/2 sine and saw tooth. Total 36 hits.
5. Standard air-flow is 8 cfm at sea level. Some higher-powered products may require additional airflow. Consult the factory for details.
6. Conformal coating type is manufacturing site-specific. Please consult the factory for details.

Table 3: Specifications

Power	<34 Watts maximum, 10 Watts standby, 5V and 3.3V Power required
PMC	3.3V I/O
Weight	340 grams (est)

## Warranty

This product has a one year warranty.

## Contact Information

To find your appropriate sales representative, please visit:

Website: [www.cwcmbedded.com/sales](http://www.cwcmbedded.com/sales)

Email: [sales@cwcmbedded.com](mailto:sales@cwcmbedded.com)

For technical support, please visit:

Website: [www.cwcmbedded.com/support1](http://www.cwcmbedded.com/support1)

Email: [support1@cwcmbedded.com](mailto:support1@cwcmbedded.com)

The information in this document is subject to change without notice and should not be construed as a commitment by Curtiss-Wright Controls Inc., Embedded Computing (CWCEC) group. While reasonable precautions have been taken, CWCEC assumes no responsibility for any errors that may appear in this document. All products shown or mentioned are trademarks or registered trademarks of their respective owners.

## AcPC8635 CompactPCI®, Nonintelligent, 3U IP Carrier Card

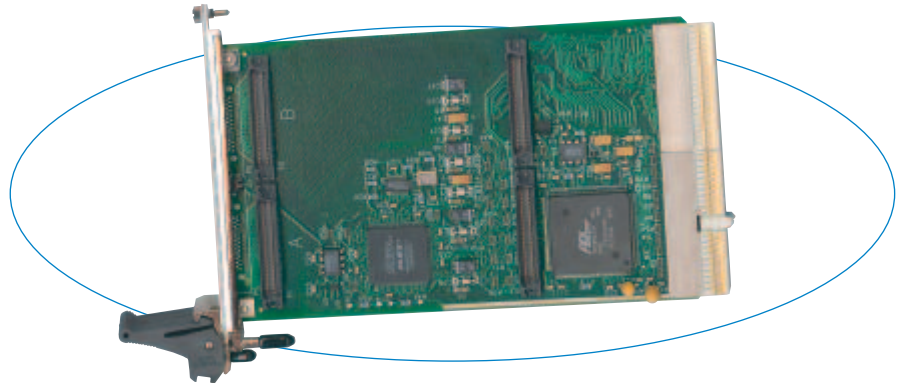
The AcPC8635 is a nonintelligent slave board that interfaces two IP modules to the CompactPCI® (cPCI) bus. All 100 I/O points are brought out the rear J2 connector. This convenience eliminates messy cables from hanging out the front of the cage. In addition to a more efficient cage wiring design, it is also much easier to insert and replace boards.

### Features

- Two industry-standard IP module slots
- Board resides in memory space
- Supports IP module I/O, ID and INT spaces
- 100 I/O points with rear access
- High-density rear connectors
- Compatible with 32-bit CompactPCI® backplane
- Plug-and-play carrier configuration and interrupt support
- Two interrupt channels per IP module
- Front panel LEDs
- Supervisory circuit for reset generation
- Individually filtered and fused power to each IP
- Ruggedized with ESD strip and EMC front panel
- Easily integrate IPs with your software using RTOS VxWorks, QNX, Linux, or Win DLL for Windows® 95/98/2000/XP.

### Benefits

- Clean system cabling.
- Easy board replacement as I/O needs change.
- Simplified debugging with status LEDs.
- Quick development of custom I/O boards.
- Flexibility to mix and match I/O functions as requirements change.



Mix and match plug-in modules with different I/O functions to quickly create custom I/O boards.

### Operation

Acromag's carrier boards provide full data access to the IP module's I/O, ID and interrupt spaces. With full access to the programmable registers, you can easily configure and control the operation of the IP modules from the cPCI bus.

Up to two interrupt requests are supported for each IP module. All board interrupts are mapped to PCI bus INTA# signal.

Individual passive filters on each IP power supply line provide optimum filtering and noise isolation between the IP modules and the carrier board.

### Specifications

#### IP Compliance (ANSI/VITA 4)

Meets IP specs per ANSI/VITA 4-1995 (8MHz operation only) and IP I/O mapping to J2 per PICMG 2.4 R1.0.

Electrical/mechanical interface:

Supports single or double size IP modules.  
32-bit IP modules are not supported.

IP Module I/O space, ID space, and INT space supported.

IP Module Memory space: Not supported.

Interrupts: Supports two interrupt requests per IP module and interrupt acknowledge cycles via access to IP INT space.

#### CompactPCI bus Compliance

Meets PCI spec. V2.1 and PICMG 2.0, R2.1.

Data transfer bus: Slave with 32-bit, 16-bit, and 8-bit data transfer operation. 32-bit read/write accesses are implemented as two 16-bit transfers to the IPs.

Interrupts: CompactPCI bus INTA# interrupt signal. Up to two requests sourced from each IP mapped to INTA#. Interrupts come from IP modules via access to IP module INT space.

32-bit memory space: Upon power-up, the system auto-configuration process (plug & play) maps the carrier's base address (for a 1K byte block of memory) into the PCI bus 32-bit memory space.

### Environmental

Operating temperature: 0 to 70°C (AcPC8635 model) or -40 to 85°C (AcPC8635E model).

Storage temperature: -55 to 100°C.

Relative humidity: 5 to 95% non-condensing.

Power:

+5V (±5%): 200mA maximum.

±12V (±5%): 0mA (not used).

Plus IP module load.

MTBF: Consult factory.

### Ordering Information

#### Industry Pack Carriers

**AcPC8635:** CompactPCI carrier. Holds two IP modules.

**AcPC8635E:** Same as AcPC8635 with extended temp. range.

**Software** (see [software documentation](#) for details)

**IPSW-API-VXW:** VxWorks® software support package

**IPSW-API-QNX:** QNX® software support package

**IPSW-API-WIN:** Windows® DLL driver software support pkg.

**IPSW-LINUX:** Linux™ support (website download only)

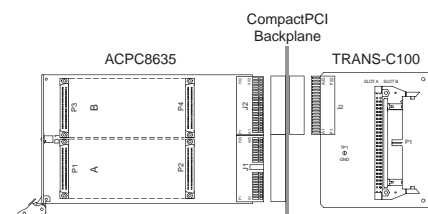
**Accessories** (see [accessories documentation](#) for details)

**5025-550:** Cable, unshielded, 50-pin header both ends

**5025-551:** Same as 5025-550 except shielded

**5025-552:** Termination panel, 50-pin connector, 50 screw terminals

**TRANS-C100:** Transition module



All trademarks are the property of their respective owners.



## IP409 Differential Digital Input/Output

The IP409 provides 24 differential I/O channels with interrupts. Each channel is programmable as an input or an output on a bit basis, in any combination. All channels can generate change-of-state (COS), low, or high level transition interrupts.

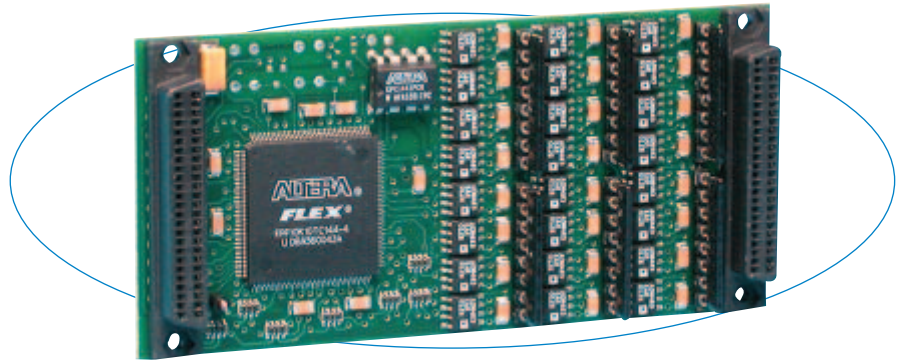
Each channel uses a robust RS485/422A transceiver that supports bi-directional data transfer in one direction at a time (half-duplex). Differential data transmission enables reliable, high speed communication across distances of up to 4000 feet, even through noisy environments. Differential transmission nullifies the effects of ground shifts and noise signals which appear as common-mode voltages on the line.

### Features

- 24 digital input and/or output channels
- Output channels support readback monitoring
- Socketed termination resistors
- Ruggedized RS422A/485 transceivers
- Interrupt support on all channels
  - change-of-state
  - high or low level transition
- Positive and negative current limiting
- Parallel I/O for up to 24 bits

### Benefits

- All channels programmable as inputs or outputs.
- Differential data transmission is ideal for high-speed, long distance communication in noisy environments.



The IP409 has 24 channels with interrupts for reliable, high-speed serial or parallel data transfer across noisy environments.

### Specifications

#### RS485 Transceivers

Bus common mode range: -7 to 12V.  
 Channel configuration: 24 independent, non-isolated RS485/422A serial ports with a common signal return connection.  
 Data rate: 250K bits/second, maximum.  
 Cable length: 4000 feet, maximum. Use of a signal repeater can extend transmission distances.  
 Termination resistors: 120 ohm resistors installed in board sockets at network endpoints only.  
 Differential output voltage: 5V, maximum. 1.5V minimum (with 27 ohm load).  
 Common mode output voltage: 3V, maximum.  
 Output short circuit current: 250mA, maximum.  
 Rise/fall time: 250nS, minimum, 800nS, typical. 2000nS, maximum.  
 Receiver input impedance: 12K ohms.

#### IP Compliance (ANSI/VITA 4)

Meets IP specifications per ANSI/VITA 4-1995.  
 IP data transfer cycle types supported:  
 Input/output (IOSel\*), ID read (IDSel\*).  
 Access Time (8MHz clock): 0 wait states (250nS cycle).  
 Interrupt handling format: An 8-bit vector is provided during interrupt acknowledge cycles on D0 - D7.

#### Environmental

Operating temperature: 0 to 70°C (IP409) or -40 to 85°C (IP409E).  
 Storage temperature: -55 to 125°C (all models).  
 Relative Humidity: 5 to 95% non-condensing  
 Power:  
 +5V (±5%): 50mA maximum.  
 ±12V (±5%) from P1: Not used.  
 MTBF: 5,258,978 hrs at 25°C, MIL-HDBK-217F, Notice 2.

### Ordering Information

#### Industry Pack Modules

##### IP409

Differential digital I/O module

##### IP409E

Same as IP409 plus extended temperature range

Acromag offers a wide selection of [Industry Pack Carrier Cards](#).

#### Software (see [software documentation](#) for details)

##### IPSW-API-VXW

VxWorks® software support package

##### IPSW-API-QNX

QNX® software support package

##### IPSW-API-WIN

Windows® DLL driver software support package

##### IPSW-LINUX

Linux™ support (website download only)

See [accessories documentation](#) for additional information.

All trademarks are the property of their respective owners.

# **DYNAMIC ENGINEERING**

150 DuBois St. Suite C Santa Cruz, CA 95060

831-457-8891 **Fax** 831-457-4793

sales@dyneng.com

www.dyneng.com

Est. 1988

## **User Manual**

# **IP-1553**

**MIL-STD-1553 Interface  
1 or 2 Dual Redundant channels  
direct or transformer coupled**

**IndustryPack® Module**



Revision B

Corresponding Hardware: Revision A

PROM revision C0

10-2006-1401

## Specifications

Host Interface:	IP Module 8 and 32 MHz capable
1553 Interface:	1/2 Redundant Channels with full protocol support
Tx Data rates generated:	Programmable. 20 MHz reference to ACE
Software Interface:	Control Registers, Status Ports
Initialization:	Hardware Reset forces all registers [except vector] to 0.
Access Modes:	IO, Memory, ID, INT spaces (see memory map)
Wait States:	minimized based on programmed clock rate
Interrupt:	Channel interrupt for each 1553 channel Software interrupt
Onboard Options:	Most Options are Software Programmable. Shunt options for direct and transformer coupled operation
Interface Options:	IP IO connector routed through IP Carrier. ARINC 1553 compatible cable with proper termination recommended
Dimensions:	Type 1 IP Module.
Construction:	High temp FR4 Multi-Layer Printed Circuit, Through Hole and Surface Mount Components. Programmable parts are socketed.
Temperature Coefficient:	.89 W/°C for uniform heat across IP
Power:	Typical <b>XX</b> mA @ 5V in Direct Coupled Mode running channel to channel test
Temperature Range	Industrial Temperature rated -40 + 85C. Conformal Coating option for condensing environments



# L-3 Targa Systems VME & cPCI SSD Storage

## OVERVIEW

Targa's VME and cPCI form factor SATA / USB SSD Storage modules have been specifically designed to replace hard disk drives in rugged and environmentally demanding applications. The single slot, module design is based on 2.5" FLASH SATA disks and is available in both convection cooled and conduction cooled form factors and is available with a user selectable SATA or USB interface, single or dual disk versions.

- SATA 1.5Ghz or USB Mass Storage Device / Bulk Transport
- Ruggedized, high reliability, solid state design, no moving parts
- SATA and USB interconnect via backplane
- Single slot Capacity: 32GB – 128GB per disk
- Dual slot Capacity: 256GB per disk
- Low power consumption
- Special Features: Write protect and Erase/Sanitize

## PRODUCT MODEL NUMBERS

Targa's SSD Storage modules are available in a broad range of memory capacities and environmental classifications. The product model designations are:

Single Disk		
VME – 6U	cPCI – 6U	cPCI – 3U
VME25/SAn-d1-ee	CPCI625/SAn-d1-ee	CPCI325/SAn-d1-ee
Dual Disk		
VME – 6U	cPCI – 6U	n/a
VME25/SAn- d1-d2-ee	CPCI625/SAn-d1-d2-ee	n/a

SAn	Disk ID	dn	capacity	ee	environmental class
Contact Targa for details			32G; 64G; 128G; 256G	00	Basic
				20	Extended
				50	Conduction Cooled



Conduction Cooled Units



communications

Targa Systems



communications

Targa Systems

Targa's Solid State Storage Solutions are available in a wide range of form factors and interfaces.

- 6U VME SATA, USB, ATA
- 6U cPCI SATA, USB, ATA
- 3U cPCI SATA, USB
- PC Card DTU's  
Ethernet NAS, SATA, USB,  
Serial, SCSI,
- Removable Disk Systems  
Ethernet NAS, USB, SATA
- USB Flash Disks - 3.5"

Website:  
[www.targasystems.com](http://www.targasystems.com)

Sales:  
Phone: 704.246.6170  
Email:  
[sales@targasystems.com](mailto:sales@targasystems.com)

Headquarters:  
Ottawa, Ontario, Canada  
Phone: 613.727.9876  
Email:  
[sales@targasystems.com](mailto:sales@targasystems.com)

# VME & cPCI SSD Storage Module

## SPECIFICATIONS

	VME25	cPCI625	cPCI325
<b>Form factor</b>	6U IEE1014-1987	6U PICMG 2.0 R3.0	3U PICMG 2.0 R3.0
<b>Power</b>	+5Vdc	4.85 – 5.25Vdc	4.85 – 5.25Vdc
	1.25A – single	1.25A – single	1.25A
	2.5A - dual	2.5A - dual	
	+3.3Vdc	3.15 – 3.45Vdc	3.15 – 3.45Vdc
	-	0.75A	0.75A
<b>Weight (nominal)</b>			
ee = 00; 20	450 g	450 g	300 g
ee = 50	750 g	750 g	375 g

<b>Interface</b> <sup>1</sup>	SATA 1.5Ghz, ATA-7, SATA 2.6	USB 2.0 Mass Storage – Bulk Transport
<b>Transfer Rates</b> <sup>2</sup>	> 30 MB/sec	> 10 MB/sec

1. Only one interface active at any one time, auto detected at power on.

2. Transfer rates are dependent on the SATA "disk ID" type and data transfer block size. Rates as stated were measured for a 500MB transfer using an /SA3 disk with 16KB block size.

<b>Data Integrity</b>	Static wear leveling and ECC/ECD (reed Solomon) defect management
<b>Write Endurance</b>	> 200 years @ 200GB/day for a 64GB unit
<b>Data Integrity</b>	> 10 Years at 25C
<b>Front Panel LEDs</b>	Power Busy Write Protect

Environmental	Basic (-00)	Extended (-20)	Conduction Cooled (-50)
Operating Temperature	0°C to +60°C	-40°C to +85°C	-40°C to +71°C
Storage Temperature	-55°C to +95°C	-55°C to +95°C	-55°C to +95°C
Altitude	50,000 ft	50,000 ft	50,000 ft
Ascent, Descent	10 m/s, 13 m/s	10 m/s, 13 m/s	10 m/s, 13 m/s
Humidity	10 – 85%	----- 10 – 100% with condensation -----	
Shock	n/a	8g, 11ms, ½ sine	20g, 11ms, ½ sine
Vibration	n/a	0.02 g <sup>2</sup> /Hz 5 to 2000 Hz	0.04 g <sup>2</sup> /Hz 5 to 2000 Hz
Stiffening Ribs	No	Yes	Yes
Conformal Coat	No	Yes	Yes

Specifications are subject to change without notice.

Targa Systems Division L-3 Communications Canada Inc. Code 08152009

## *Appendix C. CTE<sub>x</sub> Imaging System Component Datasheets*

## DATA SHEET

### v710

Ultra-fast – 1.4 million fps

1280 x 800 at 7500 fps

300 ns digital exposure

Phantom CineMag® compatible



#### Key Benefits:

#### WHEN IT'S TOO FAST TO SEE, AND TOO IMPORTANT NOT TO®

**Introducing** the Phantom v710 – a megapixel camera capable of taking 1,400,000 pictures-per-second.

Building on the architecture of the award winning Phantom v12.1 digital high-speed camera, the Phantom v710 goes beyond ultra-high-speeds and delivers the user-convenience features you need: remote/automatic black referencing, Versatile Dual HD-SDI outputs, a component viewfinder port, high-speed synchronization, range data input and Phantom CineMag support.

**Take the wide view** with our custom-designed 1280 x 800 CMOS sensor. The wide aspect ratio of the v710 – 25% wider than square cameras – allows you to keep moving targets in-frame longer and see more of the event you are recording. The v710's widescreen aspect ratio also provides the unique ability to shoot 1280 x 720 HD with a one megapixel camera.

Get over 7500 frames-per-second (fps) at full megapixel resolution. At lower resolutions, you will get even higher frame rates, up to **1,400,000 fps** (optional).

#### Key Features:

Over 7500 frames-per-second (fps) at full resolution.

Maximum fps (128 x 8): 680,000 standard, 1,400,000 (optional & export controlled)

1280 x 800 CMOS sensor

Exposure Time (shutter speed): 1 µs standard

Sub-microsecond shuttering: 300 ns (optional & export controlled)

High-resolution timing system: Better than 20 ns resolution

Extreme Dynamic Range (EDR): Two different exposures within a single frame

Internal Shutter: Hands-free/remote current session reference (CSR)

Memory Segmentation: Up to 63 segments

Non-volatile, hot-swappable Phantom CineMag memory magazines (128 GiB, 256 GiB & 512 GiB)

Range Data input

Built-in Memory: 8 GiB, 16 GiB, 32 GiB

ISO (ISO-12232 SAT): 7000 Mono, 2100 Color

Pixel Bit-depth: 8- and 12-bit

Gb Ethernet

View recordings immediately via video-out port

Versatile Dual HD-SDI ports configured to meet your needs



Phantom v710  
a megapixel  
camera  
capable  
of taking  
1,400,000  
pictures-  
per-  
second...

With an active pixel size of 20 microns and improved quantum efficiency, the Phantom v710 camera has unsurpassed **sensitivity**. So, even if you are using our sub-microsecond shuttering, you'll get the highest sensitivity with the lowest noise possible.

That's right. You can eliminate blur and see the most minute detail by using our optional **sub-microsecond shuttering**. Down to 300 nanoseconds, programmable in 18 ns increments.

Each camera supports **8- and 12-bit pixel depth**. Smaller bit-depth gives you more recording time and smaller files. Greater bit-depth gives you more gray levels and finer detail. With the greater latitude of 12-bits, you can pull more detail out of the image.

The v710's **high-resolution timing** system yields a timing resolution of better than 20 ns. Frame rate, frame synchronization and exposure accuracy are all improved over previous generations of high-speed cameras. And, a frame synchronization signal is now available via a dedicated BNC for easier cabling and increased signal integrity. This makes the camera perfect for **PIV applications** with a 500 nanosecond straddle time and no image lag. Another PIV-specific feature is the v710's unique shutter-off setting which keeps the electronic global shutter open throughout the entire frame acquisition time allowing external strobe lights or pulsed lasers to control the exposure for each frame.

Of course, the v710 offers our unique **Extreme Dynamic Range (EDR)** feature giving you the ability to get two different exposures within a single frame. And, with **auto exposure**, the camera adjusts to changing lighting conditions automatically.

There is an **internal shutter** for shading the sensor when doing a session-specific black reference (CSR). Whenever you do a CSR from the Phantom Software, the shutter closes automatically. You no longer have to manually shade the sensor with a lens cap!



The v710 comes with 8 GiB of high-speed dynamic RAM standard, but you can order 16 GiB or 32 GiB versions. Our **segmented memory** allows you to divide this into up to 63 segments so you can take multiple shots back-to-back without the need to download data from the camera.

Or, record directly to our **Phantom CineMag** non-volatile, hot-swappable memory magazines. They mount on the CineMag compatible version of the camera. Continuously record full resolution cines into non-volatile memory at up to 800 fps. That's just over 2 minutes into the 128 GiB CineMag, 4.25 minutes into the 256 GiB CineMag, or 8.5 minutes into the 512 GiB CineMag. Or, record at even higher speeds into camera RAM, then manually or automatically move your cine to the CineMag. With CineMag storage you get maximum data protection and an ideal storage medium for secure environments.

Move the CineMag from the camera to a **CineStation** connected to a PC and view, edit, and save your cines using the Phantom Software supplied with the camera. Keep them in their original cine raw format, or convert them to TIFF, QuickTime, AVI, or a number of other formats. Move the files from the CineStation to a disk or tape deck via 10Gb Ethernet, 4:4:4 HD-SDI, or Component Video outputs.

H	V	FPS
1280	800	7,500
1280	720 (720p)	8,360
1024	768	9,520
896	480 (DVD)	17,000
768	576 (PAL)	16,100
768	480 (NTSC)	19,300
640	480	22,400
512	512	25,000
512	256	49,500
512	128	97,200
384	256	60,900
256	256	79,000
256	128	153,200
256	64	288,800
128	128	215,600
128	64	397,100
128	32	685,800
128	16*	1,077,500
128	8*	1,400,000

\*Assumes FAST option installed, option is export controlled



# DATA SHEET

## v710

### Additional Features:

Analog Viewfinder Out: PAL, NTSC & HD Component (720p)

Lensing: F-mount, C-mount, PL-mount

Size (without lens): 12.25 x 5.5 x 5.0 in. (L,W,H)  
31.1 x 14 x 12.7 cm

Weight (without lens): 12 lbs (5.4 Kg)

Power: 90 Watts @ 24 VDC, without CineMag

Operating Temperature: 0°C to 40°C @ 8% to 80% RH

Storage Temperature: -10°C to 55°C

Non-operational Shock: 33G, half sine wave, 11ms,  
all axes without lens

Operational Shock: 30G, half sine wave, 11ms,  
10 times all axes (without  
CineMag or lens) to Mil-Std-810 G

Operational Vibration: 0.25G, 5-500 Hz, all axes

### Focused

Since 1950, Vision Research has been shooting, designing, and manufacturing high-speed cameras. Our single focus is to invent, build, and support the most advanced cameras possible.

**VISION**  
**RESEARCH**

An **AMETEK**® Company

100 Dey Road  
Wayne, NJ 07470 USA  
+1.973.696.4500  
phantom@visionresearch.com

[www.visionresearch.com](http://www.visionresearch.com)

All specifications are subject to change without notice.

Rev Dec 2009



AMETEK Vision Research's digital high-speed cameras are subject to the export licensing jurisdiction of the Export Administration Regulations. As a result, the export, transfer, or re-export of these cameras to a country embargoed by the United States is strictly prohibited. Likewise, it is prohibited under the Export Administration Regulations to export, transfer, or re-export AMETEK Vision Research's digital high-speed cameras to certain buyers and/or end users.

Customers are also advised that some models of AMETEK Vision Research's digital high-speed cameras may require a license from the U.S. Department of Commerce to be: (1) exported from the United States; (2) transferred to a foreign person in the United States; or (3) re-exported to a third country. Interested parties should contact the U.S. Department of Commerce to determine if an export or a re-export license is required for their specific transaction.



## V-SERIES ANALOG SIGNAL ACQUISITION MODULE W/ PHANTOM SAM-3-USB

**Product #:** VRI-DAQ-DT9802

Price: \$2,625.00

**ADD TO CART**

Usually ships in 1-2 weeks

[click for larger view](#)

### Signal Acquisition Module-3

View and analyze your sensor and support instrumentation data right from the Phantom application Software.

The SAM-3 unit is used to provide the Data Acquisition Unit with the necessary signals (READY and STROBE) to guarantee the sampled source data from an environment or from a unit under test will be synchronized with the Phantom image frames.

#### SAM-3 Key Features:

- \* Embeds multiple sample per image (frame rate dependent)
- \* Easy to interpret graphical representation of source data measurement information
- \* Quick and easy setup
- \* Supports data collection up to 100K samples per second
- \* Collects and analyzes up to 16 channel inputs simultaneously (Channels shared by 16 analog and 8 digital inputs)
- \* Synchronizes Data Acquisition Unit with Phantom imaging system

#### Solution includes:

- \* Phantom SAM3 module
- \* SAM3 BNC capture cable (Ready/Strobe/Trigger/Fsync/Video)
- \* DT9802, USB enabled data acquisition Module

The SAM-3 unit is used to provide the Data Acquisition Unit with the necessary signals (READY and STROBE) to guarantee the sampled source data from an environment or from a unit under test will be synchronized with the Phantom image frames.

The types of source data that can be collected and analyzed may vary widely, including both physical parameters such as temperature, pressure, distance, and light and sound frequencies and amplitudes, and also electrical parameters including voltage, current, and frequency. To sample these parameters a transducer may be employed to sense changes in a physical parameter, such as temperature or pressure, and to convert the sensed information into electrical signals, such as voltage or frequency variations.

Other types of sampled data that may be collected include data from oscilloscopes, spectrum analyzers and digital multimeters. The Phantom high-speed digital imaging analysis system is capable of supporting a maximum of 32 analog, or 16 digital inputs simultaneously.

*Appendix D. Attitude Determination System Component Datasheets*



The Terma HE-5AS Star Tracker is a new but fully qualified design, offering a favourable combination of arc-second performance at an affordable price. Robust algorithms provide full autonomy in initial attitude acquisition and attitude update. Terma quality standards, documentation and component screening meet the requirements of discerning customers including the European Space Agency and the U.S. Department of Defence.

## Camera

The Camera is separate to make it easier to place on the satellite, and to minimise heat dissipation (1.6W) near the sensor. The camera is a very compact unit, weighing less than 1,000g. The compact optics provides a 22° field of view and – although compact – provides enough light to track across the entire celestial vault. A cable provides digital data-link (LVDS) and power supply from the processor unit. The Camera can be supplied with a thermo-mechanically stable bracket.

## Baffle

Standard baffles are available providing a Sun exclusion half-angle as low as to 30°. Where the mission calls for a custom designed baffle, Terma has the know-how to optimise baffle design in dialogue with the customer.

## Processor

The processing unit houses the star catalogue and the software algorithms for initial attitude determination and continuing attitude update. Also, the unit provides power to the camera. The interface towards the spacecraft is redundant RS-422 or MIL-STD-1553, and a power supply voltage from 22 V to 34 V. Dissipation is 5.2 W.

## Ground Support Equipment

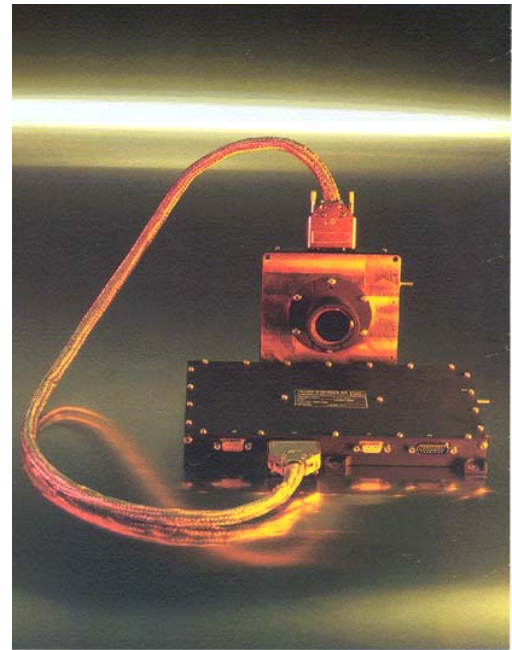
The star tracker may be delivered with Ground Support Equipment, developed for ease of use and with comprehensive User Manuals. The options are:

- Optical Stimulus: A light-weight optical stimulator reproducing the star field for a fixed attitude. Requires only a power interface and mounts without tools directly onto the baffle.
- Electrical Stimulus: Provides a stimulus reproducing the starfield at any attitude. May be used stand-alone or to close the loop for avionics testing. The equipment is delivered as a PC, with interface cards, and provides both a user interface for the definition of attitude manoeuvres, and an RS-422 interface for commanding from higher-level test equipment.
- EGSE: Provides TM/TC interface to the star tracker for unit testing. Delivered as a PC with software and interface cards.

## Heritage

The HE-5AS Star Tracker is used on satellites owned by the European Space Agency (Cryosat 1 and 2, Aeolus, and LISA Pathfinder), the U.S. Naval Research Laboratory (Nemo, Tacsat-1/Mitex), the U.S. Air Force Research Laboratory (Tacsat-2/Roadrunner) and the U.S. Missile Defence Agency (Distributed Sensing Experiment).

Independent test and validation of the star tracker have been jointly performed by the NRL and the AFRL under the DOD



*Terma HE-5AS star tracker*



*Cryosat with star trackers and baffles*

### Quaternion Reference Frame

The reference frame for quaternions is the Hipparcos Reference Frame, a barycentric inertial coordinate system consistent with the equatorial system for the mean equinox and equator of J2000: An Earth-centered system with the x-axis pointing toward the mean vernal equinox, and z-axis toward the mean rotating axis of the Earth on January 1, 2000 at 12 UTC

### Data Summary

Accuracy:

- <1 arc-seconds RMS pitch, yaw
- <5 arc-seconds RMS roll

Update Rate:

- 4 Hz maximum

Acquisition Time

- 3 sec typical, 5 sec worst case

Slew Rate

- 0.5 deg/sec full performance
- 2.0 deg/s reduced performance

Operating Temperature

- -40°C to +20°C.

Power Dissipation

- 1.6 W in Camera
- 5.2 W in Processor

Electrical Interfaces

- Power 22 V to 34 V, 6.8 W average
- Dual TM/TC interface RS-422 or MIL-STD-1553B
- Dedicated clock signal interface
- LVDS interface between Camera and Processor

Radiation Hardness

- EEE components 100 kRad(Si)

Dimensions and Mass

- Camera 120 by 120 by 33 mm (optics protrude 58 mm), 1,000 g
- Processor 245 by 165 by 29 mm, 1200 g

Baffle Exclusion Angle, Dimensions and Mass

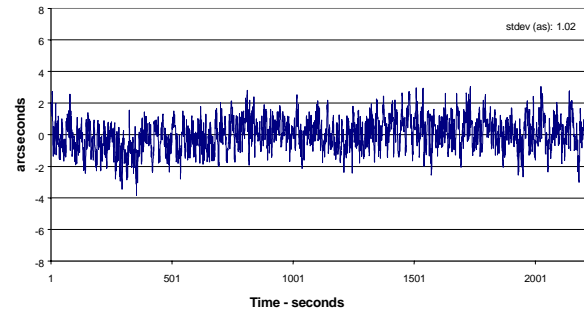
- 30° Sun Excl., Ø234 by 346 mm, 800 g
- 60° Sun Excl., Ø170 by 211 mm, 530 g

Component Screening Standards

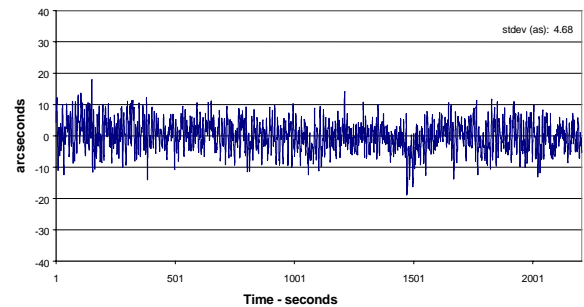
- MIL-B grade or full MIL-S grade
- Additional screening on customer request

Data Package

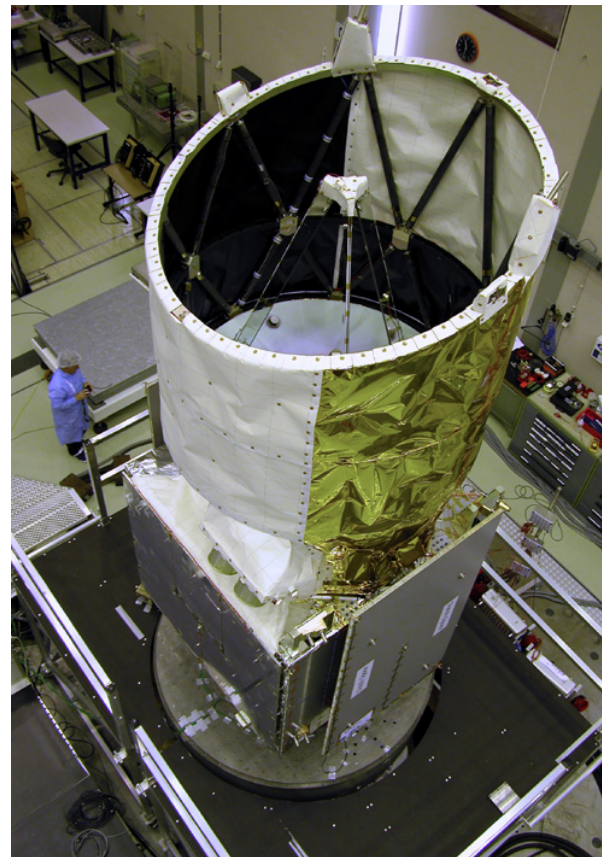
- Management and PA plans and progress reports
- CDR data package for product baseline
- End-Item Data Package for all deliverables
- Project specific documentation on customer request



*Pointing Performance*



*Roll Performance*



*Aeolus Structural Test Model*

**Terma Space**

Email: [space@terma.com](mailto:space@terma.com) Web: [www.terma.com](http://www.terma.com)

# SGR-07 – Space GPS Receiver

## Navigation and Timing

### Applications

- Navigation for LEO Missions
- Orbit and Position Determination
- Accurate Timing and Synchronisation
- Payload Data Time Stamping
- Post-maneuvre Orbit Determination

### Features

- 12 Channel L1 C/A Code Space GPS Receiver
- Flight Heritage
- Manufactured to ECSS standards
- Exceptionally Fast Start-up
- Low Mass and Power
- Radiation Tolerant Design
- Active Patch Antenna Included
- 7 Year Design Life

### Interfaces

- 50 Ohm antenna interface (SMA)
- CAN (ISO11898) and RS422 TM/TC Interface
- Pulse-Per-Second (IEE442) (TTL, RS422, LVDS)

### Key Specifications

- Position to 10 m (95%)
- Velocity to 15 cm/s (95%)
- Typical Time to First Fix (TTFF) 90 - 180 s
- 28 V Unregulated Supply, 1.6 W
- 120 x 78 x 48 mm, 0.45 kg

### Options

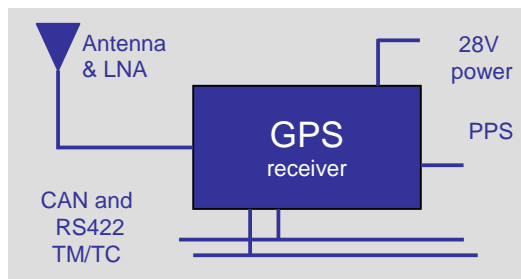
- Spacewire or other interface options
- Several Antenna options

### Heritage (launch date)

- Software derived from SGR-10/20
- GIOVE-A (2006)
- UK-DMC2 (2008)
- In manufacture for additional programmes



GPS receiver and antennas



### Other SSTL Navigation Products

- SGR-10 (2 Antennas, 24 Channels)
- SGR-20 (4 Antennas, 24 Channels)
- SGR-05 Low Cost Receiver
- SGR-GEO Receiver for GEO
- SGR Orbit Determination Solutions
- SGR Attitude Determination Solutions

Positioning and timing information provided  
By the receiver can be processed to obtain orbital  
information. SSTL can provide expertise on orbit  
determination solutions using the SSTL Space  
GPS Receiver



# SGR-07 – Space GPS Receiver

## Navigation and Timing

**Radiation:** Mitigation by using TMR memory and electronic fuse protection

**Antenna:** Active patch antenna weighing 50g with 45x45x20mm dimensions

**Non-Volatile Memory:** Flash memory stored software to allow rapid booting and upgrades. Almanacs and Orbital Elements also stored in flash memory to enable fast Time to First Fix (TTFF)

**Flight Software:** Extensive flight heritage software used on many missions

**User Interface:** PC software provided for receiver monitoring, control and data processing

### Performance

Based on circular polar low earth orbit with typical ionospheric and ephemeris error levels on signals and co-visible antenna configuration

	Typical (95%)	Max (95%)
Orbital Position (3-D)	10 m	20 m
Orbital Velocity (3-D)	0.15 m/s	0.25 m/s
Time	0.5 $\mu$ s	1 $\mu$ s
Time to First Fix		
- Self initialised	90 s	180 s
- First time	200 s	350 s
Mass	450 g	
Dimensions	120 x 78 x 48 mm	
Power	1.6 W at 28 V (Supply 18-38 V)	
Temperature	Operating -20° C to +50° C	
Random Vibration	15g <sub>rms</sub> in all axis	
Radiation tolerance	10kRad (Si)	

### Typical Measurement Precision

Pseudorange	0.9 m
Carrier-Smoothed Range	0.15 m
Carrier Phase Noise	1.5 mm
Doppler Velocity	0.5 m/s
Carrier Range Rate Velocity	0.03 m/s
Filtered Velocity	0.01 m/s

SSTL is ISO9000:2000 certified

- Manufacture and rework to
  - ECSS Q-70-80A
  - ESA PSS-01-738
  - ECSS Q-70-28A
  - Test to SSTL ISO9000:2000

Standard Delivery Service Includes

- Compliance Testing
- Vibration Test
- Thermal Cycling
- User Manual
- Test Results
- Export License and Shipping
- Thermal Vacuum Testing available
- Unit can be supplied prior to environmental testing

## Surrey Satellite Technology Limited

SSTL has launched over 30 satellites gaining almost 200 years in-orbit experience. SSTL draws on its world-class expertise in both small satellite platform technology and high and medium resolution optical instruments. SSTL provides complete turn-key system solutions; spacecraft, ground station, launch, operations and image processing.

SSTL is unique in the space industry; able to design, manufacture and integrate multiple satellites in-house.

Changing the economics of space  
[www.sstl.co.uk](http://www.sstl.co.uk)



## *Appendix E. Telescope Assembly Component Datasheets*

# ADRS Series

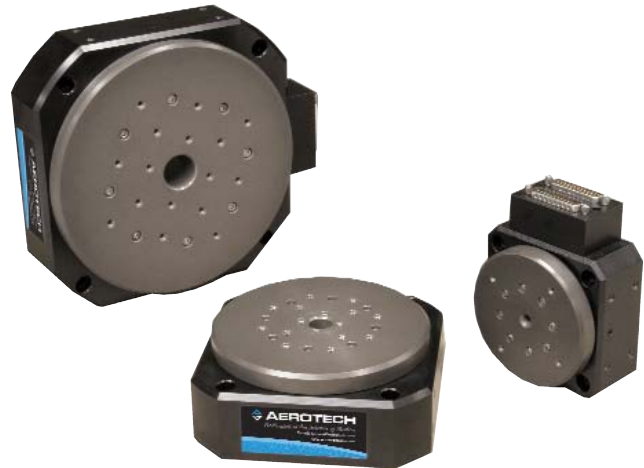
## Mechanical-Bearing Rotary Stage

High torque output, direct-drive brushless servomotor

Cog-free slotless motor design for outstanding velocity stability

Direct coupled, high-accuracy rotary encoder

Ultra-low-profile minimizes working height



Aerotech's ADRS series with its direct-drive technology and low profile provide a superior alternative to belt- and worm-drive stages.

### Compact Package

The design of the ADRS series direct-drive rotary stage was optimized to minimize stage height. The low profile of the stage reduces the effective working height of the system minimizing “stack-up” related errors. In addition to the low overall height, the ADRS series provides a clear aperture that can be used for product feed-through or laser beam delivery.

### Brushless Direct-Drive

To maximize positioning performance, the ADRS series utilizes direct-drive brushless motor technology. Direct-drive technology is optimized for 24/7 production environments, as there are no brushes to replace and no gear trains or belts to maintain. Direct drive also provides quicker acceleration and higher top speeds than gear- or belt-driven mechanisms, yielding higher total overall throughput.

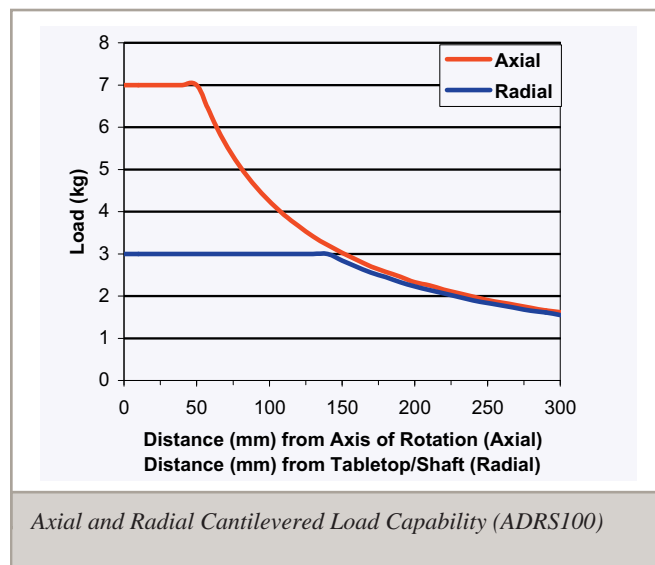
The low maintenance and high-throughput characteristics of the ADRS series provide a stage that yields the lowest total cost of ownership.

### Slotless Motor

The ADRS series uses a slotless stator design that eliminates torque ripple. This motor technology provides ultra-smooth velocity stability comparable to a high-quality DC brush motor without all the DC motor's inherent maintenance requirements. Since the slotless motor is directly coupled to the tabletop, velocity disturbances created by toothed belt drives or worm gears are eliminated.

### Multiple Configurations

The ADRS series is available in 100 mm, 150 mm, and 200 mm versions. Each stage has options for different motor windings to better match the stage to different operating conditions. The -B winding option provides the highest possible speed operation for a given available bus voltage, while the -A winding gives greater output torque for comparable current levels. Metric and “English” pattern tabletops are available and slotted mounting holes enable attachment to 25 mm and 1 inch hole pattern breadboards. The tabletop of the ADRS series has a labyrinth seal that protects the bearings and encoder from contamination. An optional shaft end seal is available for applications where the bottom of the stage is exposed to contamination.



## ADRS Series SPECIFICATIONS

ADRS Series		ADRS-100		ADRS-150		ADRS-200	
Tabletop Diameter		95 mm		140 mm		190 mm	
Aperture		6 mm		15 mm		25 mm	
Motor (-A/-B)		S-76-35-A	S-76-35-B	S-130-39-A	S-130-39-B	S-180-44-A	S-180-44-B
Continuous Current, Stall	A <sub>pk</sub>	2	4	3.8	7.6	2.7	5.3
	A <sub>rms</sub>	1.4	2.8	2.7	5.4	1.9	3.8
Bus Voltage		320	160	320	160	320	160
Resolution		0.87-87.3 $\mu$ rad (0.18-18 arc sec)		0.315-31.5 $\mu$ rad (0.065-6.5 arc sec)			
Max Speed <sup>(1)</sup>		1500 rpm		600 rpm		400 rpm	
Accuracy	Uncalibrated			388 $\mu$ rad (80 arc sec)			
	Calibrated <sup>(2)</sup>	29.1 $\mu$ rad (6 arc sec)		48.5 $\mu$ rad (10 arc sec)		48.5 $\mu$ rad (10 arc sec)	
Repeatability		14.6 $\mu$ rad (3 arc sec)		19.4 $\mu$ rad (4 arc sec)		19.4 $\mu$ rad (4 arc sec)	
Max Load <sup>(3)</sup>	Axial	7 kg		20 kg		40 kg	
	Radial	3 kg		10 kg		20 kg	
Axial Error Motion <sup>(4)</sup>		2 $\mu$ m		5 $\mu$ m		5 $\mu$ m	
Radial Error Motion <sup>(4)</sup>		3 $\mu$ m		5 $\mu$ m		5 $\mu$ m	
Tilt Error Motion		48.5 $\mu$ rad (10 arc sec)		97 $\mu$ rad (20 arc sec)		97 $\mu$ rad (20 arc sec)	
Inertia	Unloaded	0.00038 kg-m <sup>2</sup>		0.00242 kg-m <sup>2</sup>		0.00843 kg-m <sup>2</sup>	
Total Mass		2.0 kg		4.3 kg		7.6 kg	
Finish	Tabletop			Hardcoat			
	Stage			Black Anodize			

Notes:

1. Maximum speed is based on stage capability. Actual speed may depend on encoder resolution, load, amplifier bus voltage, and motor. See the S-series rotary motor for more information.

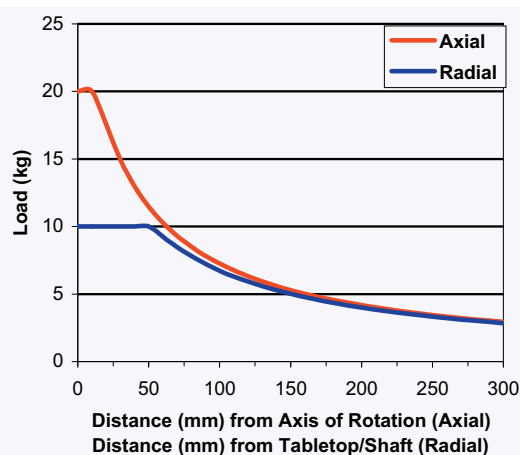
2. With HALAR.

3. Maximum loads are mutually exclusive.

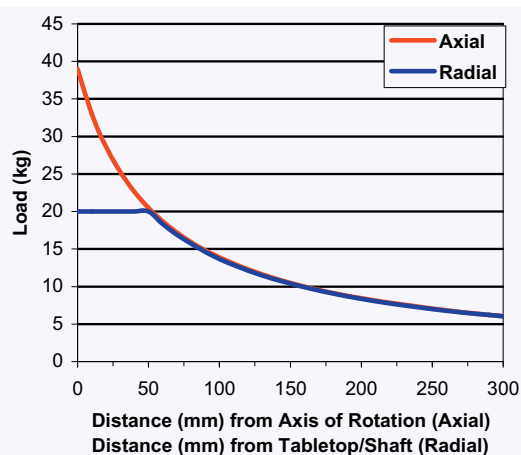
4. For the ADRS-100, error motion specifications are below 700 rpm. Above 700 rpm, the max radial error is 5 microns. Errors measured 50 mm (2 in) above the tabletop.

## ADRS Maximum Encoder Frequency

Resolution-Speed	ADRS-100	ADRS-150	ADRS-200
AS/X5/X10	1500 rpm	600 rpm	600 rpm
X25	1067 rpm	384 rpm	384 rpm
X50	533 rpm	192 rpm	192 rpm

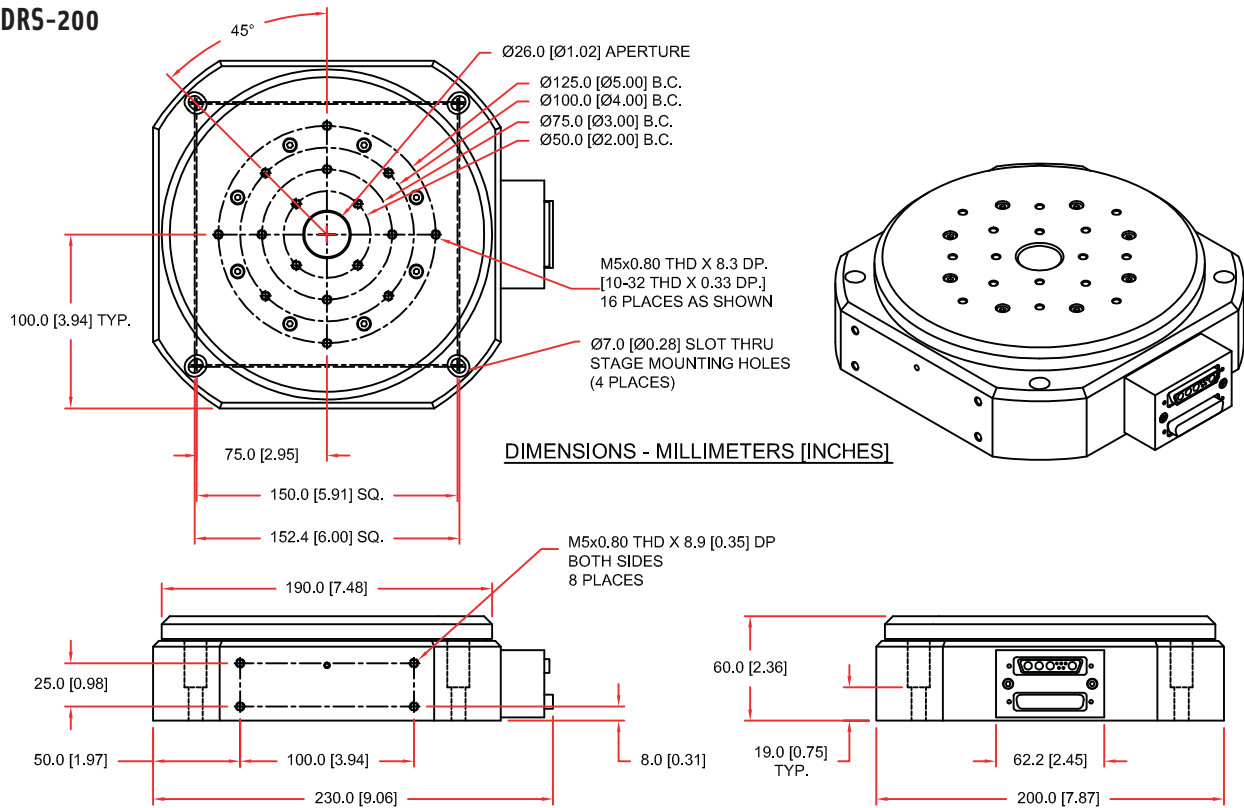


Axial and Radial Cantilevered Load Capability (ADRS150)

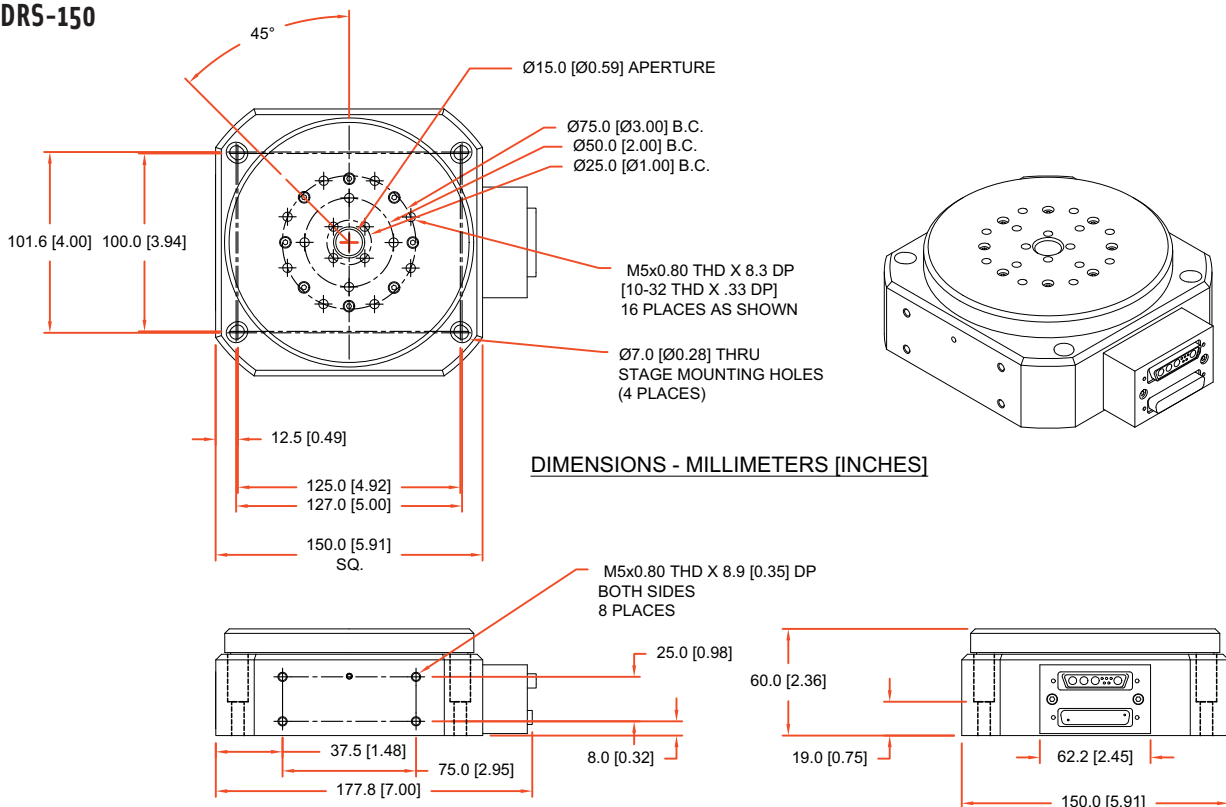


Axial and Radial Cantilevered Load Capability (ADRS200)

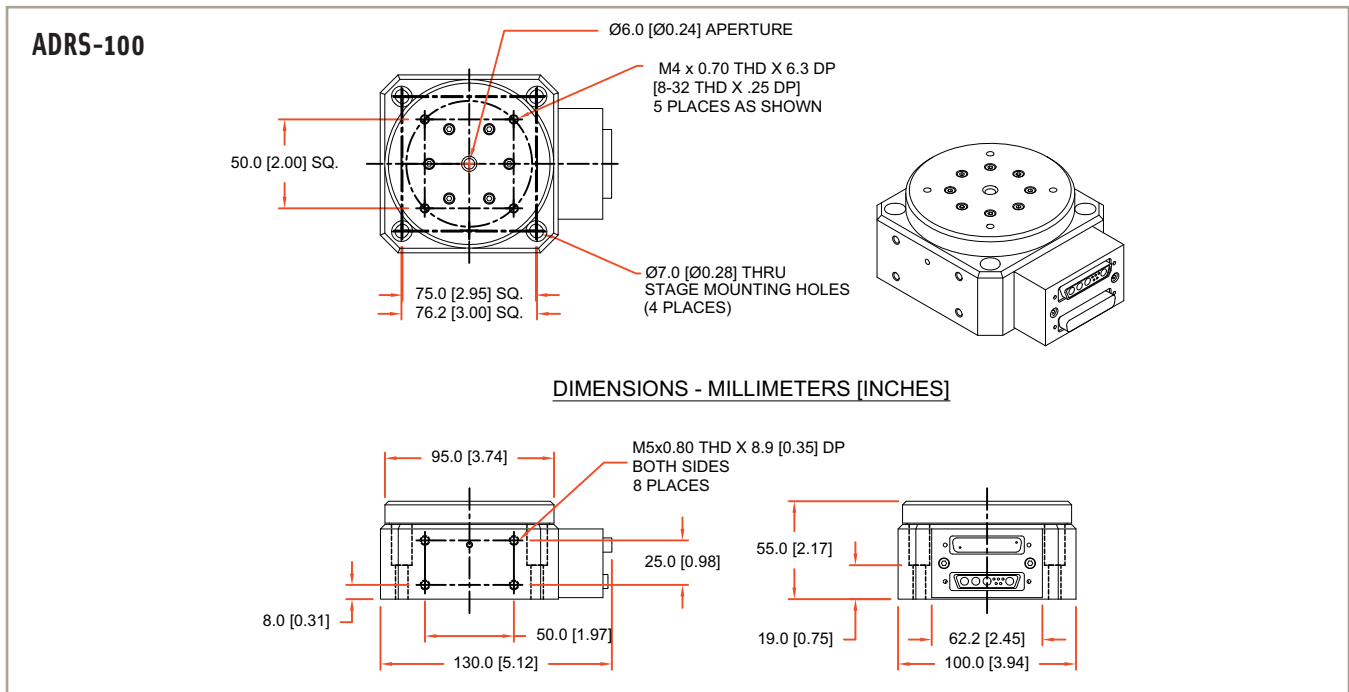
### ADRS-200



### ADRS-150



## ADRS Series DIMENSIONS and ORDERING INFORMATION



### Ordering Example

ADRS	-200	-M	-A	-AS	-S
Series	Width (mm)	Mounting Pattern	Winding Option	Position Transducer	Construction Options
	-100	-M	-A	-AS	-S
	-150	-U	-B	-X	
	-200				

### ADRS Series Direct-Drive Rotary Stage

ADRS-100	100 mm wide direct-drive rotary stage with 1.8 N-m peak torque output
ADRS-150	150 mm wide direct-drive rotary stage with 11.7 N-m peak torque output
ADRS-200	200 mm wide direct-drive rotary stage with 30 N-m peak torque output

### Mounting Pattern

-M	Metric-dimension mounting pattern and holes
-U	English-dimension mounting pattern and holes

### Winding Options

-A	Low speed, high torque-constant winding option
-B	High speed, low torque-constant winding option

### Position Transducer

-AS	Standard feedback device, 1 Vpp sine wave output, 10,000 cycles per rev on ADRS-200/150, 3600 cycles per rev on ADRS-100
-X5	Square wave digital output, 50,000 cycles per rev on ADRS-200/150 and 18,000 cycles per rev on ADRS-100
-X10	Square wave digital output, 100,000 cycles per rev on ADRS-200/150 and 36,000 cycles per rev on ADRS-100
-X25	Square wave digital output, 250,000 cycles per rev on ADRS-200/150 and 90,000 cycles per rev on ADRS-100
-X50	Square wave digital output, 500,000 cycles per rev on ADRS-200/150 and 180,000 cycles per rev on ADRS-100

Note: Digital output encoder signals are synthesized with a 16 MHz clock. Care must be taken to ensure that the encoder sample rate on the controller is at least 16 MHz or higher. Slower clock rates are available on request.

### Construction Options (ADRS 150 & 200)

-S	Bottom shaft seal (not available on ADRS-100; ADRS-100 has an integral bottom labyrinth seal)
-NS	No bottom shaft seal

# Ensemble™

## Multi-Axis Motion Controller Software



**Up to 10 axes of coordinated motion**

**Multiple 10-axis systems can be controlled by a single PC via Ethernet or USB**

**Controller architecture capable of coordinating motion of up to five independent tasks**

**Capable of driving and controlling linear or rotary brushless, DC brush servo, and micro-stepping motors**

**Complete motion capabilities include: point-to-point, linear and circular interpolation, electronic gearing, velocity profiling**

**Program in AeroBASIC™ with the IDE, Microsoft .NET including C#, VB.NET®, Managed C++, or LabVIEW®**

**Remote ASCII interface provided for Windows® or non-Windows® programs (including Linux) to command the Epaq through standard Ethernet, RS-232 port, and optional IEEE-488**

**Fully compatible with EPICS set of software tools and applications, making Ensemble ideal for use in synchrotron and general laboratory facilities**

**Advanced Windows®-based remote diagnostics, tuning, and programming interface software**

**Axis jogging/control with optional joystick**

**Allen-Bradley EtherNet/IP™ interface provides full integration with the Ensemble; program the Ensemble directly from RSLogix™ 5000**



The Ensemble™ is Aerotech's next-generation, multi-axis controller for moderate- to high-performance applications with high speed communication through 10/100 Base T Ethernet or USB interfaces. It offers easy to use, affordable multi-axis motion programming for laboratory experimentation, production testing, or advanced OEM automated manufacturing systems.

### Versatile, Stand-Alone Multi-Axis Control

With the Ensemble stand-alone controller, up to ten axes of synchronized motion are offered in a distributed network of panel-mounted drives. This is excellent for applications where drives must be embedded into a machine at various locations or where panel space is at a premium. For desktop and rack-mount installations, the Ensemble is offered in a stand-alone 6-axis unit with integrated drives. Three additional panel mounted linear or PWM drives may be added externally to the six-axis unit for up to nine axes of motion control. The Ensemble can control any Aerotech brushless, brush, or stepper motors or stages in any combination. The simple parameter interface also allows easy integration to third-party motors and stages. The controller encoder interface includes TTL quadrature input or analog encoder input. Multiple Ensemble controllers can be controlled from a single Windows® PC through Ethernet or USB, allowing many more than ten axes of motion to be operated from one host PC.

### Powerful and Intuitive Programming Functionality

Unlike most controllers on the market today, there is no need to understand a cryptic command set to generate motion. The intuitive interface allows a user to begin programming immediately. Ensemble online help further simplifies writing motion programs and includes many functional examples that can be easily modified for customer applications.

## Ensemble DESCRIPTION

The Ensemble Integrated Development Environment software offers a graphical user interface in Windows® featuring an intuitive Program Editor, Variable Output window, Compiler Output window, Task State monitor, Network Explorer, and Solution Explorer. This interface enables users to easily monitor all aspects of their positioning system, no matter how complex. The Axis Control and Diagnostic screen interfaces are further supplemented by a fully functional autotuning utility that minimizes startup time and allows easy optimization of motion axes. System diagnostics are easily read from the interface. The Windows-based remote software package is included with each unit, which allows the user to upload/download programs, modify parameter files, and analyze motion with Aerotech's advanced graphical tuning package, all from the convenience of a remote PC.

Each Ensemble axis uses the processing power of a 225 MHz double precision, floating-point DSP to offer exceptional performance in a variety of applications, including point-to-point motion, linear and circular interpolation, multi-axis error correction, 2D error mapping, direct commutation of linear and rotary brushless servomotors, and on-board servo autotuning. High-speed interrupts and data logging capabilities provide a real-time link to external systems. The Ensemble also offers high-speed position latching capability and optional single-axis PSO (Position Synchronized Output). Whether the requirement is simple point-to-point motion or complex velocity profiled contours with output on the fly, Ensemble ensures peak performance for critical applications.

### Flexible Drives

Because the Ensemble can control many different types of motors, users have excellent flexibility in their motion system design. High accuracy linear motor air-bearings can be controlled from the same controller running lower precision drives with servo or stepper motors. Parameters are easily reconfigured for these various motors and feedback devices, so customers can adapt to changing system needs.

### Allen-Bradley Interface

Combine proven PLC with proven motion control for easier integration, startup, and maintenance of medium- and high-end automation projects. The Aerotech EtherNet/IP™ interface enables AB PLCs (MicroLogix, CompactLogix™, or ControlLogix) to be integrated directly with the Ensemble. Motion can be directly programmed in the RSLogix 5000 environment or separate programs can be written on the controller and triggered from the AB PLC. Aerotech has two interfaces: ASCII and Register. Choose the PLC, motion controller, and interface that best fits your application needs.

### EPICS Drivers

Each Ensemble installation includes full compatibility with the EPICS open source distributed control system. EPICS is used worldwide at leading light source (synchrotron) facilities and other government laboratories, allowing Ensemble to seamlessly integrate into applications at all major research institutions.

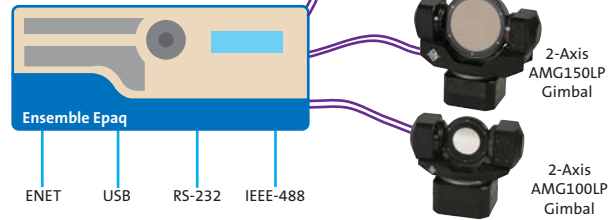
### Enhancing a Legacy of Success

Although Ensemble is envisioned as a general-purpose, stand-alone controller, it carries forward a legacy of success built from Aerotech's hugely successful A3200 and Soloist™ controllers. It offers enhanced capabilities that will make it an ideal choice for many aggressive motion control applications. The Ensemble motion control architecture builds upon the Soloist intuitive graphical user interface, while offering advanced features appropriate for multi-axis control. Ease of use is further improved with pre-coded LabVIEW® VIs, AeroBASIC™ programming functionality, .NET tools for C#, VB.NET, and managed C++ compatibility.

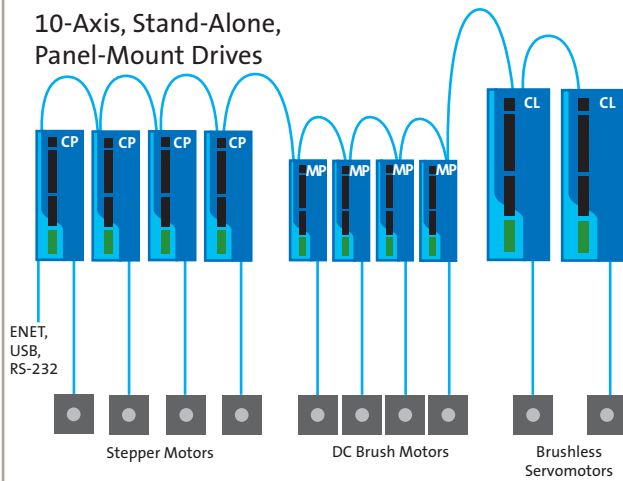


## Ensemble DESCRIPTION

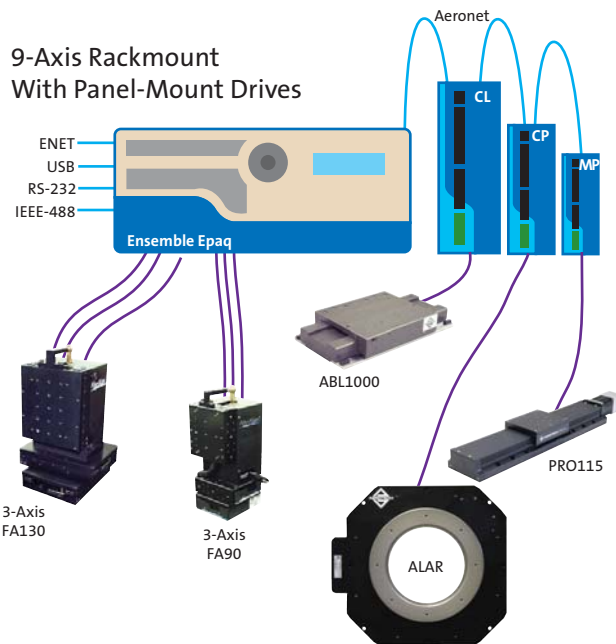
### 6-Axis, Stand-Alone, Rackmount or Desktop



### 10-Axis, Stand-Alone, Panel-Mount Drives



### 9-Axis Rackmount With Panel-Mount Drives



*The Ensemble can be used to control multiple axes (from one to ten axes) of both brush and brushless drives and motors.*



# Ensemble™ HPe/HLe/CP/CL/MP

## Networked, Panel-Mount Drives

Network drives through a high-speed serial interface to coordinate up to ten axes of motion

Select linear (HLe/CL) or pulse width modulation (HPe/CP/MP) amplifiers

Coordinate motion using up to five independent tasks

Drive and control linear or rotary brushless, DC brush servo, and micro-stepping motors

Command various motion types including: point-to-point, linear and circular interpolation, electronic gearing, and velocity profiling

Program in AeroBASIC™, Microsoft .NET (C#, VB.NET, and Managed C++), or LabVIEW®

Remotely command drives over Ethernet, USB, or RS-232 with an ASCII interface available for both Windows® and non-Windows® programs (including Linux)

Diagnose, tune, and program through an advanced Windows-based interface

UL listed, CE approved

The Ensemble™ is Aerotech's next-generation, multi-axis controller for moderate- to high-performance applications. Versatility, power, and affordability make the Ensemble ideal for applications from basic laboratory experimentation and general-purpose positioning to advanced OEM systems.

### Versatile, Flexible, Stand-Alone Multi-Axis Control

Network multiple Ensemble HPe/HLe/CP/CL/MP combination controllers/drives for up to ten axes of coordinated motion, and seamlessly mix and match amplifiers (linear and PWM) and motor types (brush, brushless, and stepper) within the same positioning system using a common programming and control platform. High-



*Clockwise from upper left: Ensemble HPe, Ensemble HLe, Ensemble CL, Ensemble MP, and Ensemble CP.*

accuracy linear motor air-bearing stages can be directed from the same controller/drive running lower precision stages with servo or stepper motors. Each controller/drive can be reconfigured to accept different motors and feedback devices, allowing customers to adapt to changing system needs. Optional on-board encoder interpolation provides programmable axis resolution, including the ability to change interpolation (multiplication) values through software.

### Powerful and Intuitive Programming

Monitor and control all aspects of the positioning system, no matter how complex, through the Ensemble GUI

## Ensemble HPe/HLe/CP/CL/MP DESCRIPTION

Integrated Development Environment software. An Autotuning utility minimizes startup time by allowing easy optimization of motion axes. Functional programs that can be modified and used in customer applications are included in the online Help. Pre-coded LabVIEW® VIs, AeroBASIC™ programming functionality, .NET tools for C#, VB.NET, and managed C++, make the Ensemble even easier to use.

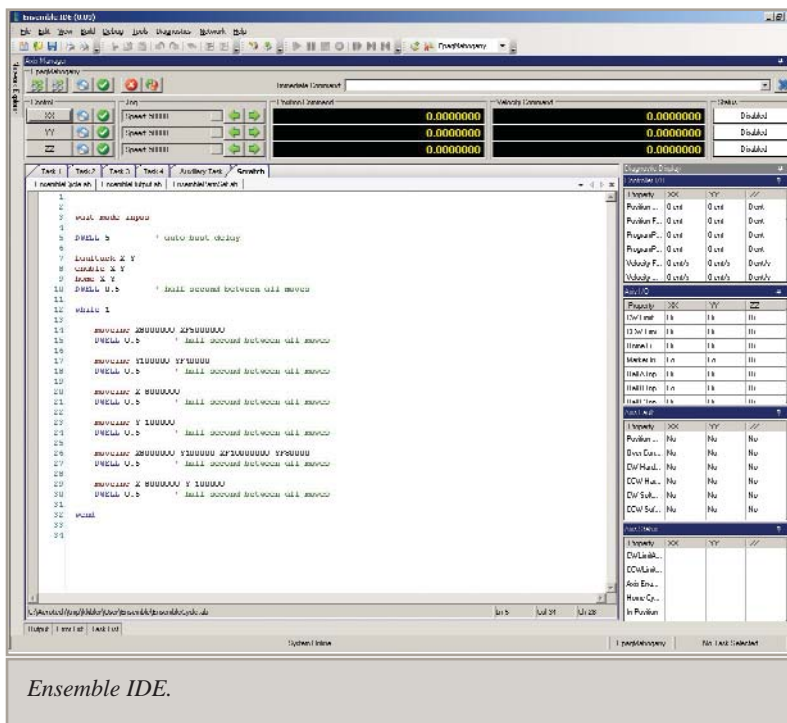
### Advanced DSP Control

The processing power of a 225 MHz double precision, floating-point DSP supplies exceptional performance in a variety of applications including point-to-point motion, linear and circular interpolation, multi-axis error correction, 2D error mapping, direct commutation of linear and rotary brushless servomotors, and on-board servo autotuning. High-speed interrupts and data logging capabilities provide

a real-time link to external systems. The Ensemble HPe/HLe/CP/CL/MP controller/drive combination also offers high-speed position latching capability and single-, dual-, or triple-axis PSO (Position Synchronized Output), depending on model. Whether the requirement is simple point-to-point motion or complex velocity-profiled contours with output on the fly, Ensemble ensures peak performance for critical operations.

### Enhancing a Legacy of Success

Ensemble carries forward a legacy of success that originated in Aerotech's A3200 and Soloist™ controllers. Enhanced capabilities make it an obvious choice for aggressive motion control applications. The Ensemble motion control architecture builds upon the Soloist™ intuitive graphical user interface, while improving multi-axis control through advanced features.



Ensemble IDE.

## Ensemble HPe/HLe/CP/CL/MP COMPARISON



**Ensemble HPe**  
Width: 99 mm  
Height: 232.4 mm



**Ensemble HLe**  
Width: 206.9 mm  
Height: 234.3 mm



**Ensemble CP**  
Width: 63.5 mm  
Height: 198.2 mm



**Ensemble CL**  
Width: 103.7 mm  
Height: 265.2 mm



**Ensemble MP**  
Width: 41.1 mm  
Height: 141.2 mm

Ensemble Comparison Chart	Ensemble HPe	Ensemble HLe	Ensemble CP	Ensemble CL	Ensemble MP
PC Interface	Ethernet or USB	Ethernet or USB	Ethernet or USB	Ethernet or USB	Ethernet or USB
Current Output, Peak	10-150 A	10-20 A	10-30 A	10 A	10 A
Current Output, Continuous	5-75 A	5-10 A	5-15 A	5 A	5 A
Bus Voltage	10-320 V	40-80 V	10-320 V	40 V	10-80 V
Amplifier Type	PWM	Linear	PWM	Linear	PWM
Input Type	2 or 3 Phase AC	2 Phase AC	2 Phase AC	2 Phase AC	DC
Motor Style	Brush, Brushless, Stepper	Brush, Brushless, Stepper	Brush, Brushless, Stepper	Brush, Brushless, Stepper	Brush, Brushless, Stepper
Base I/O	4-DO/6-DI 1-AO/1-AI	4-DO/6-DI 1-AO/1-AI	4-DO/6-DI 1-AO/1-AI	4-DO/6-DI 1-AO/1-AI	1-AI
Additional I/O (Additional to Base I/O)	16-DO/16-DI 3-AO/3-AI	16-DO/16-DI 3-AO/3-AI	16-DO/16-DI 1-AO/1-AI	16-DO/16-DI 1-AO/1-AI	8-DO/8-DI 1-AO/1-AI
ESTOP Input	Yes	Yes	Yes	Yes	Yes
Brake Input Capable	Yes	Yes	Yes	Yes	Yes
Single Axis PSO <sup>(1)</sup>	Yes	Yes	Yes	Yes	Yes
Dual Axis PSO <sup>(1)</sup>	Yes	Yes	No	No	No
Triple Axis PSO <sup>(1)</sup>	Yes	Yes	No	No	No
Ethernet Capable for Third-Party I/O	Yes	Yes	No	No	No
Auxiliary Keep Alive	Yes	Yes	Yes	Yes	Yes

Notes:

1. PSO not available on Ensemble CP/MP when using integral MXU.

## Ensemble HPe SPECIFICATIONS

Ensemble HPe	Units	10	20	30	50	75	100	150
Output Voltage <sup>(1)</sup>	VDC	10-320 <sup>(2)</sup>						
Peak Output Current (1 sec)	A <sub>pk</sub>	10	20	30	50	75	100	150
Continuous Output Current <sup>(3)</sup>	A <sub>pk</sub>	5	10	15	25	37	50	75
Power Amplifier Bandwidth	kHz	Selectable Through Software						
PWM Switching Frequency	kHz	20						
Minimum Load Inductance	mH	0.1 @ 160 VDC (1.0 mH @ 320 VDC)						
Operating Temperature	°C	0 to 50						
Storage Temperature	°C	-30 to 85						
Weight	kg (lb)	2.36 (5.2)			6.64 (14.6)			11.06 (24.4)
Maximum Shunt Regulator Dissipation	W	40 (Optional)		40	440	440	440	440
Power Input	VAC	Single- or Three-Phase 7-240 VAC, 50-60 Hz <sup>(4)</sup>						
Encoder Input Frequency	kHz	200 kHz Amplified Sine (For Onboard Multipliers), 40 MHz TTL Square Wave						
Current Loop Update Rate	kHz	20 kHz						
Servo Loop Update Rate	kHz	1 to 20 kHz						
Keep Alive/Auxiliary Power Supply <sup>(5)</sup>	—	Optional						
Brake Output	—	Optional						
Position Synchronized Output	—	Single Axis Standard, Two/Three Axis Optional						
Digital Inputs	—	6 Optically-Isolated (2 High Speed)						
Digital Outputs	—	4 Optically-Isolated						
Analog Inputs	—	One 16-bit Differential						
Analog Outputs	—	One 16-bit Single-Ended						
Additional I/O <sup>(6)</sup>	—	16/16 Digital; 3/3 In/Out						
MXH	—	Up to x65536						
Ethernet	—	Optional						
Emergency Stop Sense Input (ESTOP) <sup>(7)</sup>	—	Yes						
Resolver Interface	—	Optional <sup>(8)</sup>						
Shared Bus for Regen	—	No						Yes

## Notes:

- Output voltage dependent on input voltage.
- 10-120 VDC bus requires external transformer and auxiliary power option for logic power.
- Peak value of the sine wave; rms current for AC motors is 0.707(A<sub>pk</sub>).
- Optional three-phase input available on Ensemble HPe models.
- Auxiliary power option requires single phase 115-240 VAC 50-60 Hz.
- Requires IO option.
- Requires external relay to remove AC power.
- One- or two-channel input.

## Ensemble HLe SPECIFICATIONS

Ensemble HLe	Units	10-40	20-40	10-80
Output Voltage <sup>(1)</sup>	VDC	±40	±40	±80
Peak Output Current (1 sec) <sup>(8)</sup>	A <sub>pk</sub>	10	20	10
Continuous Output Current <sup>(2,8)</sup>	A <sub>pk</sub>	5	10	5
Power Amplifier Bandwidth	kHz	Selectable Through Software		
Minimum Load Inductance	mH	0		
Operating Temperature	°C	0 to 50		
Storage Temperature	°C	-30 to 85		
Weight	kg (lb)	10.36 (22.8)		
Maximum Shunt Regulator Dissipation	W	N/A		
Power Input	VAC	Single-Phase 7-240 VAC, 50-60 Hz		
Encoder Input Frequency	kHz	200 kHz Amplified Sine (For Onboard Multipliers), 40 MHz TTL Square Wave		
Current Loop Update Rate	kHz	20 kHz		
Servo Loop Update Rate	kHz	1 to 20 kHz		
Keep Alive/Logic Power Input <sup>(4)</sup>	—	Optional		
Brake Output	—	Optional		
Position Synchronized Output	—	Single Axis Standard, Two/Three Axis Optional		
Digital Inputs	—	6 Optically-Isolated (2 High Speed)		
Digital Outputs	—	4 Optically-Isolated		
Analog Inputs	—	One 16-bit Differential		
Analog Outputs	—	One 16-bit Single-Ended		
Additional I/O <sup>(5)</sup>	—	16/16 Digital; 3/3 In/Out		
MXH	—	Up to x65536		
Ethernet	—	Optional		
Emergency Stop Sense Input (ESTOP) <sup>(6)</sup>	—	Yes		
Resolver Interface	—	Optional <sup>(7)</sup>		

## Notes:

1. Output voltage dependent upon input voltage.
2. Peak value of the sine wave; rms current for AC motors is  $0.707(A_{pk})$ .
3. 10-120 VDC bus requires external transformer and auxiliary power option for logic power.
4. Auxiliary power option requires single phase 115-240 VAC 50-60 Hz.
5. Requires IO option.
6. Requires external relay to remove AC power.
7. One- or two-channel input.
8. Load dependent.

## Ensemble CP/CL/MP SPECIFICATIONS

CP Electrical Specifications		
Logic Input Voltage	VAC	85 to 240
Bus Input Voltage	VAC	14 to 240
Output Voltage	VDC	20 to 340
Peak Output Current	$A_{pk}$	10 to 30
Continuous Output Current	$A_{pk}$	5 to 15
PWM Switching Frequency	kHz	20
Power Amplifier Bandwidth	kHz	Software Selectable
Minimum Load Inductance	mH	0.1 @ 160 VDC (1 mH @ 320 VDC)
Digital Inputs and Outputs	Standard	4 opto inputs; 2 high-speed opto inputs; 4 opto outputs
	Optional	16 additional opto inputs; 16 additional opto outputs
Analog Inputs and Outputs	Standard	1 ( $\pm 10$ VDC, 16-bit) input; 1 ( $\pm 10$ VDC, 16-bit) output
	Optional	1 additional ( $\pm 10$ VDC, 12-bit) input; 1 additional ( $\pm 10$ VDC, 16-bit) output
Encoder Inputs		TTL RS-422 standard, and auxiliary encoder input; optional amplified sine encoder input on primary encoder channel; programmable resolution up to 1024 times the analog encoder resolution; 250 kHz amplified sine primary
Operating Temperature	°C	0 to 50
Storage Temperature	°C	-30 to 85
Weight	kg (lb)	1.6 (3.6)

CL Electrical Specifications		
Logic Input Voltage	VAC	85-240
Bus Input Voltage	VAC	56 VAC (center tapped transformer; two 28 VAC windings)
Output Voltage	VDC	$\pm 40$
Peak Output Current	$A_{pk}$	10 (load dependent)
Continuous Output Current	$A_{pk}$	5 (load dependent)
Power Amplifier Bandwidth	kHz	Software Selectable
Minimum Load Inductance	mH	0
Digital Inputs and Outputs	Standard	4 opto inputs; 2 high-speed opto inputs; 4 opto outputs
	Optional	16 additional opto inputs; 16 additional opto outputs
Analog Inputs and Outputs	Standard	1 ( $\pm 10$ VDC, 16-bit) input; 1 ( $\pm 10$ VDC, 16-bit) output
	Optional	1 additional ( $\pm 10$ VDC, 12-bit) input; 1 additional ( $\pm 10$ VDC, 16-bit) output
Encoder Inputs		TTL RS-422 standard, and auxiliary encoder input; optional amplified sine encoder input on primary encoder channel; programmable resolution up to 1024 times the analog encoder resolution; 250 kHz amplified sine primary
Operating Temperature	°C	0 to 50
Storage Temperature	°C	-30 to 85
Weight	kg (lb)	3.8 (8.4)

MP Electrical Specifications		
Logic Input Voltage	VDC	24 to 80
Bus Input Voltage	VDC	10 to 80
Output Voltage	VDC	10 to 80
Peak Output Current	$A_{pk}$	10
Continuous Output Current	$A_{pk}$	5
PWM Switching Frequency	kHz	20
Power Amplifier Bandwidth	kHz	Software Selectable
Minimum Load Inductance	mH	0.1 @ 80 VDC
Digital Inputs and Outputs	Standard	None
	Optional	8 opto inputs; 8 opto outputs
Analog Inputs and Outputs	Standard	1 ( $\pm 10$ VDC, 16-bit) input
	Optional	1 additional ( $\pm 10$ VDC, 12-bit) input; 1 additional ( $\pm 10$ VDC, 16-bit) output
Encoder Inputs		TTL RS-422 standard, and auxiliary encoder input; optional amplified sine encoder input on primary encoder channel; programmable resolution up to 1024 times the analog encoder resolution; 250 kHz amplified sine primary
Operating Temperature	°C	0 to 50
Storage Temperature	°C	-30 to 85
Weight	kg (lb)	0.45 (1.0)



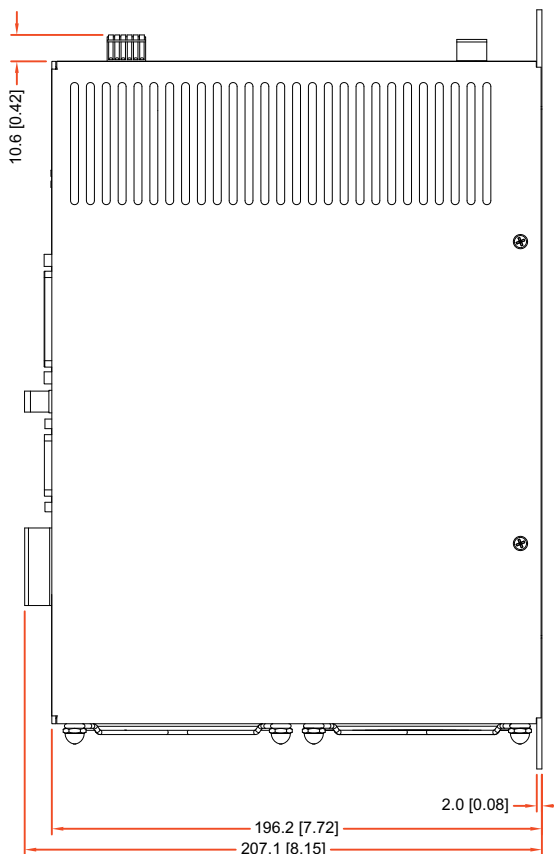
## Ensemble CP/CL/MP FEATURES

Feature	Details	
<b>Axes</b>	Up to 10 axes of coordinated motion	
<b>Axis Loop Type/Update Rate</b>	PID loop with up to 20 kHz servo update rate with feedforward; four user-configurable digital filters (e.g., notch, low pass)	
<b>On-Board Memory</b>	Program Storage	2 MB flash memory for user programs, parameters, miscellaneous storage
	Program Execution	8 MB RAM
<b>Driver Type Compatibility</b>	Brushless (linear or rotary) servo with on-board commutation DC brush servo Stepper/microstepper (on-board commutation)	
<b>Position Feedback</b>	Encoder interface, differential RS-422 signal, sine, cosine, and marker; 32 MHz input data rate; optional onboard analog encoder interpolation (of up to 1024-times encoder multiplication)	
<b>Position Modes</b>	Absolute, incremental, dynamic trajectory correction	
<b>Motion Types</b>	Independent Motions	Point-to-point incremental; target position or velocity; velocity profiles; time based; free run
	Coordinated Motions	Advanced queuing and deferred execution features for simultaneous command execution
	Interpolated Motions	Up to 10-axis linear and circular interpolation
	Digitally Geared Motions	Gearing with optional auxiliary encoder input
	Advanced Features	Automatic PID loop gain computation (autotuning)
	Contouring	Cubic spline curve-fitting; velocity profiling
	Error Mapping	2D error mapping, backlash compensation
<b>Acceleration Profiles</b>	Linear and jerk limiting parabolic; independent acceleration and deceleration profiles possible	
<b>Acceleration Ramp</b>	Rate, time, or distance based; independent acceleration and deceleration capability	
<b>Programmable Multitasking</b>	Up to 5 independent tasks	
<b>Programming</b>	Command Set	AeroBASIC™, LabVIEW®, VB.Net, C#
<b>Command Execution Modes</b>	AUTO	Program runs complete upon startup
	SINGLE	Full debug capability to step, step over, step into individual program lines
	IMMEDIATE	Commands are executed upon entry
	REMOTE	Command execution controlled by remote host through Ethernet, RS-232, or IEEE-488 communications port via ASCII strings
<b>Process Time</b>	Command execution up to 1000 lines of code per 1 ms (from command sent to motion start); read request @ 1 ms; average is 7 µs per program line (e.g., c = a + b)	
<b>Additional Interfaces</b>	Serial	10/100 Base-T Ethernet communication interface for system setup, application networking, embedded programming, immediate commands, and Modbus over TCP; USB communication interface for system setup, application networking, Windows® PC control interface
	Machine Control	Estop discrete input to stop all axes

The technical drawings show the front and side views of the Ensemble Aerotech room. The front view includes labels for various components: EMPTY, POWER, SENSORS, INPUT, ETHERNET, MOTOR PERFORMANCE, SETUP TEST, AUDIO, EXTERNAL TRANSFORMER REQUIRED, and DANGER! High Voltage. Dimensions are provided in inches [millimeters].

View	Dimension	Value (inches)	Value (millimeters)
Front View	Total Width	103.7	[4.08]
	Top Panel Width	102.0	[4.01]
	Left Side Mounting Hole Spacing	13.7	[0.54]
	Internal Top Panel Width	76.2	[3.00]
	Top Panel Hole Diameter	Ø4.8	[Ø0.19]
	Top Panel Hole Diameter	Ø10.4	[Ø0.41]
	Total Height	265.2	[10.44]
	Bottom Panel Thickness	4.8	[0.19] (TYP.)
	Bottom Panel Mounting Hole Spacing	18.1	[0.71]
	Bottom Panel Mounting Hole Diameter	8.9	[0.35]
Side View	Depth	10.6	[0.42]
	Bottom Panel Thickness	2.0	[0.08]
	Bottom Panel Mounting Hole Spacing	196.2	[7.72]
	Bottom Panel Mounting Hole Diameter	207.1	[8.15]

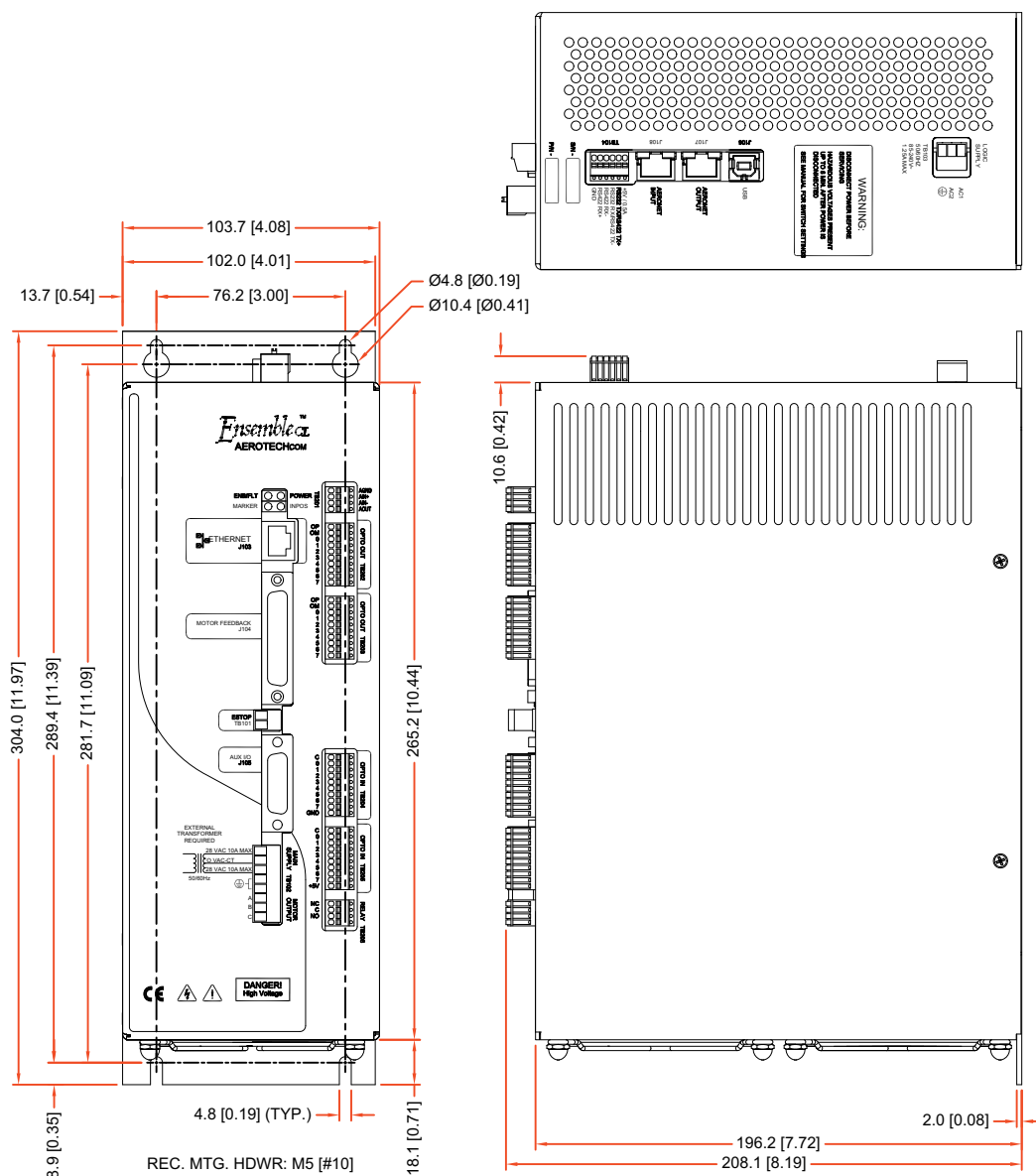
REC. MTG. HDWR: M5 [#10]





## Ensemble CL DIMENSIONS

## Ensemble CL with additional IO



# S-340

## High-Speed Piezo Tip/Tilt Platforms



- Fixed Orthogonal Axes with a Common Pivot Point
- 4 mrad Optical Beam Deflection
- For Mirrors to 100 mm Ø
- Sub-μrad Resolution
- Closed-Loop Versions for Better Linearity
- Differential Design for Excellent Temperature Stability
- Zero Friction Flexure Guides
- Single-Moving-Platform, Parallel-Kinematics Design: Equal Dynamics for all Axes, Better Linearity & Temperature Stability

S-340 piezo tip/tilt platforms are fast and compact tilt units, providing precise angular movements of the top platform in two orthogonal axes. The tip/tilt range is 2 mrad (equivalent to 4 mrad optical beam deflection) with sub-μrad reso-

lution. Closed-loop versions are available for highest accuracy and repeatability. S-340 systems are designed for mirrors up to 100 mm diameter and have outstanding angular stability over a wide temperature range.

To match the CTEs (coefficients of thermal expansion) of various mirror materials, platforms made from different materials are available (see ordering information).

### Open / Closed-Loop Operation

In open-loop operation, the platform angle roughly corresponds to the drive voltage (see page 4-17 in the "Tutorial" section for behavior of open-loop piezos). The open-loop

**This product family has been replaced  
by the following new product:  
>> S-340 Piezo Tip / Tilt-Platform**

models are ideal for applications where the position is controlled by an external loop, based on data provided by a sensor (e.g. PSD, quad cell, CCD chip, etc.).

The closed-loop versions are equipped with two pairs (one per axis) of LVDT (linear variable differential transformer) sensors operated in a bridge circuit for ultra-high resolution and angular stability. They provide sub-μrad resolution and repeatability.

### Higher Performance Through Parallel Kinematics

S-340 tip/tilt platforms feature a single moving platform, parallel-kinematics design with a common pivot point. Compared to stacked, multi-axis systems, the parallel-kinematics design provides faster response and better linearity with equal dynamics for all axes in a smaller package.

### Working Principle / Lifetime

S-340 tip/tilt platforms are equipped with two pairs of long-life, ceramic-encapsulated, high-performance PICMA® piezo drives operating as a unit in push/pull mode. The aluminum case is equipped with an integrated, FEA-modeled (finite element analysis) circular flexure featuring zero stiction, zero friction and exceptional guiding precision. Since drives and guides are frictionless and not subject to wear and tear, these units offer an exceptionally high level of reliability.

### Notes

See the "Selection Guide" on p. 3-8 for comparison with other steering mirrors.

See the "Piezo Drivers & Nanopositioning Controllers" section

### Ordering Information

#### S-340.A0

$\Theta_x$ ,  $\Theta_y$  Piezo Tip/Tilt Platform, 2 mrad, Aluminum Top Plate

#### S-340.i0

$\Theta_x$ ,  $\Theta_y$  Piezo Tip/Tilt Platform, 2 mrad, Invar Top Plate

#### S-340.S0

$\Theta_x$ ,  $\Theta_y$  Piezo Tip/Tilt Platform, 2 mrad, Steel Top Plate

#### S-340.T0

$\Theta_x$ ,  $\Theta_y$  Piezo Tip/Tilt Platform, 2 mrad, Titanium Top Plate

#### S-340.AL

$\Theta_x$ ,  $\Theta_y$  Piezo Tip/Tilt Platform, 2 mrad, Aluminum Top Plate, Closed-Loop

#### S-340.iL

$\Theta_x$ ,  $\Theta_y$  Piezo Tip/Tilt Platform, 2 mrad, Invar Top Plate, Closed-Loop

#### S-340.SL

$\Theta_x$ ,  $\Theta_y$  Piezo Tip/Tilt Platform, 2 mrad, Steel Top Plate, Closed-Loop

#### S-340.TL

$\Theta_x$ ,  $\Theta_y$  Piezo Tip/Tilt Platform, 2 mrad, Titanium Top Plate, Closed-Loop

Ask about custom designs!

for our comprehensive line of low-noise modular and OEM control electronics for computer and manual control.

### Materials Match

Platform	Recommended Models	Mirror
Aluminum	Aluminum	S-340.Ax
Invar	Zerodur glass	S-340.ix
Titanium	BK7 glass	S-340.Tx
Steel		S-340.Sx

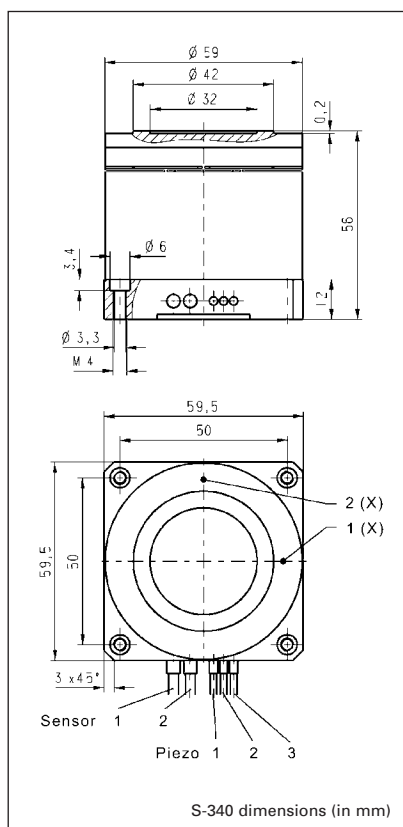
### Application Examples

- Image stabilization
- Laser beam stabilization
- Beam switching
- Adaptive optics systems
- Laser beam steering & scanning
- Correction of polygon scanner errors
- Interlacing, dithering

**This product family has been replaced  
by the following new product:  
>> S-340 Piezo Tip / Tilt-Platform**

Piezo • Nano • Positioning

**PI**



#### Technical Data

Models	S-340.x0	S-340.xL	Units	Notes see page 3-26
Active axes	$\Theta_x, \Theta_y$	$\Theta_x, \Theta_y$		
* Open-loop tilt angle 0 to 100 V	2 (4 optical)	2 (4 optical)	mrad $\pm 20\%$	A2
* Closed-loop tilt angle	-	2 (4 optical)	mrad	A3
Integrated feedback sensor	-	4 x LVDT		B
** Closed-loop / open-loop resolution	- / 0.1	0.5 / 0.1	$\mu\text{rad}$	C1
Closed-loop linearity (typ.)	-	$\pm 0.1$	%	
Full-range repeatability (typ.)	-	$\pm 1$	$\mu\text{rad}$	C3
Electrical capacitance	6.0 / axis	6.0 / axis	$\mu\text{F} \pm 20\%$	F1
*** Dynamic operating current coefficient (DOCC)	0.38 / axis	0.38 / axis	$\mu\text{A}/(\text{Hz} \times \mu\text{rad})$	F2
**** Unloaded resonant frequency ( $f_0$ )	1.4	1.4	$\text{kHz} \pm 20\%$	G2
**** Resonant frequency w/ $\varnothing 50 \times 15$ mm glass mirror	0.9	0.9	$\text{kHz} \pm 20\%$	G3
**** Resonant frequency w/ $\varnothing 75 \times 22$ mm glass mirror	0.4	0.4	$\text{kHz} \pm 20\%$	G3
Distance, pivot point to platform surface (T)	7.5	7.5	mm	
**** Platform moment of inertia	18000	18000	$\text{g} \cdot \text{mm}^2$	
Operating temperature range	- 20 to 80	- 20 to 80	$^{\circ}\text{C}$	H2
Voltage connection	3 x VL	3 x VL		J1
Sensor connection	-	2 x L		J2
Weight (w/o cables)	335	335	$\text{g} \pm 5\%$	
Material (case / platform)	Al / depends on version	Al / depends on version		L
Recommended amplifier/controller (codes explained page 3-9)	G <sup>a</sup> , C	H <sup>a</sup> , E		

\* Mechanical tilt, optical beam deflection is twice as large.

\*\* For calibration information see p. 3-7.

Resolution of PZT tip/tilt platforms is not limited by friction or stiction. Noise equivalent motion with E-503 amplifier.

\*\*\* Dynamic Operating Current Coefficient in  $\mu\text{A}$  per  $\text{Hz}$  and  $\mu\text{rad}$ . Example: Sinusoidal scan of 100  $\mu\text{rad}$  at 10 Hz requires approximately 0.38 mA drive current.

\*\*\*\* Value for aluminum top plate. Lower resonant frequency for other platforms due to higher moment of inertia: titanium: +60%; invar: +200%; steel: +190%.  
\* With (1 x E-505.00S + 2 x E-505.00) or 1 x E-503.00S

## E-616 Controller for Multi-Axis Piezo Tip/Tilt Mirrors and Platforms

### Flexible Multi Channel OEM Electronics with Coordinate Transformation



#### Ordering Information

**E-616.SS0**  
Multi Channel Servo-Controller /  
Driver for Piezo Tip/Tilt Mirror  
Platforms with SGS and Differential  
Drive

**E-616.S0**  
Multi Channel Servo-Controller /  
Driver for Piezo Tip/Tilt Mirror  
Platforms with SGS and Tripod  
Drive

- **Three Integrated Amplifiers Provide up to 10 W Peak Power**
- **Closed-Loop and Open-Loop Versions**
- **Internal Coordinate Transformation Simplifies Control of Parallel Kinematics Designs (Tripod & Differential Drive)**
- **Compact and Cost-Effective Design for OEMs**

The E-616 is a special controller for piezo based tip/tilt mirrors and tip/tilt platforms. It contains two servo controllers, sensor channels and power amplifiers in a compact unit. The controller works with high-resolution SGS position sensors used in PI piezo mechanics and provides optimum position stability and fast response in the nanometer and  $\mu$ rad-range respectively. A high output power of 10 W per channel allows dynamic operation of the tip/tilt mirrors for applications such as (laser) beam steering and stabilization.

#### **Tripod or Differential Piezo Drive? One for All!**

PI offers two basic piezo tip/tilt mirror designs. Both are parallel-kinematics designs where the individual piezo actuators affect the same moving platform. With the tripod design (e.g. S-325, see p. 2-92) the platform is driven by three piezo actuators placed with 120° spacing. The differential drive design (S-330, see p. 2-88 or S-334, see p. 2-90) with two orthogonal axes and a fixed pivot point is based on two pairs of actuators operating in

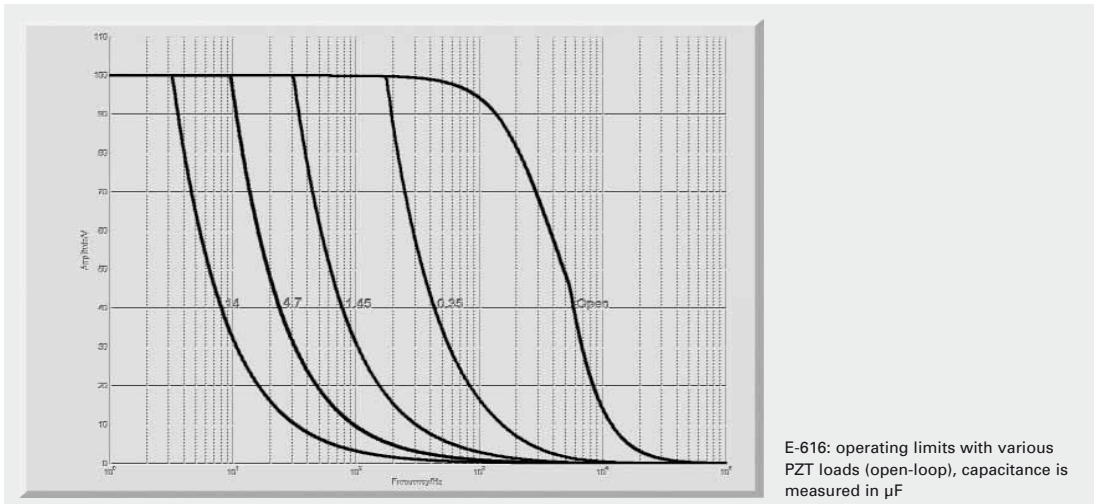
push / pull-mode. The differential evaluation of two sensors per axis provides an improved linearity and resolution.

#### **Internal Coordinate Transformation Simplifies Control**

Parallel-kinematics require the transformation of the commanded tilt angles into the corresponding linear motion of the individual actuators. In the E-616.S0, this is taken care of by an integrated circuit, eliminating the need of additional external hardware or software. Additionally with the E-616.S0 all actuators can be commanded by an offset-voltage simultaneously. As a result a vertical movement, for example for optical path tuning, is obtained.

#### **Simple Setup and Operation**

To facilitate integration, setup and operation the E-616 features both front and rear panel connections: The 25 pin sub-D piezo & sensor connector is located on the front, along with offset trim pots and LEDs for Power and Overflow. A 32 pin rear connector allows commanding and reading the sensor and amplifier monitor outputs.



## Technical Data

Model	E-616.S0	E-616.SS0
Function	Controller for parallel-kinematics piezo tip/tilt mirror systems with strain gauge sensors, tripod design	Controller for parallel-kinematics piezo tip/tilt mirror systems with strain gauge sensors, differential design
Tilt axes	2	2
<b>Sensor</b>		
Servo characteristics	P-I (analog), notch filter	P-I (analog), notch filter
Sensor type	SGS	SGS
Sensor channels	3	2
External synchronization	200 kHz TTL	200 kHz TTL
<b>Amplifier</b>		
Control input voltage range	-2 V to +12 V	-2 V to +12 V
Output voltage	-20 V to +120 V	-20 V to +120 V
Amplifier channels	3	3
Peak output power per channel	10 W	10 W
Average output power per channel	5 W	5 W
Peak current	100 mA	100 mA
Average current per channel	50 mA	50 mA
Current limitation	Short-circuit-proof	Short-circuit-proof
Voltage gain	10	10
Amplifier bandwidth, small signal	3 kHz	3 kHz
Amplifier bandwidth, large signal	See frequency diagram	See frequency diagram
Ripple, noise, 0 to 100 kHz	<20 mVpp	<20 mVpp
Amplifier resolution	<1 mV	<1 mV
<b>Interfaces and operation</b>		
Piezo / sensor connector	25-pin sub-D connector	25-pin sub-D connector
Analog input	32-pin connector	32-pin connector
Sensor monitor output	0 to +10 V for nominal displacement	0 to +10 V for nominal displacement
Sensor monitor socket	32-pin connector	32-pin connector
Display	Power-LED and sensor OFL display	Power-LED and sensor OFL display
<b>Miscellaneous</b>		
Operating temperature range	5 °C to 50 °C	5 °C to 50 °C
Overheat protection	Max. 75 °C, deactivation of the piezo voltage output	Max. 75 °C, deactivation of the piezo voltage output
Dimensions	160 mm x 100 mm x 10 TE	160 mm x 100 mm x 10 TE
Mass	700 g	700 g
Operating voltage	12 to 30 V DC	12 to 30 V DC
Power consumption	30 W	30 W

## Linear Actuators & Motors

### Nanopositioning / Piezoelectrics

#### Piezo Flexure Stages / High-Speed Scanning Systems

Linear

Vertical & Tip/Tilt

2- and 3-Axis

6-Axis

#### Fast Steering Mirrors / Active Optics

### Piezo Drivers / Servo Controllers

Single-Channel

**Multi-Channel**

Modular

Accessories

Piezoelectrics in Positioning

## Nanometrology

## Micropositioning

## Index



# M-122 Precision Micro-Translation Stage

## Fast & Compact with Direct Position Measurement



The M-122.2DD miniature translation stage features an optical linear encoder with 0.1  $\mu\text{m}$  position resolution and a highly efficient ballscrew

- Travel Range 25 mm
- 0.1  $\mu\text{m}$  Optical Linear Encoder for Highest Accuracy & Repeatability
- Min. Incremental Motion to 0.2  $\mu\text{m}$
- Max. Velocity 20 mm/s
- Cross-Roll Bearings
- Recirculating Ball Screw Drives Provide High Speeds & Long Lifetimes

The M-122 palm-top-sized translation stage combines small dimensions, high speeds and very high accuracy at a competitive price. It features a space-saving, folded drive train with the servo motor and drive screw side-by-side. Equipped with a non-contacting optical linear encoder and a preloaded, precision-ground, ball-screw, these stages can provide much higher accuracy and better repeatability than conventional stepper motor stages or rotary encoder-equipped servo motor stages.

### Low Friction, High Speed, Maintenance-Free

Due to its low-friction, the backlash-free ball screw yields significantly higher mechanical

efficiency than leadscrews, and allows maintenance-free, high duty-cycle operation at high velocities up to 20 mm/sec.

### XY and XYZ Combinations

M-122 stages can be combined to very compact XY and XYZ systems. The M-122.AP1 mounting bracket is available to mount the Z-axis.

### Limit and Reference Switches

For the protection of your equipment, non-contact Hall-effect limit and reference switches are installed. The direction-sensing reference switch supports advanced automation applications with high precision.

### Low Cost of Ownership

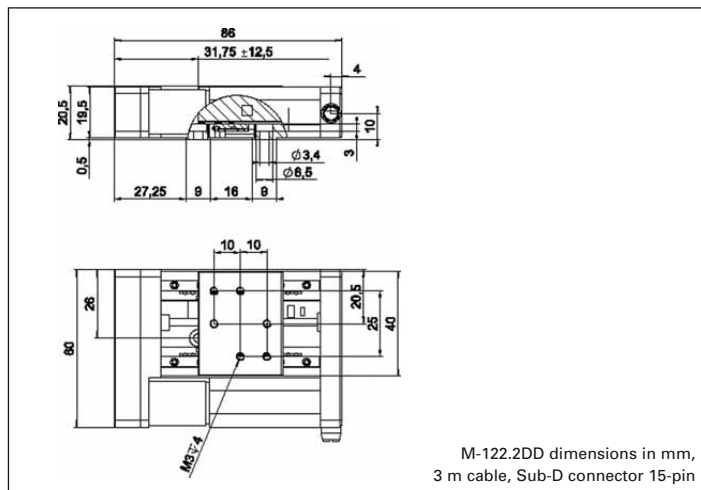
The combination of these positioners with the networkable, single-channel C-863 Mercury™ servo motor controller (s. p. 4-114) offers high performance for a very competitive price in both single- and multi-axis configurations. For multi-axis applications, the C-843 PC plug-in controller board with on-board servo amplifiers (s. p. 4-120) is another cost-effective alternative.

### Ordering Information

**M-122.2DD**  
High-Precision Translation Stage,  
25 mm, Direct-Drive DC Motor,  
Ballscrew

### Accessories

**M-122.AP1**  
Angle bracket for vertical  
mounting of M-122 stages  
**Ask about custom designs**



M-122.2DD dimensions in mm,  
3 m cable, Sub-D connector 15-pin

### Technical Data

Model	M-122.2DD
Active axes	X
<b>Motion and positioning</b>	
Travel range	25 mm
Integrated sensor	Linear encoder
Sensor resolution	0.1 $\mu\text{m}$
Design resolution	0.1 $\mu\text{m}$
Min. incremental motion	0.2 $\mu\text{m}$
Backlash	0.2 $\mu\text{m}$
Unidirectional repeatability	0.15 $\mu\text{m}$
Pitch	$\pm 150 \mu\text{rad}$
Yaw	$\pm 150 \mu\text{rad}$
Max. velocity	20 mm/s
Origin repeatability	1 $\mu\text{m}$
<b>Mechanical properties</b>	
Drive screw	Recirculating ballscrew
Thread pitch	0.5 mm
Stiffness in motion direction	0.25 N/ $\mu\text{m}$
Max. load	50 N
Max. push/pull force	20 N
Max. lateral force	25 N
<b>Drive properties</b>	
Motor type	DC motor
Operating voltage	0 to $\pm 12 \text{ V}$
Electrical power	2.25 W
Limit and reference switches	Hall-effect
<b>Miscellaneous</b>	
Operating temperature range	-20 to +65
Material	Aluminum, steel
Dimensions	86 x 60 x 20.5 mm
Mass	0.22 kg
Recommended controller/driver	C-863 (single-axis) C-843 PCI board (up to 4 axes)

### Application Examples

- Photonics packaging
- Fiber positioning
- Metrology
- Quality assurance testing
- Testing equipment
- Micromachining

## M-227 DC-Mike High-Resolution Linear Actuator

### Non-Rotating Tip, Long Stroke to 50 mm



M-227.10 (w/ piezo tip), M-227.25, M-227.50 (w/ ball tip), high-resolution DC-Mike actuators and several tip options

#### Ordering Information

**M-227.10**  
High-Resolution DC-Mike Linear Actuator, 10 mm

**M-227.25**  
High-Resolution DC-Mike Linear Actuator, 25 mm

**M-227.50**  
High-Resolution DC-Mike Linear Actuator, 50 mm

**M-219.10**  
Ball Tip

**P-855.20**  
Piezo Actuator for Micrometer Drive

- Travel Ranges 10, 25 and 50 mm
- Min. Incremental Motion to 0.05  $\mu\text{m}$
- Non-Rotating Tip
- Closed-Loop DC-Motors
- Sub-nm Resolution with Optional PZT Drive
- MTBF >5,000 h

M-230 (see p. 1-46 ff), M-235 (see p. 1-50 ff) and M-238.

M-227 are ultra-high-resolution linear actuators providing linear motion up to 50 mm with sub-micron resolution in a compact package. They consist of a micrometer with non-rotating tip, driven by a closed-loop DC-motor/gearhead combination with motor-shaft-mounted high-resolution encoder. The combination of an extremely low stiction/friction construction and high-resolution encoder allows for a minimum incremental motion of 50 nanometers at speeds up to 1 mm/sec.

#### Compact, High-Precision, Cost-Effective

M-227 actuators provide a cost-effective solution for industrial and OEM environments.

#### Integrated Line Drivers

All actuators include an integral 0.5 m cable with 15-pin sub-D connector and come with a 3 m extension cable. On the DC servo versions, the connector features integrated line drivers for cable lengths up to 10 meters between actuator and controller.

#### Non-Rotating Tip

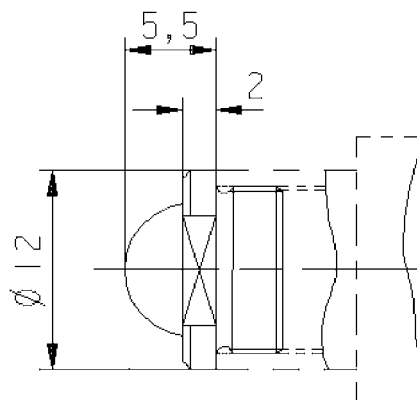
Compared to conventional rotating-tip micrometer drives, the non-rotating-tip design offers several advantages:

- Elimination of torque-induced positioning errors
- Elimination of sinusoidal motion errors
- Elimination of wear at the contact point
- Elimination of tip-angle-dependent wobble

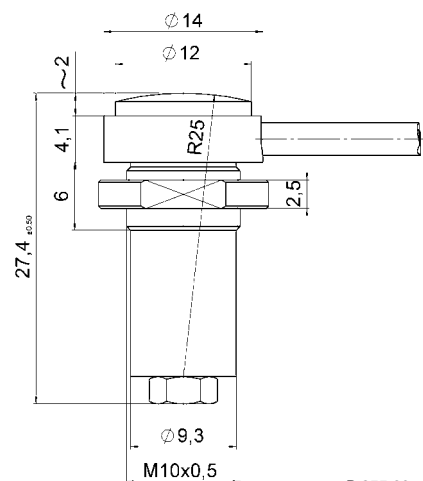
#### High-Resolution Piezo Option

All models come with standard flat tips. A variety of other tips are also available, such as a piezoelectric tip featuring 20  $\mu\text{m}$  travel with sub-nanometer resolution for dynamic scanning and tracking see p. 1-73 and 1-58.

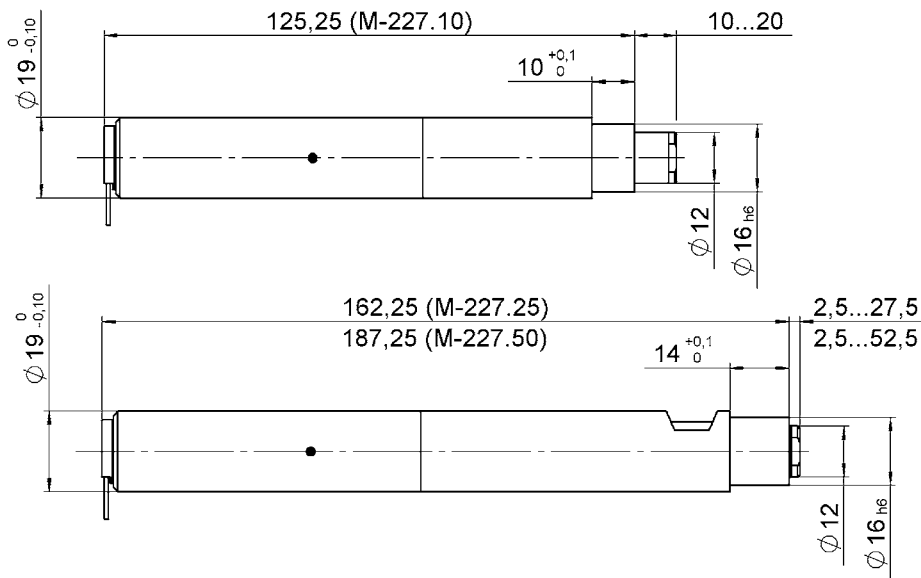
For higher loads and integrated limit switches refer to the



M-219.10 ball tip option



P-855.20 piezo tip option



M-227 DC-Mike, dimensions (in mm). C-815.38 motor cable included: 3 m, sub-D, 15/15 pin (m/f)

#### Linear Actuators & Motors

PiezoWalk® Motors / Actuators

PILine® Ultrasonic Motors

#### DC-Servo & Stepper Actuators

Piezo Actuators & Components

Guided / Preloaded Actuators

Unpackaged Stack Actuators

Patches/Benders/Tubes/Shear..

#### Nanopositioning / Piezoelectrics

Nanometrology

Micropositioning

Index

#### Technical Data

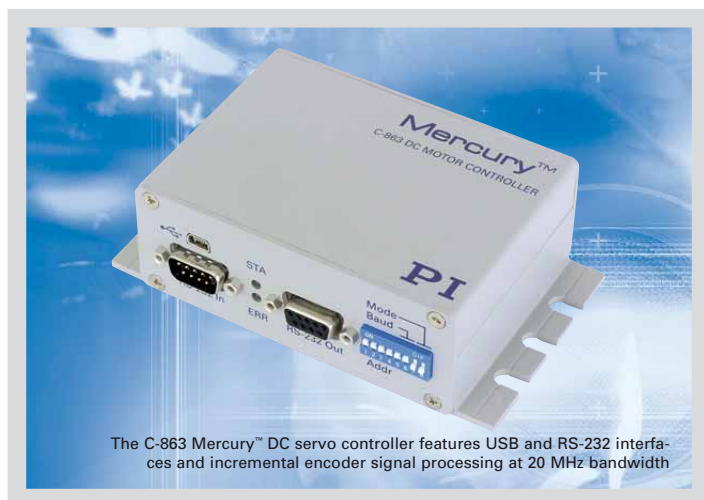
Model	M-227.10	M-227.25	M-227.50	Units
Active axes	X	X	X	
<b>Motion and positioning</b>				
Travel range	10	25	50	mm
Integrated sensor	Rotary encoder	Rotary encoder	Rotary encoder	
Sensor resolution	2048	2048	2048	Cts./rev.
Design resolution	0.0035	0.0035	0.0035	µm
Min. incremental motion	0.05	0.05	0.05	µm
Backlash	2	2	2	µm
Unidirectional repeatability	0.1	0.1	0.1	µm
Max. velocity	0.75	0.75	0.75	mm/s
<b>Mechanical properties</b>				
Drive screw	Leadscrew	Leadscrew	Leadscrew	
Thread pitch	0.5	0.5	0.5	mm
Gear ratio	69.12:1	69.12:1	69.12:1	
Max. push/pull force	40	40	40	N
Max. lateral force	0.1	0.1	0.1	N
<b>Drive properties</b>				
Motor type	DC-motor, gearhead	DC-motor, gearhead	DC-motor, gearhead	
Operating voltage	0 to ±12	0 to ±12	0 to ±12	V
Electrical power	1.25	1.25	1.25	W
<b>Miscellaneous</b>				
Operating temperature range	-20 to +65	-20 to +65	-20 to +65	°C
Material	Al (anodized), steel	Al (anodized), steel	Al (anodized), steel	
Mass	0.16	0.22	0.26	kg
Cable length	0.1	0.1	0.1	m
Connector	15-pin sub-D connector	15-pin sub-D connector	15-pin sub-D connector	
Recommended controller/driver	C-863 single-axis C-843 PCI-board, for up to 4 axes	C-863 single-axis C-843 PCI-board, for up to 4 axes	C-863 single-axis (see p. 4-114) C-843 PCI-board, for up to 4 axes (see p. 4-120)	

\*Higher forces on request



## C-863 Mercury™ Servo Controller

### 1-Axis DC-Servo-Motor Controller with Network Feature



The C-863 Mercury™ DC servo controller features USB and RS-232 interfaces and incremental encoder signal processing at 20 MHz bandwidth

- High Performance at Low Cost
- DC Servo-Motor Controller Supplies up to 30 W
- 20 MHz Encoder Input for High Speed & Resolution
- Macro Programmable Stand-Alone Functionality
- Network Capability for Multi-Axis Applications
- Non-Volatile EEPROM for Macros and Parameters
- Digital I/O Lines (TTL)
- Motor-Brake Control
- USB and RS-232 Interface
- Optional Joystick for Manual Control
- Works with All PI Micropositioners

The latest generation Mercury™ C-863 servo motor controller is even more powerful and versatile than its predecessors. Easy data interchange with laptop or PC is possible via the USB interface. The RS-232 interface provides for easy integration in industrial applications. The compact design with its integrated amplifier makes it ideal for building high-performance,

cost-effective micropositioning systems.

#### Flexible Automation

The Mercury™ offers a number of features to achieve automation and handling tasks in research and industry in a very cost-effective way. Programming is facilitated by the high-level mnemonic command language with macro and compound-command functionality. Macros can be stored in the non-volatile memory for later recall.

Stand-alone capability is provided by a user-programmable autostart macro to run automation tasks at power up (no runtime computer communication required!).

For easy synchronization of motion with internal or external trigger signals four input and four output lines are provided.

#### Multi-Axis Control, Combination of DC & Stepper Motors

Up to 16 C-863 Mercury™ DC servo controllers and C-663 stepper motor controllers can be daisy-chained and addressed via the same interface.

The networking feature allows the user to start out with one controller and add more units later for multi-axis setups.

#### Easy Programming

All servo and stepper motor controllers of the Mercury™ family can be operated using the PI general command set (GCS). PI-GCS allows networking of different controller units, both for piezo-based and motorized positioning units, with minimal programming effort. In addition, the C-863 can be programmed using the native command set of previous Mercury™ controllers.

#### Cost-Saving Due to Integrated Amplifier and PWM Outputs

The unique Mercury™ concept combines a high-performance motion controller and an integrated power amplifier in a small package. Additional PWM control outputs allow the direct operation of any DC-motor-driven PI micro-positioning system—even high-speed stages such as the M-500 ActiveDrive™ Translation Stages—reducing costs, increasing reliability and simplifying the setup.

#### Contents of Delivery

Each controller is delivered with a wide-range power sup-

#### Ordering Information

**C-863.10**  
Mercury™ DC-Motor Controller, 1 Channel, with Wide-Range Power Supply

**C-819.20**  
2-Axis Analog Joystick for Mercury™ Controller

**C-819.20Y**  
Y-Cable for Connecting 2 Controllers to C-819.20

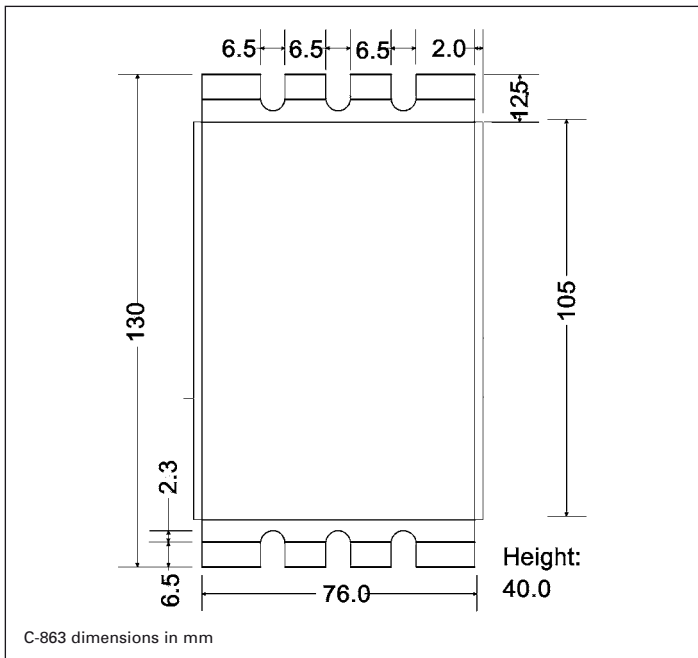
**C-170.IO**  
I/O Cable, 2 m, Open End

**C-170.PB**  
Push Button Box, 4 Buttons and 4 LEDs

ply, RS-232 communication cable, a daisy-chain network cable and a comprehensive software package.

#### Application Examples

- Fiber positioning
- Automation
- Photonics / integrated optics
- Quality assurance testing
- Testing equipment



## Technical Data

<b>Model</b>	<b>C-863.10</b>
Function	DC-servo-motor controller, 1 channel
<b>Motion and control</b>	
Servo characteristics	P-I-D servo control, parameter change on-the-fly
Trajectory profile modes	Trapezoidal, point-to-point
Encoder input	AB (quadrature) single-ended or differential TTL signal, 20 MHz
Stall detection	Servo off, triggered by programmable position error
Input limit switch	2 x TTL (pull-up/pull-down, programmable)
Input reference switch	1 x TTL
Motor brake	1 x TTL, software controlled
<b>Electrical properties</b>	
Output power	max. 30 W (PWM)
Output voltage	0 to 15 V
Current	80 mA + motor current (3 A max.)
<b>Interfaces and operation</b>	
Communication interfaces	USB, RS-232 (9-pin [m] sub-D)
Motor connector	15-pin (f) sub-D
Controller network	Up to 16 units on single interface
I/O ports	4 analog/digital in, 4 digital out (TTL)
Command set	Mercury Command Set, GCS (via DLL)
User software	PIMikroMove®, MMCRun
Software drivers	GCS (PI General Command Set)-DLL, LabVIEW drivers, native Mercury™ DLL
Supported functionality	Start-up macro; internal safety circuitry: watchdog timer
Manual control (optional)	2-axis joystick, Y-cable for 2D motion, pushbutton box
<b>Miscellaneous</b>	
Operating voltage	15 to 30 V included: external power supply, 15 V / 2 A
Operating temperature range	+5 to +50 °C
Mass	0.3 kg
Dimensions	130 x 76 x 40 mm

Linear Actuators &amp; Motors

Nanopositioning / Piezoelectrics

Nanometrology

## Micropositioning

Hexapod 6-Axis Systems /  
Parallel Kinematics

Linear Stages

Translation (X)

Vertical (Y)

Multi-Axis

Rotary &amp; Tilt Stages

Accessories

## Servo & Stepper Motor Controllers

Single-Channel

Hybrid

Multi-Channel

Micropositioning  
Fundamentals

Index

### *Appendix F. Proposed AFIT Ground Station Parts List*

THE following is a list of components to be used on the AFIT ground station. This list was obtained from a proposal quote from Front Range Aerospace Inc.

**Proposed AFIT Ground Station Equipment List**

<b><u>Quan</u></b>	<b><u>Description</u></b>	<b><u>Model Number/Item Number</u></b>
1	M2 VHF Yagi Antenna	2MCP14
1	M2 UHF Yagi Antenna	436CP32 U/G
2	Antenna Controllers	RT21
1	Antenna Tower w/thrust bearing	N/A
1	UHF Preamplifier	MSP432VDG-160
1	DC Voltage injector for PreAmp	DCINJ-N-PWR
1	ICOM 910 H Tranceivers	ICOM 910H
1	Astron Rack Mount Power Supply	RM60M
1	"Eye" Pattern Monitor Oscilloscope	TDS 1001B
1	Rack Mount for O-scope	RM2000B
1	Win Radio Spectrum Analyser	WR-G305e
1	Win Radio Advanced Digital Suite	WR-ADS-FULL
1	Diawa Power Meter	CN-103NL
1	NOVA Software for Tracking Control	WINNOVA
1	Terminal Node Controller	TNC31S (U-S96)
1	Equipment Rack (19")	

## Bibliography

1. Ebbing, D., *General Chemistry*, Houghton Mifflin Company, 5th ed., 1996.
2. Short, N., "The Remote Sensing Tutorial," <http://rst.gsfc.nasa.gov>, Jan 2010.
3. Clifford, G., "HICO/RAIDS Experiment Payload (HREP)," Presentation provided to AFIT, Jan 2010.
4. TERMA, "Star Tracker HE-5AS," [http://www.terma.com/multimedia/Star\\_Trackers5.pdf](http://www.terma.com/multimedia/Star_Trackers5.pdf), Jan 2010.
5. Troxel, I., Fehring, M., and Chenoweth, M., "Achieving Multipurpose Space Imaging with the ARTEMIS Reconfigurable Payload Processor," *Proc. Aerospace Conference*, 2008.
6. Troxel, I., Fehring, M., and Chenoweth, M., "Flexible Fault Tolerance Using The ARTEMIS Reconfigurable Payload Processor," Military and Aerospace FPGA and Applications (MAFA) Meeting, Nov 2007.
7. Moody, D., *Microprocessor-Based Systems Control For The Rigidized Inflatable Get-Away-Special Experiment*, Master's thesis, Air Force Institute of Technology, 2004.
8. United States Naval Academy, "MidSTAR Homepage," <http://www.usna.edu/Satellite/midstar/>, Jan 2010.
9. Black, J. and Cobb, R., "AFIT-0801 Space Chromotomography Experiment (CTEx)," Briefing to the DoD Space Experiments Review Board (SERB), Oct 2009.
10. LeMaster, D., *Design and Model Verification of an Infrared Chromotomographic Imaging System*, Master's thesis, Air Force Institute of Technology, 2004.
11. O'Dell, D., *Development and Characterization of a Field-Deployable Fast Chromotomographic Imager*, Master's thesis, Air Force Institute of Technology, 2010.
12. Atkins, P. and Jones, L., *Chemistry: Molecules, Matter, and Change*, W. H. Freeman and Company, 3rd ed., 1997.
13. Wolfson, R. and Pasachoff, J., *Physics: For Scientists and Engineers*, Harper Collins College Publishers, 2nd ed., 1995.
14. University of Nebraska-Lincoln, "Spectral Types of Stars - Eclipsing Binary Stars -NAAP," <http://astro.unl.edu/naap/ebs/spectraltype.html>, Jan 2010.
15. Niece, B., "Light Sources Tutorial - Line Sources," [http://www1.assumption.edu/users/bniece/Spectra/Tutorials/LS\\_Line.html](http://www1.assumption.edu/users/bniece/Spectra/Tutorials/LS_Line.html), Jan 2010.
16. Japanese Aerospace Exploration Agency, "Payload:H-II Transfer Vehicle (HTV) - International Space Station - JAXA," <http://iss.jaxa.jp/en/htv/mission/htv-1/payload/>, Jan 2010.
17. National Aeronautics and Space Administration, "NASA - HICO and RAIDS Experiment Payload," [http://www.nasa.gov/mission\\_pages/station/science/experiments/HREP-HICO.html](http://www.nasa.gov/mission_pages/station/science/experiments/HREP-HICO.html), Jan 2010.
18. Starr, W., *Analysis of Slewing and Attitude Determination Requirements for CTEx*, Master's thesis, Air Force Institute of Technology, 2010.

19. PCI Industrial Computer Manufacturers Group, "PCIMG - Resources - Compact-PCI," <http://www.picmg.org/v2internal/compactpci.htm>, Jan 2010.
20. Warren, K., "Air Force's satellite-loaded Atlas V is 50th launch success," *Air Force News*, 2007.
21. Roddy, D., *Satellite Communications*, McGraw-Hill, 4th ed., 2006.
22. Mooney, J., Brodzik, A., and An, M., "Principal component analysis in limited-angle chromotomography," *Imaging Spectrometry III*, Vol. 3118, 1997, pp. 170–178.
23. Mooney, J., "Spectral Imaging Via Computed Tomography," *Proc. of the 1994 Meeting of the Infrared Information Symposia Special Group on Passive Sensors*, Vol. 1, DTIC, 1994, pp. 203–215.
24. Dearing, A., *Simulating A Chromotomographic Sensor For Hyperspectral Imaging In The Infrared*, Master's thesis, Air Force Institute of Technology, 2004.
25. Gustke, K., *Reconstruction Algorithm Characterization and Performance Monitoring in Limited-Angle Chromotomography*, Master's thesis, Air Force Institute of Technology, 2004.
26. Bostick, R. and Perram, G., "Hyperspectral Imaging Using Chromotomography: A Fieldable Visible Instrument For Transient Events," *International Journal of High Speed Electronics and Systems*, Vol. 20, No. 10, 2006, pp. 1/11/2010.
27. Book, T., *Design Analysis of a Space Based Chromotomographic Hyperspectral Imaging Experiment*, Master's thesis, Air Force Institute of Technology, 2010.
28. European Space Agency, "Call for ideas Annex 1: Experiments for global climate change from the ISS," [http://www.esa.int/SPECIALS/HSF\\_Research/SEM3VBZRA0G\\_0.html](http://www.esa.int/SPECIALS/HSF_Research/SEM3VBZRA0G_0.html), Feb 2010.
29. Wind River Systems, "Wind River VxWorks: Embedded RTOS with support for POSIX and SMP," <http://www.windriver.com/products/vxworks/>, Feb 2010.

<b>REPORT DOCUMENTATION PAGE</b>			Form Approved OMB No. 0704-0188	
<p>The public reporting burden for this collection of information is estimated to average 1 hour per response, including the time for reviewing instructions, searching existing data sources, gathering and maintaining the data needed, and completing and reviewing the collection of information. Send comments regarding this burden estimate or any other aspect of this collection of information, including suggestions for reducing this burden to Department of Defense, Washington Headquarters Services, Directorate for Information Operations and Reports (0704-0188), 1215 Jefferson Davis Highway, Suite 1204, Arlington, VA 22202-4302. Respondents should be aware that notwithstanding any other provision of law, no person shall be subject to any penalty for failing to comply with a collection of information if it does not display a currently valid OMB control number. PLEASE DO NOT RETURN YOUR FORM TO THE ABOVE ADDRESS.</p>				
1. REPORT DATE (DD-MM-YYYY) 25-03-2010		2. REPORT TYPE Master's Thesis		3. DATES COVERED (From — To) Sep 2008 – Mar 2010
4. TITLE AND SUBTITLE  Preliminary Electrical Designs for CTE <sub>x</sub> and AFIT Satellite Ground Station			5a. CONTRACT NUMBER	
			5b. GRANT NUMBER	
			5c. PROGRAM ELEMENT NUMBER	
6. AUTHOR(S)  Morse, Arthur L., Capt, USAF			5d. PROJECT NUMBER	
			5e. TASK NUMBER	
			5f. WORK UNIT NUMBER	
7. PERFORMING ORGANIZATION NAME(S) AND ADDRESS(ES) Air Force Institute of Technology Graduate School of Engineering and Management (AFIT/ENY) 2950 Hobson Way WPAFB OH 45433-7765			8. PERFORMING ORGANIZATION REPORT NUMBER  AFIT/GA/ENY/10-M08	
9. SPONSORING / MONITORING AGENCY NAME(S) AND ADDRESS(ES)  Undisclosed Sponsor			10. SPONSOR/MONITOR'S ACRONYM(S)	
			11. SPONSOR/MONITOR'S REPORT NUMBER(S)	
12. DISTRIBUTION / AVAILABILITY STATEMENT APPROVED FOR PUBLIC RELEASE; DISTRIBUTION UNLIMITED				
13. SUPPLEMENTARY NOTES				
14. ABSTRACT <p>This thesis outlines the design of the electrical components for the space-based ChromoTomography Experiment (CTE<sub>x</sub>). CTE<sub>x</sub> is the next step in the development of high-speed chromotomography at the Air Force Institute of Technology. The electrical design of the system is challenging due to the large amount of data that is acquired by the imager and the limited resources that is inherent with space-based systems. Additional complication to the design is the need to know the angle of a spinning prism that is in the field of view very precisely for each image. Without this precise measurement any scene that is reconstructed from the data will be blurry and incomprehensible. This thesis also outlines how the control software for the CTE<sub>x</sub> space system should be created. The software flow is a balance of complex real time target pointing angles and simplicity to allow the system to function as quick as possible.</p> <p>This thesis also discusses the preliminary design for an AFIT satellite ground station based upon the design of the United States Air Force Academy's ground station. The AFIT ground station will be capable of commanding and controlling satellites produced by USAFA and satellites produced by a burgeoning small satellite program at AFIT.</p>				
15. SUBJECT TERMS chromotomography, hyperspectral				
16. SECURITY CLASSIFICATION OF:			17. LIMITATION OF ABSTRACT  UU	18. NUMBER OF PAGES  151
a. REPORT  U	b. ABSTRACT  U	c. THIS PAGE  U		
			19a. NAME OF RESPONSIBLE PERSON Dr. Jonathan T. Black, AFIT/ENY	
			19b. TELEPHONE NUMBER (Include Area Code) (937)255-3636, ext 4578	